NON-LINEAR DYNAMICS OF MARINE ECOSYSTEM MODELS

By

Georgina Anne Gibson

RECOMMENDED:

Advisory Committee Chair

Head, Graduate Program in
Marine Science and Limnology

APPROVED:

Dean, School of Fisheries and Ocean Sciences

Dean of the Graduate School

Date

NON-LINEAR DYNAMICS OF MARINE ECOSYSTEM MODELS

A

DISSERTATION

Presented to the Faculty

Of the University of Alaska Fairbanks

In Partial Fulfillment of the Requirements

For the Degree of

DOCTOR OF PHILOSOPHY

By

Georgina Anne Gibson, B.Sc.

Fairbanks, Alaska

December 2004

ABSTRACT

Despite a rapid trend towards more realistic Nutrient-Phytoplankton-Zooplankton (NPZ) models, in which zooplankton are presented with multiple nutritional resources, investigations into the fundamental dynamics of these newer models have been limited. The objective of this dissertation was to explore the dynamical behavior of such NPZ models parameterized for the coastal Gulf of Alaska. With alternative stationary forcing regimes and zooplankton grazing functions, the dynamics of one-dimensional NPZ models were investigated for a range of specific predation rates (h) and predation exponents (q), which together define the form of the predation (model closure) function. Oscillations in state variables are shown to be an intrinsic property of the NPZ models, not dependent on variable seasonal forcing for their existence. Increasing mixed layer diffusivity or reducing mixed layer depth increased model excitability; it is hypothesized that this is due to the resultant increase in flux of utilizable nutrient. Model behavior was also strongly influenced by the form of both the grazing and predation functions. For all of the grazing functions implemented, Hopf bifurcations, where the form of the solution transitioned between steady equilibrium and periodic limit cycles, persisted across the q-h parameter space. Regardless of the values of h and q, with some forms of the grazing function steady equilibrium solutions that simultaneously comprised non-zero concentrations for all model components could not be found. The inclusion of sinking detritus in the model had important implications for the composition and excitability of model solutions, generally increasing the region of q-h space for which oscillatory solutions were found. Therefore, in order to correctly simulate the depth-explicit concentrations of model components, or to have an accurate understanding of the potential excitability of the system, inclusion of this component is valuable. This dissertation highlights the importance of understanding the potential impact that choice of functional response may have on the intrinsic oscillatory nature of a model prior to interpreting results from coupled bio-physical simulations. As we come to rely more on ecosystem models as a tool to interpret marine ecosystem functionality it will be important to improve our understanding of the non-linear behavior inherent in these models.

TABLE OF CONTENTS

LIST OF FIGURES

LIST OF TABLES

LIST OF NOTATIONS

α_1	Fraction of organic materiel lost from the microzooplankton considered dissolved
α_2	Fraction of organic materiel lost from the mesozooplankton considered dissolved
α	Real portion of eigenvalue
β	Imaginary portion of eigenvalue
C_i	Concentration of model component
C_i^*	Equilibrium concentration of model component
C_i'	Perturbed concentration of model component
d	Detrital degregation rate
D	Bacterial degregation of detritus
Dt	Detritus
e_{11}	Prey ratio independent microzooplankton capture efficiency for small phytoplankton
e_{12}	Prey ratio independent microzooplankton capture efficiency for large phytoplankton
e_{21}	Prey ratio independent mesozooplankton capture efficiency for small phytoplankton
e_{22}	Prey ratio independent mesozooplankton capture efficiency for large phytoplankton
e_{ZZ}	Prey ratio independent mesozooplankton capture efficiency for microzooplankton
ε_{11}	Prey ratio dependent microzooplankton capture efficiency for small phytoplankton
ε_{12}	Prey ratio dependent microzooplankton capture efficiency for large phytoplankton
ε_{21}	Prey ratio dependent mesozooplankton capture efficiency for small phytoplankton
ε_{22}	Prey ratio dependent mesozooplankton capture efficiency for large phytoplankton
ε_{ZZ}	Prey ratio dependent mesozooplankton capture efficiency for microzooplankton
g	Zooplankton specific natural mortality rate (Edwards model)
G	Grazing rate
G_{11}	Grazing by microzooplankton on small phytoplankton
G_{12}	Grazing by microzooplankton on large phytoplankton
G_{21}	Grazing by mesozooplankton on small phytoplankton
G_{22}	Grazing by mesozooplankton on large phytoplankton
G_{ZZ}	Grazing by mesozooplankton on microzooplankton
h	Specific predation rate for mesozooplankton
H	Undefined predation on mesozooplankton
i_{max}	Zooplankton maximum ingestion rate
i_{max1}	Maximum ingestion rate for microzooplankton

$i_{\max 2}$	Maximum ingestion rate for mesozooplankton
k_P	Phytoplankton half-saturation constant for nutrient
k_Z	Zooplankton half-saturation constant for phytoplankton
k_{11}	Small phytoplankton half-saturation constant for nitrate
k_{12}	Large phytoplankton half-saturation constant for nitrate
k_{21}	Small phytoplankton half-saturation constant for ammonium
k_{22}	Large phytoplankton half-saturation constant for ammonium
k_{31}	Half-saturation coefficient for microzooplankton grazing
k_{32}	Half-saturation coefficient for mesozooplankton grazing
k_{ext}	Light extinction coefficient
Kh	Horizontal diffusion coefficient
Kv	Vertical diffusion coefficient
Kv_m	Mixed layer vertical diffusion coefficient
Kv_b	Background vertical diffusion coefficient
m	Phytoplankton specific natural mortality rate (Edwards model)
m_1	Specific natural mortality rate of small phytoplankton
m_2	Specific natural mortality rate of large phytoplankton
m_z	Specific natural mortality rate of microzooplankton
M_1	Natural mortality of small phytoplankton
M_2	Natural mortality of large phytoplankton
M_Z	Natural mortality of microzooplankton
MLD	Mixed layer depth
N	Nutrient
N_1	Nitrate
N_2	Ammonium
N_T	Total nitrogen
P	Phytoplankton
P_1	Small phytoplankton
P_2	Large phytoplankton
$P_{\max}$	Maximum growth rate of phytoplankton
$P_{\max 1}$	Maximum growth rate of small phytoplankton
$P_{\max 2}$	Maximum growth rate of large phytoplankton
q	Predation exponent

r	Specific nitrification on rate
R	Nitrification
R_m	Maximum grazing rate (Edwards model)
S	Sinking of detritus
t	Time
u	Velocity in the x-direction
U_{11}	Small phytoplankton uptake rate for nitrate
U_{12}	Large phytoplankton uptake rate for nitrate
U_{21}	Small phytoplankton uptake rate for ammonium
U_{22}	Small phytoplankton uptake rate for ammonium
v	Velocity in the y-direction
V_m	Maximum uptake rate of nutrients by the phytoplankton (Edwards model)
w	Velocity in the z-direction
W_s	Detrital sinking rate
ψ	Inhibition parameter for uptake of nitrate by ammonium
ω	Shape parameter for diffusion profile
z	Depth
Z	Zooplankton
Z_1	Microzooplankton
Z_2	Mesozooplankton
γ	Unassimilated grazing fraction (Edwards model)
γ_1	Assimilation efficiency of microzooplankton
γ_2	Assimilation efficiency of mesozooplankton
Φ	Shape parameter for diffusion profile
Λ	Ivlev saturation constant for grazing (Edwards model)
λ	Eigenvalue
θ	Zooplankton feeding threshold concentration

PREFACE

Here the organization of this dissertation is described as a convenience for the reader, and to point out the relationship between the material to be included in manuscripts for publication, and the general background material. This dissertation includes the text of a manuscript (Chapter 4) that has been submitted to Journal of Plankton Research. The other chapters are material that would either be inappropriate for inclusion in a journal article, but nevertheless, provides insight into the work conducted as part of this dissertation (Chapters 1-3, 6), or the basis for a second manuscript (Chapter5). Due to the format of this dissertation there may be some redundancy in material, such as equations and references, but an effort has been made to keep this to a minimum.

Chapter 1 outlines the general motivation for this dissertation. A background on NPZ models is provided along with a discussion on the importance of understanding the non-linear dynamics inherent in these models. The contribution of ecosystem modeling as a supplement to the traditional observational studies is discussed, as is the importance of the Gulf of Alaska ecosystem and the variability in productivity that has been observed on a decadal timescale. Finally, the objectives of this dissertation and the specific hypothesis addressed are presented.

Chapter 2 is concerned with the details of NPZ model development. It includes an outline of how the models used in this dissertation were developed from a simpler model whose dynamics have been previously investigated. The modeling approach is detailed, and the biological equations that comprise the six-component model are presented along with a discussion concerning the incorporation of stationary, depth-explicit physical forcing. In this chapter the reliability of the six-component model is examined through a comparison of time-series solutions to equivalent results produced by and existing three component model.

In Chapter 3 an attempt to use the traditional eigenvalue analysis approach to determine the behavior of the six-component NPZ model is outlined. This approach is illustrated to be non applicable for complex depth-explicit diffusive models such as the ones under investigation in this dissertation. The realizations presented in this chapter led to an alternative approach for investigating the non–liner dynamics of the model. This is the subject of Chapter 4.

In Chapter 4, the dynamics of a six-component NPZ model in which zooplankton can graze on a mixed prey field are explored. Five alternative functional forms were implemented to describe zooplankton grazing, and the form for predation on mesozooplankton was prescribed by a product of a specific predation rate (h) and the mesozooplankton concentration raised to a power (q) which was varied between one and two. This work has been submitted as a manuscript to the Journal of Plankton Research.

Although a sub-surface chlorophyll maximum is known to persist in the coastal Gulf of Alaska during the summer months, no sub-surface chlorophyll maximum was observed for any of the simulations with the six-component model. To address this discrepancy, in Chapter 5, a detritus component is added to the model and behavior of the seven-component model is investigated for sinking and non-sinking detritus. The impact of alternative stationary physical regimes is also examined.

Chapter 6 provides a summary and discussion of key results that emerged from this dissertation, and their implications for ecosystem modeling. Areas where our understanding falls short have been highlighted and suggested as possible paths for future work in this field.

ACKNOWLEDGEMENTS

I have been fortunate in receiving support in many shape and forms, without which this dissertation would not have been possible. Early funding for this research was provided by the University of Alaska Foundation Presidents Special Project Fund, and the past four years of this research were generously funded through fellowships from the Rasmuson Fisheries Research Center; I would like to express my gratitude to both funding bodies. I am also indebted to Dr. D. L. Musgrave for funding numerous trips to meetings and conferences and for providing the computer hardware upon which this research was heavily dependent. I would like to express my appreciation for the support and encouragement that I have had from my advisory committee: Dave Musgrave (major advisor), Sarah Hinckley, Terry Whitledge, Russell Hopcroft and Ken Coyle. They have all been very generous with their time and provided effective guidance while I was working on this research. Their critical reviews and helpful comments have vastly improved the content of this dissertation. I owe a special thank you to Dave Musgrave and Sarah Hinckley for their input and guidance to the work presented in Chapter 4 of this dissertation. We have jointly submitted this chapter to the Journal of Plankton Research. And last, but by no means least, I would like to express my eternal gratitude to both my parents Margaret and Keith, and my husband Michael for always believing in me and providing support and encouragement when I needed it most.

Chapter 1 . General Introduction

1.1 The role of modeling in ecosystem studies.

A full understanding of marine ecosystem dynamics requires knowledge of the influence of physical forcing on the temporal and spatial distribution and abundance of plankton, and of the interaction between the different trophic levels. Study of the temporal and spatial distribution and abundance of plankton in the marine environment has traditionally required the collection of numerous samples, usually with the aid of horizontal and vertical net tows at designated locations (stations) of interest. While essential to our understanding, observational methods do have drawbacks. Data collection is generally heavily dependent on ship or laboratory time, and restricted with respect to the time frame and the geographic area covered or the number of species under consideration. In light of the drawbacks of observational studies, computer simulation models are becoming increasingly prevalent tools in marine ecosystem studies. Models can be used to gain understanding of how a system works or to make predictions of the future state of the ecosystem. Models can enable synchronous 'coverage' of an ecosystem of interest, and are a relatively cost-effective research tool. Models can also be used to perform "experiments" in ways it is impossible to do in a real ecosystem. Physical forcing, initial conditions or model parameters can be varied and the effects on the biological system examined. Additionally, models can also be used to focus, direct or help design field studies by clarifying areas, parameters or processes of particular importance or that are critical to ecosystem function. While such computer simulation models are not a substitute for the traditional observational approach, they do provide a valuable way of studying the details of the links between physical forcing, nutrient availability, and zooplankton abundance. The ability to explore the impact of the influence of physical forcing on phytoplankton and zooplankton communities provides valuable insights into marine ecosystem functionality, and contributes towards our understanding of observed spatial and temporal variations in ecosystem productivity.

1.2 Ecosystem variability in the Gulf of Alaska

The Gulf of Alaska (GOA) shelf is a very productive region and amongst the world's largest fisheries with annual catches exceeding 300g/1000 m^3 (Brodeur and Ware, 1992; Ware and McFarland, 1989). Five salmon species spawn and are harvested in Alaskan waters; together they provide an important source of revenue to the state of Alaska. Recently, fisheries managers and biologists are finding that escapement estimates alone are insufficient for determining the observed recruitment in salmon fishery stocks (Kruse, 1998; Brodeur *et al.*, 2000). On a decadal time scale the total abundance of salmon in the North Pacific has undergone one complete cycle since the 1920's: high in the 1930's; low in the 1960's, and high again since the 1980's (Beamish and Bouillon, 1995). Reconstructions of salmon abundance from lake core sediments have revealed that similar cycles in salmon abundance have occurred over the past 300 years (Finney *et al.*, 2000). It is hypothesized that ocean survival of salmon is determined primarily by survival of juvenile salmon in coastal regions. Survival appears to be related to changes in circulation and hydrography that result from the climate forcing associated with the Pacific Decadal Oscillation, a recurring pattern of pan-Pacific atmosphere-ocean variability (Francis and Hare, 1994; US GLOBEC, 1996; Hare *et al.*, 1999).

The exact mechanism for the climatic control on salmon is not known although large shifts in salmon productivity are associated with changes in productivity of the juveniles' zooplankton prey, which is driven by changes in circulation and hydrography of the Gulf of Alaska (Beamish and Bouillon 1995). Throughout spring and summer juvenile pink salmon predominantly prey on small and large copepods (Cooney *et al.*, 1981, Sturdevant *et al.*, 1996, Landingham, *et al.*, 1998). By late summer more of the prey tend to come from larger crustaceans, especially hyperiid amphipods and euphausiids (Purcell and Sturdevant, 2001; Boldt and Halderson, 2004), although larvaceans at times also dominate juvenile salmon diets (Purcell and Strudevant, 2001).

Juvenile pink salmon utilize the Alaska Coastal Current (ACC) as a migratory corridor for moving from nearshore nursery areas located in productive coastal estuaries or fjords, into open shelf or deep oceanic feeding areas in the North Pacific Ocean (Williams and Weingartner, 1999). The ACC dominates the GOA shelf circumscribing the inner shelf of the GOA from British Columbia in the east to the Bering sea in the west (Stabeno *et al.*, 2004). The current is primarily driven by the combination of a large but widely distributed source of fresh water from the surrounding mountains, and downwelling favorable winds. While the flow is continuous, its properties are influenced by large variations in coastal geometry, seasonally changing winds, and coastal discharge (Williams and Weingartner, 1999). During the winter, precipitation in southern Alaska is stored as snow in snowfields and glaciers. Therefore, the current is at a maximum during summer due to the influence of melt water on freshwater runoff (Stabeno *et al.*, 2004). Mean winds in this region cause an onshore surface Ekman transport over the slope and shelf, resulting in coastal convergence and downwelling for much of the year (September-May); in the summer the winds are weakly upwelling (Royer, 1998).

One of the core hypothesis of the Northeast Pacific Global Ocean Ecosystem Dynamics (GLOBEC) research group is that "Ocean survival of salmon is primarily determined by survival of the juveniles in coastal regions, and is affected by interannual and interdecadal changes in physical forcing and by changes in food web dynamics". In an attempt to address this hypothesis, the GLOBEC Long Term Observation Program (LTOP), has made a series of multi-year observations on the physical, chemical and biological properties in the coastal Gulf of Alaska ecosystem. Observational efforts have been focused on the Seward transect line (Figure 1-1). Suites of biological process rates; phytoplankton growth rates, and zooplankton growth, grazing and reproductive rates, have also been determined for the key species in the coastal Gulf of Alaska through the work conducted as part of the GLOBEC Process program.

Figure 1-1 The cGOA, showing the location of the Seward transect line.
GAK 1 is the most inshore station on the transect line.

1.3 The GOA GLOBEC Ecosystem Model

Observations provide much needed information on the dynamics of both the phytoplankton and zooplankton, as well as on the interaction between these two trophic levels. However, the ability to accurately model the effects of physical forcing on the primary and secondary production on the Alaska continental shelf will be critical in gaining an understanding of year class strength of salmonids under different physical forcing regimes that may arise with natural climatic variation. Ecosystem modeling is thus an essential component of the GLOBEC program.

The full GLOBEC NPZ model for the coastal Gulf of Alaska (cGOA) consists of eleven compartments: iron, nitrate, ammonium, small phytoplankton, large phytoplankton, large

and small microzooplankton, small coastal copepods, large oceanic copepods, euphausiids and detritus. The biology model is embedded within a three-dimensional physical circulation model. This model is being used to explore the mechanisms by which interannual/interdecadal variability of physical fields affects zooplankton species and the feeding of juvenile salmon in the cGOA (Hinckley *et al.*, in progress). The eleven biology components were selected to enable representation of both the coastal and oceanic regimes observed in the Gulf of Alaska. The food webs in these two regions are fundamentally different, in that the oceanic ecosystem is based on small phytoplankton, whose community structure is generally dominated by autotrophic flagellates, and to a lesser extent small pennate diatoms and cyanobacteria (Boyd and Harrison, 1999; Strom *et al.*, 2001), while the coastal ecosystem is dominated by blooms of large phytoplankton including dinoflagellates and larger diatoms (Boyd and Harrison, 1999; Strom *et al.*, 2001). The two phytoplankton size classes exhibit different response to nutrients, iron and light. Both phytoplankton size classes can uptake nitrate and ammonium, although their use and response to each of these nutrient sources differs (Dugdale and Goering, 1967; Eppley and Peterson, 1979). Inclusion of nitrate, ammonium, and iron in the model therefore enabled correct representation of primary production throughout the Gulf of Alaska; additionally the proportion of new versus recycled production, and the effect of the two nitrogen sources on the food web can be examined. Due to different foraging strategies these two phytoplankton size classes are preyed upon by different sizes of zooplankton. In the GLOBEC model both small and large microzooplankton were considered. The small microzooplankton component is assumed to represent mainly heterotrophic nanoflagellates, ciliates and medium dinoflagellates, and can eat only the small phytoplankton. The large microzooplankton component is assumed to represent large heterotrophic dinoflagellates that are only able to graze on the large phytoplankton. The three mesozooplankton components were also selected to reflect their differing roles in the coastal and oceanic food webs. The coastal copepod component was assumed to represent *Pseudocalanus, spp* which reproduce in response to the spring phytoplankton bloom. Both large oceanic copepods, representative of the dominant *Neocalanus, spp.*

(Dagg, 1993), and euphausiids were included in the model due to their importance as a food source for juvenile salmon (Sturdevant *et al.*, 1996, Landingham, *et al.*, 1998; Purcell and Sturdevant, 2001; Boldt and Halderson, 2004).

During development of the cGOA GLOBEC model it became apparent that an understanding of the inherent dynamics of a biology model of this complexity has been essentially ignored. This realization provided the motivation behind the work presented in this dissertation. Previous investigations into dynamics of NPZ models have focused on models comprising only a single phytoplankton and zooplankton species. To extend on this work in a logical fashion I have investigated the dynamics of a six and a seven-component model that have a complexity between the simple three-component models previously investigated and the full eleven-component GLOBEC model. I retained the assumption of two nitrogen sources, and two phytoplankton size classes, however, for simplicity I only considered one microzooplankton component and one mesozooplankton component. Detritus was not included in the original six-component model but was subsequently added to produce the seven-component model.

1.4 Introduction to NPZ models

There have been many approaches to marine ecosystem modeling, for example conceptual compartmental models (e.g. Roff *et al.*, 1990) and chemostat models (e.g. Frost and Franzen, 1992). Dynamic models, however, have proved to be the most common and successful approach to ecosystem understanding. Dynamic Nutrient-Phytoplankton-Zooplankton (NPZ) models are composed of mathematical equations that describe the changes over time of quantities representing the systems state variables (Haefner, 1996). Since the historical works of Riley (1946) and Steele (1974) the use of Nutrient-Phytoplankton-Zooplankton (NPZ) computer simulation models as tools to understand temporal and spatial dynamics of marine ecosystem dynamics has become common practice.

Although NPZ models used in most ecosystem studies today are often quite complex, the original NPZ models were very simple, comprising only a few state variables (*i.e.*, one phytoplankton, one zooplankton, and one nutrient) and simple functional forms to describe the biological processes. The gross groupings embodied in these simple models required many assumptions and oversimplifications. For example, the 'zooplankton' group was assumed representative of all zooplankton species and age classes. This simplicity was due not only to the limited knowledge of the ecosystem at the time of their development, but also due to the limitations of the computational power available at that time (Gentleman, 2002). Additionally, the simplicity of these earlier models has roots in good modeling practice. To fully understand the dynamics of an ecosystem, or even of a single interaction within an ecosystem, the goal should be to capture the key features of the ecosystem with a model that is as simple as possible (Haeffner, 1996). Despite the many gross generalizations in these early simple models, they still proved to be useful research tools for testing understanding of marine ecosystem functionality. Both the ever-expanding knowledge of the marine ecosystem and the ever-increasing availability of computational power prompted a rapid trend towards the development of complex high-resolution three-dimensional coupled NPZ-physical models that can perform realistic simulations of a marine ecosystem. These more complex models, which attempt to reflect current understanding of the marine ecosystem, have been used in attempts to address more complex questions concerning ecosystem dynamics. Such coupled models are now frequently an integral part of research programs geared to understand ecosystem dynamics, for example JGOFS (Loukos *et al.* 1997), GLOBEC (Franks and Chen, 2001), and PICES (Aita *et al.* 2003).

The differential equations that comprise an NPZ model describe the change in concentration of each of the state variables over time. For example, phytoplankton concentration changes over time as a result of phytoplankton growth, natural mortality, grazing by zooplankton, and advective and diffusive processes. The differential equation for phytoplankton in a simple NPZ model can be written in words as:

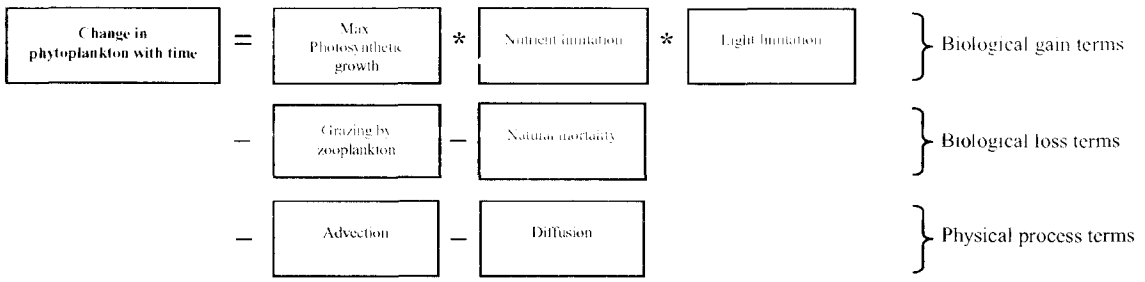

Each box on the right hand side of the equation represents a process that contributes to the rate of change of phytoplankton over time. Each of these process rates has to be described by a mathematical formulation or 'function' that describes its contribution to the change in phytoplankton over time. The biological processes are generally dependent on the concentration of one or more of the state variables, but may also be dependent on environmental factors, for example, temperature.

While the functional form of some of the biological processes is generally well understood and agreed upon, this is not the case for many of the processes that are included in an NPZ model. The limitation on phytoplankton growth due to nutrient availability is perhaps the best understood process, due to its ease of measurement within a laboratory environment. It is currently widely accepted this biological process is best represented by the hyperbolic function first introduced by Monod (1942), for example:

$$\text{Nutrient limitation} = \frac{N}{k_P + N} \qquad \text{Eq. 1.1}$$

where N is the nutrient concentration and k_P is the half saturation constant. A graphic representation of this function is shown below (Figure 1-2).

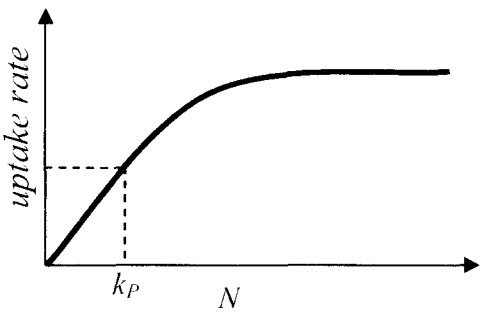

Figure 1-2 Schematic to illustrate the Monod nutrient uptake function.

Initially as the concentration of nutrient (N) increases, the phytoplankton uptake rate increases linearly. The steepness of this line depends on the phytoplankton's half-saturation constant, (k_P). At some N the increase in uptake rate slows and a maximum rate is approached. Any subsequent increase in N does not result in an increase in uptake rate - the phytoplankton has become saturated with respect to the nutrient.

Unlike nutrient limitation, there is no such agreement on the best functional form to describe the rate of zooplankton grazing on phytoplankton despite much observational effort. A 'Michaelis-Menten' type formulation was traditionally a common choice (Ivlev, 1961; Frost, 1987). This hyperbolic function is equivalent to the Monod equation for nutrient uptake, with the grazing rate (G) first increasing linearly with phytoplankton concentration (P) before becoming saturated. Several more complex grazing formulations have also been developed and are commonly used in NPZ models. The most common alternatives provide phytoplankton with a refuge from zooplankton grazing pressure when their concentrations are low. These formulations arose as a result of both observational studies and the desire of the modeler to prevent extinction of phytoplankton due to zooplankton grazing. The most notable of these modified grazing functions are the 'threshold' function (Steele, 1974; Mullin and Fuglister, 1975; Wroblewski 1977), which incorporates a critical prey concentration below which grazing ceases, and the sigmoidal function, in which the grazing rate is reduced at low prey concentrations (Evans and Parslow, 1985; Steele and Henderson, 1992; Denman and Peña, 1999). It is probable that

no one equation is correct for all scenarios and the modeler will have to ascertain which is most appropriate for the situation of interest. This could depend on the key zooplankton species or stage of interest and the nature of the available prey. Examples of alternative functions that have been used to describe zooplankton grazing on a single prey field are illustrated below (Figure 1-3).

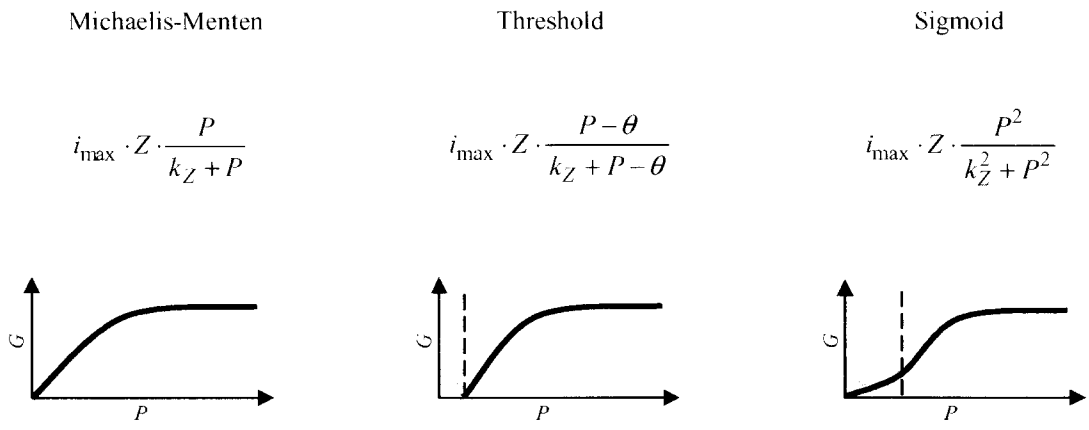

Figure 1-3 Illustration of three common single resource grazing functions.
P and Z are the concentrations of phytoplankton and zooplankton respectively, θ is the threshold concentration below which zooplankton cease to graze, k_Z is the half saturation constant for grazing and i_{max} is the maximum grazing rate. The shaded area represent regions where the grazing rate is reduced, thus providing a refuge for the prey.

By determining the appropriate functional form to describe each biological process a differential equation can be constructed to describe the time rate of change of each of the models state variables. The marine environment, however, is not a static medium in which biological processes are conducted unhindered. Rather it is a three dimensional medium that varies on a temporal scale from seconds to years and a spatial scale from nanometers to ocean basins. To understand the influence of environment factors, such as diffusion (mixing) and light, on the purely biological dynamics, it is necessary to

determine the important scales of these physical processes and to include their influence in the model.

Considering the influence of vertical diffusivity on biological interactions, the differential equation to describe the change in phytoplankton concentration with time could have the following form:

$$\frac{dP}{dt} = \underbrace{P * P_{\max}}_{\text{maximum photosynthetic rate}} * \underbrace{e^{-z \cdot k_{ext}}}_{\text{light limitation}} * \underbrace{\frac{N}{k_P + N}}_{\text{nutrient limitation}} - \underbrace{i_{\max}}_{\text{maximum grazing rate}} * Z * \underbrace{\frac{P}{k_Z + P}}_{\text{resource limitation}} - \underbrace{m * P}_{\text{natural mortality}} + \underbrace{Kv \cdot \frac{\partial P}{\partial z}}_{\text{diffusion}} \qquad \text{Eq. 1.2}$$

Where P, N and Z are the concentrations of phytoplankton, nutrient and zooplankton, respectively, P_{max} is the maximum photosynthetic rate, k_{ext} is the light extinction coefficient, k_P is the half saturation uptake constant for nutrient, k_Z is the half saturation constant for grazing, i_{max} is the maximum grazing rate, m is phytoplankton natural mortality rate, Kv is the vertical diffusion coefficient and z is depth.

1.5 The importance of NPZ models non-linear dynamics

Without a good understanding of how these models behave when subjected to steady forcing, the time dependent behavior of coupled biological-physical ecosystem models could mistakenly be attributed to variable physical forcing rather than as an inherent property of the model's biology. Over the past few decades, the application of non-linear systems dynamics has provided a basis for understanding the behavior of NPZ models (Oaten and Murdoch, 1975; Edwards and Brindley, 1996; Edwards *et al.*, 2000). Incorporating moderate levels of vertical diffusion into a purely biological NPZ model has been shown to impart model stability (Edwards *et al.*, 2000), an important consideration for the realm of coupled bio-physical models. The formulations for both zooplankton grazing (Franks *et al.*, 1986) and predation on zooplankton (Steele and

Henderson, 1992; Edwards and Yool, 2000) have also been found to influence the fundamental dynamics of simple NPZ model, determining whether a model's time-dependent behavior will approach steady state or exhibit oscillatory behavior, such as periodic limit cycles. To date, the influence of most terms in the NPZ model on model dynamics has not been rigorously considered. In the case of nutrient uptake and natural mortality, there is general agreement on the most appropriate functional form for these processes, and thus less variability in the modeling literature. Conversely, there is much contention on which formulations most appropriately simulate zooplankton grazing and undefined predation (the model closure term). Despite a rapid trend towards more realistic NPZ models, in which zooplankton grazers are presented with multiple nutritional resources, investigations into the fundamental dynamics of these newer models have been limited (Armstrong, 1994; Ryabchenko *et al.,* 1997; Yool, 1998). Without a good understanding of the fundamental behavior of the more complex NPZ models now commonly employed in ecosystem studies, time-dependent behavior simulated with coupled biological-physical models, as in periodic or chaotic solutions, could be interpreted as due to variable physical forcing rather than as an inherent property of an ecosystem model. It is important that we extend our understanding of NPZ system dynamics to these more complex models and develop an appreciation of how our choice of formulations for simulating biological processes can affect their behavior.

The two most common forms of solutions observed in ecosystem models are steady equilibrium or periodic limit cycle. A steady equilibrium is one in which, following initial transient behavior, the time rate of change of each model component goes to zero (Figure 1-4 a and b), whereas a solution entering a periodic limit cycle oscillates indefinitely between a maximum and minimum value (Figure 1-4 c and d). Other more complex model solutions in which model trajectories have multiple periods or are chaotic have also been observed (Hastings and Powell, 1991, Popova *et al.,* 1997). Oscillations in nature appear rare, although this is possibly as a result of insufficient sampling on a temporal scale, Oscillations have, however, been observed at Ocean Weather Station I in the north-east Atlantic Ocean (Williams, 1988) and in several freshwater plankton

populations (McCauley and Murdoch, 1987). Predator-prey interactions and high nutrient supply, due to strong upwelling and high pycnocline nutrient concentrations, have been shown to play an important role in oscillatory behavior (Popova *et al.*, 1997), as has the thickness of the mixed layer and the annual entrainment velocity (Ryabchenko *et al.*, 1997).

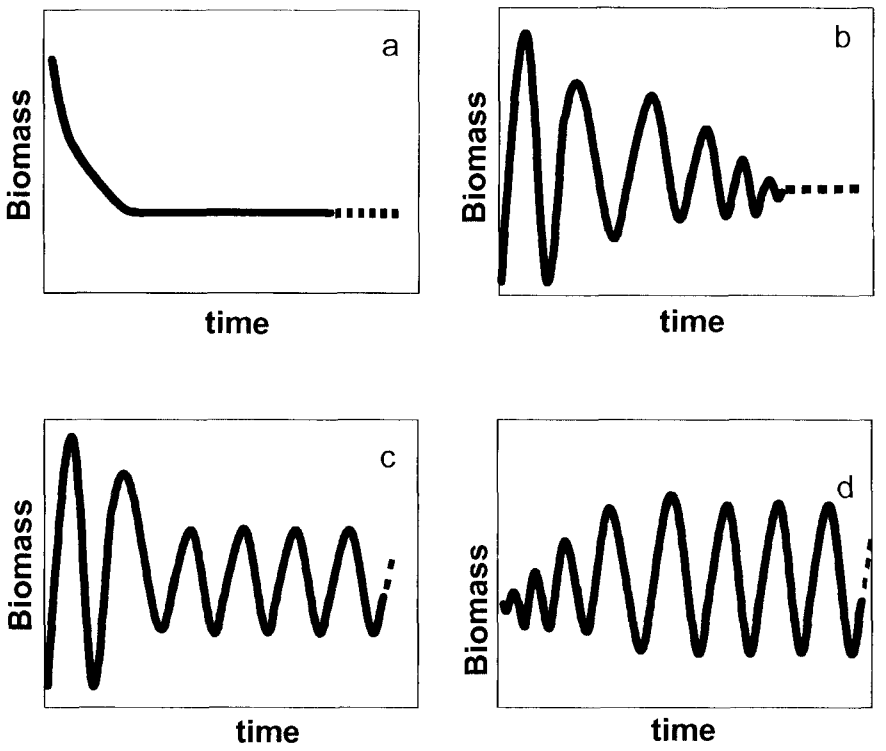

Figure 1-4 Examples of time series solutions that approach an equilibrium.
Two alternative approaches to steady equilibrium (a) monotonic and (b) spiral sink, and two alternative approaches to periodic limit cycle solutions (c and d).

Previous investigations into model stability have not addressed survivorship of model components, *i.e.*, whether model components have non-zero concentrations at equilibrium. This is unlikely to be an issue since those studies consider only a single phytoplankton and zooplankton component. However, like the majority of models used in

modern ecosystem modeling studies, the model under investigation in this dissertation comprises multiple grazers and multiple prey types. It will thus be critical to know if certain model structures or parameterizations promote or inhibit the simultaneous survival of model components.

1.6 Objectives

The objective of this dissertation was to explore the dynamical behavior of intermediately complex NPZ models while simultaneously investigating the survivorship of model components. The models were parameterized for the coastal Gulf of Alaska and contained multiple grazers which could feed on multiple prey types.

Specifically, the hypotheses tested were:

1. The dynamics and survivorship of an NPZ model in which zooplankton grazers feed on multiple prey types is uninfluenced by the functional form for grazing.

2. The dynamics and survivorship of a NPZ model in which zooplankton grazers feed on multiple prey types is uninfluenced by the form of the predation function (the model closure term).

3. The dynamics and survivorship of an NPZ model in which zooplankton grazers feed on multiple prey types is not influenced by varying the stationary vertical diffusivity profile.

4. The addition of a detritus component to an NPZ model does not influence model dynamics, survivorship, or the model's ability to simulate a sub-surface chlorophyll maximum.

1.6 References

Aita, M. N., Yamanaka, Y. and Kishi, M. J. (2003) Effects of ontogenetic vertical migration of zooplankton on annual primary production - using NEMURO embedded in a general circulation model. *Fish. Oceanogr.*, **12**, 284-290.

Armstrong, R. A. (1994) Grazing limitation and nutrient limitation in marine ecosystems: Steady state solutions of an ecosystem model with multiple food chains. *Limnol. Oceanogr.*, **39**, 597-608.

Beamish R. J. and Bouillon D. R., (1993) Pacific Salmon Production Trends in Relation to Climate. *Can. J. Fish. Aquat. Sci.*, **50**, 1002-1016.

Beamish, R. J., and Bouillon, D. R. (1995) Marine fish production trends off the Pacific coast of Canada and the United States. *In* R. J. Beamish (editor), *Climate change and northern fish populations, Can. Spec. Publ. Fish. Aquat. Sci.*, **121**, 585-591.

Boldt, J. L. and Halderson, L. J. (2003) Seasonal and geographic variation in juvenile pink salmon diets in the northern Gulf of Alaska, *Transactions of the American Fisheries Society*, **132,** 1035-1052.

Boyd, P. and Harrison, P. J. (1999) *Deep-Sea Res. (II Top. Stud. Oceanogr.)*, **46 (11-12)**, 2405-2432.

Brodeur R. D., Boehlert, G. W., Casillas, E., Eldridge, M. B., Helle, J. H., Peterson, W. T., Heard, W. R., Lindley, S. T. and Schiewe, M. H. (2000) A Coordinated Research Plan for Estuarine and Ocean Research on Pacific Salmon. *Fisheries*, **25**, 7-16.

Brodeur, R. D. and Ware, D. M. (1992) Long-term variability in zooplankton biomass in the subarctic Pacific Ocean. *Fish. Oceanogr.*, **1(1)**, 32-39.

Cooney R.T., Urquhart, D., and Bernard, D. (1981) The Behavior, Feeding Biology, and Growth of Hatchery Released Pink and Chum Salmon Fry in Prince William Sound, Alaska. *Alaska Sea Grant Rep.*

Cousins, S. H. (1985) The trophic continuum in marine ecosystems: Structure and equations for a predictive model., Ecosystem Theory for Biological Oceanography. *Can. J. Fish. Aquat. Sci.*, **213**, 76–93.

Dagg, M. (1993) Grazing by the copepod community does not control phytoplankton production in the Subarctic Pacific Ocean, *Prog. Oceanogr.* **32**, 163-183.

Denman, K. L. and Peña, M. A. (1999) A coupled 1-D biological/ physical model of the northeast subarctic Pacific Ocean with iron limitation. *Deep-Sea Res. II*, **46**, 2877-2908.

Dugdale, R. C. and Goering, J. J. (1967) Uptake of new and regenerated forms of nitrogen in primary productivity, *Limnol. Oceanogr.* **12**, 196-20.

Edwards, A. M. and Brindley, J. (1996) Oscillatory behaviour in a three-component plankton population model. *Dynamics and Stability of Systems*, **11**, 347-370.

Edwards, A. M. and Yool, A. (2000) The role of higher predation in plankton population models. *J. Plankton Res.*, **22**, 1085-1112.

Edwards, C. A., Powell, T. A. and Batchelder, H. P. (2000) The stability of an NPZ model subject to realistic levels of vertical mixing. *J. Mar. Res.*, **58**, 37-60.

Eppley, R. W. and Peterson, B. J. (1979) Particulate organic matter flux and planktonic new production in the deep ocean, *Nature*, **282,** 677-680.

Evans, G. T. and Parslow, J. S. (1985) A model of annual plankton cycles. *Biol Oceanogr.*, **3**, 327-347.

Finney, B., Gregory-Eaves, I., Sweetman, J., Douglas, M. S. V., Smol, J. P. (2000) Impacts of climatic change and fishing on Pacific salmon abundance over the past 300 years, *Science,* **290**, 795-799.

Francis, R. C. and Hare, S. R. (1994) Decadal-scale regime shifts in the large marine ecosystems of the North-east Pacific: A case for historical science, *Fish. Oceanogr.*, **3**, 279-291.

Franks, P. J. S. and Chen, C. (2001) A 3-D prognostic numerical model study of the Georges bank ecosystem. Part II: biological-physical model. *Deep-Sea Res.*, **48**, 457-482.

Franks, P. J. S., Wroblewski, J. S. and Flierl, G. R. (1986) Behavior of a simple plankton model with food-level acclimation by herbivores. *Mar. Biol.*, **91**, 121-129.

Frost, B. W. (1987) Grazing control of phytoplankton stock in the open subarctic Pacific Ocean: A model assessing the role of mesozooplankton, particularly the large calanoid copepods Neocalanus spp. *Mar. Ecol. Prog. Ser.*, **39**, 49-68.

Frost, B. W. and Franzen, N. C. (1992) Grazing and iron limitation in the control of phytoplankton stock and nutrient concentration: a chemostat analogue of the Pacific equatorial upwelling zone. *Mar. Ecol. Prog. Ser.*, **83,** 291-303.

Gentleman, W. C. (2002) A chronology of plankton dynamics *in silico*: How computer models have been used to study marine ecosystems. *Hydrobiologia*, **480**, 69-85.

Haefner, J. W. (1996) *Modeling Biological Systems: Principles and Applications.* Chapman and Hall, New York.

Hare, S. R., Mantua, N. J., and Francis, R. C. (1999) Inverse Production Regimes: Alaska and West Coast Pacific Salmon, *Fisheries,* **24**, 6-15.

Hastings, A. and Powell, T. (1991) Chaos in a three-species food chain. *Ecology,* **72**, 896-903.

Hinckley, S., Dobbins, L. and Hermann, A. (in progress) A biophysical NPZ model for the Gulf of Alaska: model development and sensitivity analysis.

Ivlev, V. S. (1961) Experimental ecology of the feeding of fishes. Yale Univ. Press, New Haven, Connecticut, USA.

Kruse G.H. (1998) Salmon Run Failures in 1997-1998: A Link to Anomalous Ocean Conditions ? *Alaska Fisheries research Bulletin,* **5(1)**, *55-63.*

Landingham, J. H., Sturdevant, M. V., Brodeur, R. D. (1998) Feeding habits of juvenile Pacific salmon in marine waters of southeastern Alaska and northern British Columbia. *Fish. Bull.*, **96,** 285-302.

Loukos, H., Frost, B. W., Harrison, D. E. and Murray, J. W. (1997) An ecosystem model with iron limitation of primary production in the equatorial Pacific at 140^{O}W. *Deep-Sea Res. II,* **44**, 2221-2249.

May, R. M. (1972) Limit cycles in predator-prey communities. *Science,* **177**, 900-902.

May, R. M. (1973). Stability and Complexity in Model Ecosystems. *Princeton University Press.*

McCauley, E. and Murdoch, W.W. (1987) Cyclic and stable populations: Plankton as paradigm. *Am. Nat.*, **129**, 97-121.

Monod, J. (1942) Recherches sur la croissance des cultures bact'eriennes [studies on the growth of bacterial cultures]. *Actualities Scientifique et Industrielles,* **911**, 1-215.

Mullin, M. M. and Fuglister, F. J. (1975) Ingestion by planktonic grazers as a function of concentration of food. *Limnol. Oceanogr.,* **20**, 259-262.

Oaten, A. and Murdoch, W. W. (1975) Switching, functional response, and stability in predator-prey systems. *The American Naturalist,* **109**, 299-318.

Purcell, E. J. and Sturdevant, M.V. (2001) Prey selection and dietary overlap among zooplanktivorous jellyfish and juvenile fishes in Prince William Sound, Alaska. *Mar. Ecol. Prog. Ser.,* **210**, 67-83.

Riley, G. A. (1946) Factors controlling phytoplankton populations on Georges Bank. *J. Mar. Res.,* **6**, 54-72.

Roff, J. C., Hopcroft, R. R., Clarke, C., Chisholm, L. A., Lynn, D. H. and Gilron, G. L. (1990) Structure and energy flow in a tropical neritic planktonic community off Kingston Jamaica. *Trophic relationships in the marine environment. (Proc. 24th Europ. Mar. Biol. Symp.)* Barnes,M. and R.N. Gibson (eds), Aberdeen University Press. pp. 266-280.

Royer, T. (1998) Coastal Processes in the Northern North Pacific. *The Sea*, **11**, Wiley, New York, 395-414

Ryabchenko, V. A., Fasham, M. J. R., Kagan, B. A. and Popova, E. E. (1997) What causes short-term oscillations in ecosystem models of the ocean mixed layer? *J. Mar. Res.,* **13**, 33-50.

Stabeno, P. J., Bond, N. A., Hermann, A. J., Kachel, N. B., Mordy, C. W., and Overland, J. E. (2004) Meteorology and oceanography of the Northern Gulf of Alaska, *Cont. Shelf Res.,* **24**, 859-897.

Steele, J. H. (1974). The structure of marine ecosystems, Harvard University Press. Cambridge.

Steele, J. H. and Henderson, E. W. (1992) The role of predation in plankton models. *J. Plankton Res.*, **14**, 157-172.

Sturdevant, M. V., Wertheimer, A. C., Lum, J. L. (1996) Diets of juvenile pink and chum salmon in oiled and non-oiled nearshore habitats in Prince William Sound, 1989 and 1990. *Am. Fish.* Soc. Symp., **18**, 578-592,

U.S. GLOBEC (1996) Northeast Pacific Implementation Plan. *U.S. Global Ocean Ecosystems Dynamics.* Report Number 17.

Ware, D. M. and McFarlane, G. A. (1989) Fisheries production domains in the Northeast Pacific Ocean. *Can. Spec. Publ. Fish. Aquat. Sci.*, **108**, 359-379.

Williams W. J. and Weingartner T. J. (1999) The Response of Bouyancy driven Coastal Currents to Downwelling-Favorable Wind Stress. *EOS, Transactions, American Geophysical Union, 2000 Ocean Science Meeting*, **80**, No 49.

Williams, R. (1988) Spatial heterogeneity and niche differentiation in oceanic zooplankton. In Boxshall, G.A. and Schimke, H.K. (eds), Biology of Copepods. *Hydrobiologia*, **167/168**, 151-159.

Wroblewski, J. S. (1977) A model of phytoplankton plume formation during variable Oregon upwelling. *J. Mar. Res.*, **35**, 357-394.

Yool, A. (1998) The dynamics of open-ocean plankton ecosystem models, Ph.D. diss, University of Warwick.

Chapter 2 . Development of an NPZ model with multiple prey types

This chapter provides an overview of the development of the NPZ model whose dynamical behavior was investigated in this dissertation. The development of the biological equations that comprise the NPZ model, and the approach taken to incorporate physical forcing into the model are described. An outline of the approach taken to model analysis and the development of the computer coding is also presented. Finally, as a test of the model code, the functionality of the six-component NPZ model developed here is compared to the functionality of the three-component NPZ model that provided the basis for model development.

2.1 Development of the biological equations

Many of the NPZ models employed in ecosystem studies today are rather complex and often three-dimensional. Generally, the time dependent behavior of several state variables is represented by a system of non-linear differential equations which comprise mathematical formulations that describe each biological process of interest. These modern models often have multiple phytoplankton and zooplankton size classes. Analyses of the non-linear dynamics of these complex NPZ models are lacking. Such understanding should be stepwise, building in a logical fashion on those used in previous studies of this nature. Without studies on precursor models it is difficult to disentangle the influence of each of the additional components (and their associated functions) on the observed model dynamics. Following good modeling practice, the NPZ model that was developed was kept as simple as possible while allowing for testing of the first two hypothesis, *i.e.,* that the non linear dynamics and survivorship of NPZ models, in which zooplankton can graze on multiple prey types, are uninfluenced by the choice of grazing and mortality functions.

Over the past few decades, the application of non-linear systems dynamics has provided a basis for understanding the behavior of NPZ models (May, 1972; Oaten and Murdoch, 1975; Edwards and Brindley, 1996; Edwards *et al.*, 2000). The NPZ models investigated in these past studies generally comprised only a single phytoplankton and zooplankton size class, and with few exceptions, biological interactions were assumed to take place within a homogeneous mixed layer. Edwards *et al.* (2000) has investigated the non-linear dynamics of a three component NPZ model subject to vertical diffusion. This is one of the only studies of NPZ non-linear dynamics that is spatially explicit. This three-component NPZ model was originally developed by Franks *et al.* (1986), and considered the exchange of nitrogen between phytoplankton (P), zooplankton (Z), and nutrient (N) pools. The mathematical functions that described each biological process in the model were all of the simplest forms commonly used. This three-component model was used as a starting point for development of a one-dimensional (vertical) model that had multiple phytoplankton and zooplankton size classes. The system of three differential equations that comprise the Franks (1986) model is as follows:

$$\frac{dP}{dt} = \frac{V_m \cdot N \cdot P}{k_P + N} e^{-k_{ext} z} - R_m \cdot Z(1 - e^{-\Lambda P}) - mP \qquad \text{Eq. 2.1}$$

$$\frac{dZ}{dt} = (1-\gamma) \cdot R_m \cdot Z \cdot (1 - e^{-\Lambda P}) - gZ \qquad \text{Eq. 2.2}$$

$$\frac{dN}{dt} = -\frac{V_m \cdot N \cdot P}{k_P + N} e^{-k_{ext} z} - \gamma \cdot R_m \cdot Z \cdot (1 - e^{-\Lambda P}) + mP + gZ \qquad \text{Eq. 2.3}$$

Where P, N and Z are the concentrations of phytoplankton, nutrient and zooplankton, V_m is the maximum uptake rate of nutrients by the phytoplankton, k_P is the half-saturation uptake constant, k_{ext} is the light extinction coefficient, R_m is the maximum grazing rate, Λ

is the Ivlev saturation constant for grazing, m and g are the mortality of phytoplankton and zooplankton respectively, γ is the unassimilated grazing fraction, and z is depth.

As was often the case historically, the 'Z' component in the Franks model was originally parameterized to represent mesozooplankton. Edwards *et al.* (2000) re-parameterized the model such that the zooplankton component represented microzooplankton, although the parameterization chosen was questionable due to the unrealistically high grazing rate used. Even so, despite examining model dynamics with this alternative parameterization for the zooplankton, only one zooplankton component was considered at a time.

Our understanding of the planktonic food web has grown substantially since the development of the original three-component NPZ models. In order to adequately replicate observations, models must incorporate the expanded complexity of marine food web dynamics. For example, in the coastal Gulf of Alaska both small and large phytoplankton are known to exist and constitute an important part of the marine food web (Strom *et al.*, 2001). Representation of the two size classes is important due to their potentially different reactions to the marine environment and their different positions in the marine food web. The phytoplankton are now known to utilize both new (nitrate) and regenerated (ammonium) forms of inorganic nitrogen (Dugdale and Goering, 1967; Eppley and Peterson, 1979). However, the response of the two phytoplankton size classes to the two nutrient pools can be very different. For example, small phytoplankton have a general preference for ammonium (Legendre and Rassoulzadegan, 1995) and are generally more proficient at utilizing low levels of nutrients than the large phytoplankton (Evans and Parslow, 1985). In cold water environments, such as the coastal Gulf of Alaska, large phytoplankton preferentially take up nitrate even when ammonium is present (Lomas and Glibert, 1999). Despite the historical bias towards mesozooplankton, microzooplankton, with their ability to feed on these small phytoplankton size fractions, are now thought to be the primary grazers (Dagg, 1993) controlling the chlorophyll standing stock in many regions (Landry and Hassett, 1982; Gifford, 1988; Strom and

Welschmeyer, 1991; Dagg, 1995). In reality, both microzooplankton and mesozooplankton are able to graze on a mixed prey field comprising a range of size classes. Thus, to fully capture food web interactions it is important to have multiple size classes of both phytoplankton and zooplankton present simultaneously in the model, and zooplankton grazers capable of feeding on more than one size class.

To reflect this improved understanding of the marine ecosystem an intermediately complex six-component NPZ model was developed by adding a second phytoplankton and zooplankton component and splitting the nutrient component into nitrate and ammonium. The three original equations were thus replaced with six equations that represent the time rate of change of the nitrate (N_1) and ammonium (N_2), small phytoplankton (P_1), large phytoplankton (P_2), microzooplankton (Z_1), and mesozooplankton (Z_2). Within the model the 'small' and 'large' phytoplankton groups are considered to respectively represent the aggregate of phytoplankton <8μm in size, and the aggregate of phytoplankton >8 μm in size. This size division was chosen to mimic that selected by Strom *et al.* (2001), who have conducted the majority of the work on phytoplankton processes in the coastal Gulf of Alaska. The 'microzooplankton' component was considered to represent mainly heterotrophic dinoflagellates and ciliates, while the 'mesozooplankton' component was considered to represent mainly coastal copepods common in the coastal Gulf of Alaska. Following Franks *et al.* (1986), detritus was not initially explicitly represented as a state variable. It could be argued that this approach could increase model excitability (and, thus, the likelihood of oscillatory limit cycle behavior), however, previous studies of model dynamics (Edwards and Brindley, 1996; Edwards and Brindley, 1999; Edwards *et al.*, 2000; Edwards and Bees, 2001; Edwards and Yool, 2000), upon which this investigation builds, did not include detritus or specifically model the regeneration loop. Additionally, a study on an NPZ model which did include a detritus component (Edwards, 2001) found that did not significantly influence the model's dynamical behavior is zooplankton were unable to graze upon it. In

later studies (Chapter 5), detritus was added as a seventh model component permitting specific representation of the regeneration loop.

In the absence of advection and diffusion, the time dependent dynamics of the six model components were described by the following set of six non-linear differential equations:

$$F_{N_1} = \frac{\partial N_1}{\partial t} = -U_{11} - U_{12} + R \qquad \text{Eq. 2.4}$$

$$F_{N_2} = \frac{\partial N_2}{\partial t} = -U_{21} - U_{22} + M_1 + M_2 + M_Z + H + (1-\gamma_1)\cdot(G_{11} + G_{12}) + (1-\gamma_2)\cdot(G_{21} + G_{22} + G_{ZZ}) - R \qquad \text{Eq. 2.5}$$

$$F_{P_1} = \frac{\partial P_1}{\partial t} = U_{11} + U_{21} - M_1 - G_{11} - G_{21} \qquad \text{Eq. 2.6}$$

$$F_{P_2} = \frac{\partial P_2}{\partial t} = U_{12} + U_{22} - M_2 - G_{12} - G_{22} \qquad \text{Eq. 2.7}$$

$$F_{Z_1} = \frac{\partial Z_1}{\partial t} = \gamma_1 \cdot (G_{11} + G_{12}) - G_{ZZ} - M_Z \qquad \text{Eq. 2.8}$$

$$F_{Z_1} = \frac{\partial Z_2}{\partial t} = \gamma_2 \cdot (G_{21} + G_{22} + G_{ZZ}) - H \qquad \text{Eq. 2.9}$$

Where γ_1 and γ_2 respectively represent microzooplankton and mesozooplankton grazing efficiency, and *U, M, G, H,* and *R* respectively represent transformation rates of nitrogen due to nutrient uptake, mortality, grazing, predation, and the nitrification of ammonium to nitrate. These biological process rates, which are defined in subsequent equations, describe the interaction between the six model components (Figure 2-1).

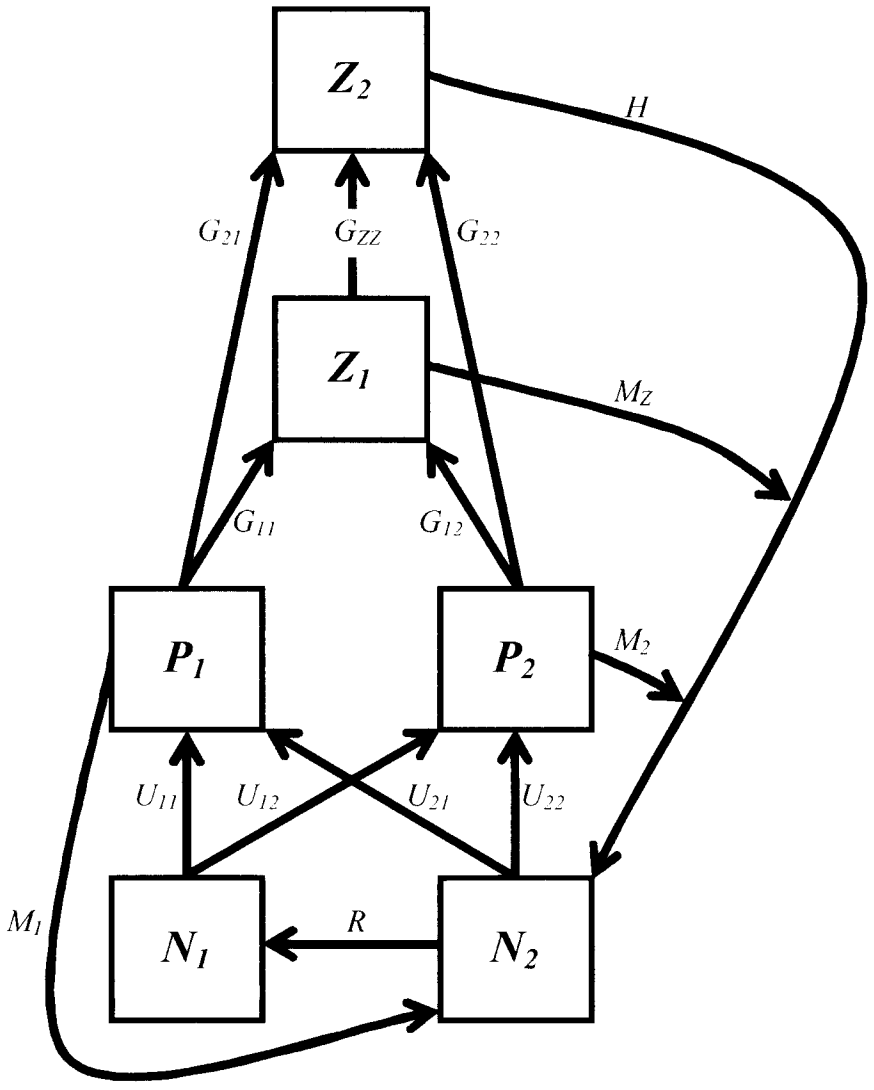

Figure 2-1 Interactions in the six-component NPZ model -repeated from Chapter 4. Nitrate (N_1), ammonium (N_2), small phytoplankton (P_1), large phytoplankton (P_2), microzooplankton (Z_1), and mesozooplankton (Z_2). The arrows indicate the direction of material flow.

Phytoplankton nutrient uptake (U), mortality of phytoplankton (M_X) and microzooplankton (M_Z) and the nitrification of ammonium to nitrate (R) were described as follows:

$$U_{1X} = P_X \cdot P_{\max X} \cdot e^{-z \cdot k_{ext}} \cdot \frac{N_1 \cdot e^{-\psi \cdot N_2}}{k_{1X} + N_1} \quad P_X \text{ uptake of } N_1 \qquad \text{Eq. 2.10}$$

$$U_{2X} = P_X \cdot P_{\max X} \cdot e^{-z \cdot k_{ext}} \cdot \frac{N_2}{k_{2X} + N_2} \quad P_X \text{ uptake of } N_2 \qquad \text{Eq. 2.11}$$

$$R = r \cdot N_2 \quad N_2 \xrightarrow{nitrification} N_1 \qquad \text{Eq. 2.12}$$

$$M_X = m_X \cdot P_X \quad \text{natural mortality of } P_X \qquad \text{Eq. 2.13}$$

$$M_Z = m_Z \cdot Z_1 \quad \text{natural mortality of } Z_1 \qquad \text{Eq. 2.14}$$

where X can be 1 or 2 to represent small and large phytoplankton respectively.

A full discussion of the formulations used to represent each of the biological processes, including definition of the subscripts, is included in Chapter 4 and so not repeated here; parameter values are given in Table 4-2. Here only the similarities and differences between the original three-component model (Franks *et al.*, 1986) and the more complex six-component model are discussed. The Monod formulation for nutrient uptake used in the original three-component model (Franks *et al.*, 1986) was applied in the six-component model to simulate the uptake of ammonium (Eq. 2.11). However, to simulate phytoplankton uptake of nitrate an additional 'ammonium inhibition function' was added to the equation (Eq. 2.10), because in the presence of ammonium, the uptake of nitrate is reduced (Wroblewski, 1977). An additional term (R) was required to describe the nitrification of ammonium to nitrate, which was assumed to occur at a simple linear rate (Eq. 2.12). As discussed above, the two phytoplankton size fractions were considered able to respond differently to the two nutrient sources. This was reflected in their half saturation nutrient uptake constants and discussed in detail in Chapter 4. Following

Franks *et al.* (1986), the natural mortality of phytoplankton, and microzooplankton, were described with simple linear functions (Eq. 2.13 and Eq. 2.14).

The mesozooplankton component was assumed to experience losses (H) due to natural mortality and to predation by undefined predators. This was effectively the model closure term and throughout this dissertation is referred to as 'predation'. In the original three-component model a single simple linear function, *i.e.,* Eq. 2.15, was used to represent these losses. In the modeling literature the predation term is also commonly represented by a quadratic formulation (Eq. 2.16).

$$H = h \cdot Z_2 \quad = LINEAR \qquad \text{Eq. 2.15}$$

$$H = h \cdot Z_2^2 \quad = QUADRATIC \qquad \text{Eq. 2.16}$$

The generic form of the mortality function can be expressed as:

$$H = h \cdot Z_2^q \qquad \text{Eq. 2.17}$$

The linear form is representative of a predator that exhibits a constant response to zooplankton prey numbers, this could be thought of as a simple filter feeding strategy. The quadratic formulation assumes that the zooplankton predators have a biomass proportional to their prey; it is thought to represent a predator that exhibits an ambush feeding strategy, attracted to large concentrations of zooplankton and less inclined to feed at low concentrations. Other formulations, *i.e.,* hyperbolic (Frost, 1987; Fasham, 1993) and sigmoidal (Malchow, 1994), are also occasionally used. The wide variety of formulations used to represent predation reflects that predation is a notoriously difficult biological process to measure, and much uncertainty exists with regards to the most appropriate formulation. The differences between the linear and quadratic predation functions are illustrated below (Figure 2-2).

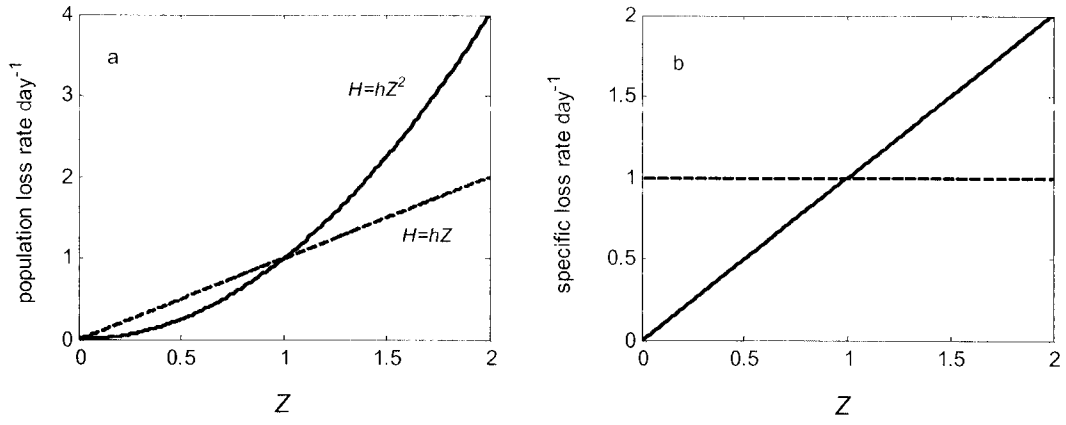

Figure 2-2 Graphic representation of the linear and quadratic predation functions. The population mortality rate (a) and the specific mortality rate (b) with the linear (dashed line) and the quadratic (solid line) formulations.

It has been proposed (Edwards and Bees, 2001) that, because "the predator's effective reaction distance varies with the turbulent energy dissipation rate, the proportion of predators adopting either the 'linear' or 'quadratic' strategy will vary in a continuous fashion depending on the environmental and physical conditions". Therefore, while in Chapter 3 only a 'linear' or 'quadratic' formulation is implemented in the model, subsequently (Chapters 4 and 5) the dynamics of the model are explored with a non-integer predation exponent that varied from linear to quadratic ($1 \leq q \leq 2$).

In the original three-component model, grazing (G) was described using the Ivlev grazing formulation (Eq. 2.18) which has a saturating response (initially linear before leveling off at a specified maximum rate), very similar to the well known Michalis–Menten function (Figure 1-3).

$$i_{\max} Z_2 (1 - e^{-\lambda P_2}) \qquad \text{Eq. 2.18}$$

In the six-component NPZ model, a zooplankton grazer was able to feed on multiple prey types. It was therefore necessary to uses a multiple resource grazing function to simulate zooplankton grazing. Several alternative functional forms have arisen which extend the single resource grazing functions to simulate zooplankton grazing on a mixed prey field (Ambler, 1986; Fasham *et al.*, 1990; Ryabchenko *et al.*, 1997; Chifflet *et al.*, 2001; Denman and Peña, 2002). In Chapters 3 and 4 five alternative grazing functions (functions I-V) are implemented in the six-component model and the impact that each had on the resulting model dynamics is investigated. In Chapter 5, the focus is on the two most different functions (functions I and V). A detailed explanation of each of the grazing functions is presented in Chapter 4, therefore not repeated here.

2.2 Adding physical forcing to the model

The time and depth dependent population dynamics due purely to the biological interactions were described by Eq. 2-4 – Eq.2-9, written in shorthand as:

$$\frac{\partial C_i(t,z)}{\partial t} = F_{C_i}\left(C_1(t,z),\ C_2(t,z),\ C_3(t,z),\ C_4(t,z),\ C_5(t,z),\ C_6(t,z)\right) \qquad \text{Eq. 2.19}$$

where C_i represents the model state variables, *i.e.*,

$$C_1 = P_1,\ C_2 = P_2,\ C_3 = Z_1,\ C_4 = Z_2,\ C_5 = N_1,\ C_6 = N_2\ ,$$

and F_{C_i} represents the biological source/sink term.

In the ocean the biological dynamics, which are dependent upon space (x,y,z) as well as time (t), are also subjected to both advection and diffusion. Therefore, the total derivative, *i.e.*, the rate of change of C_i within the moving fluid, with respect to both time and space, is given by:

$$\underbrace{\frac{dC_i(t,z)}{dt}}_{\text{TOTAL DERIVATIVE (LAGRANGIAN)}} = \underbrace{\frac{\partial C_i}{\partial t}}_{\text{LOCAL TERM (EULARIAN)}} + \underbrace{\left(u\frac{\partial C_i}{\partial x} + v\frac{\partial C_i}{\partial y} + w\frac{\partial C_i}{\partial z}\right)}_{\text{ADVECTIVE TERMS}} = \underbrace{F_{C_i}}_{\text{BIOLOGICAL DYNAMICS}} + \underbrace{Kh\left(\frac{\partial^2 C_i}{\partial x^2} + \frac{\partial^2 C}{\partial y^2}\right) + Kv\frac{\partial^2 C_i}{\partial z^2}}_{\text{DIFFUSIVE TERMS}} \qquad \text{Eq. 2.20}$$

The local term is the local rate of change with time and the advective terms are the advective rates of change due to motion, where u,v and w are the velocity component in the x,y and z directions, and Kh and Kv are the kinematic eddy diffusivities in the horizontal (x,y) and the vertical (z) directions.

The primary concern throughout this dissertation was to adequately represent the effects of vertical mixing on the dynamics of the model, therefore, diffusivity in the horizontal directions (K_h=0) were neglected and the velocity field was set to zero ($\bar{U} = 0$). This is the same approach as that taken by Edwards *et al.* (2000). The system of equations reduce to:

$$\frac{dC_i(t,z)}{\partial t} = \frac{\partial C_i}{\partial t} = F_i + \frac{\partial}{\partial z}\left(Kv \cdot \frac{\partial C_i}{\partial z}\right) \qquad \text{Eq. 2.21}$$

Thus, only a single additional term is required in each of the biological equations:

$$\frac{\partial}{\partial z}\left(Kv\frac{\partial C_i}{\partial z}\right) \qquad \text{Eq. 2.22}$$

In the investigation by Edwards *et al.* (2000) Kv was held constant throughout the water column, which was 100 meters in depth. The magnitude of diffusion (Kv=10^{-5}-10^{-2} m^2 s^{-1}) was found to have an impact on model dynamics (Edwards *et al.* 2000). In reality, perhaps with the exception of strong winter storms, the upper 100 meters of the water column will not have a constant vertical diffusion profile. In the coastal Gulf of Alaska, as in most marine environments, the upper portion of the water column is mixed by the action of the wind and is homogeneous with respect to physical properties such as density, temperature, salinity and nutrient concentration. Within this 'mixed layer' diffusivity (Kv) would be relatively high, below the wind mixed layer, diffusivity would be quite small. To reflect this difference in diffusivity within and below the mixed layer in the model a mixed layer diffusivity (Kv_m) of 10^{-3} m^2 s^{-1} and a background diffusivity (Kv_b) of 10^{-5} m^2 s^{-1} were implemented. To avoid having an unrealistic, abrupt change in diffusion a *tanh* function (Eq. 2.23) was implemented to define the diffusivity profile (Figure 2-3).

$$Kv(z) = Kv_b - \left(\frac{Kv_b - Kv_m}{\tanh(\Phi_{100}) - \tanh(\Phi_1)}\right) - \left(\frac{Kv_b - Kv_m}{\tanh(\Phi_{100}) - \tanh(\Phi_1)}\right) \cdot \tanh\left(\frac{-\Phi(z)}{\omega}\right) \qquad \text{Eq. 2.23}$$

Here, z is depth, and Φ and ω are shape parameters that define the position and thickness of the pycnocline, respectively. Further explanation of this function and parameter values and definitions are given in Chapter 4.

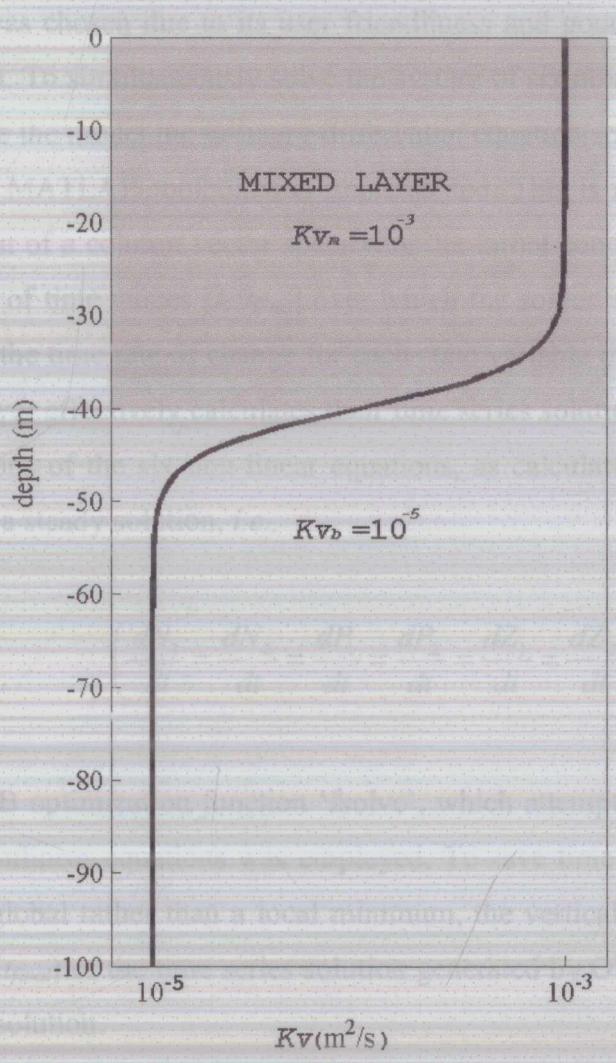

Figure 2-3. Illustration of the depth-explicit diffusivity profile.
Note the smooth transition between the mixed layer diffusivity (Kv_m) and the background diffusivity (Kv_b) below.

2.3 Model Analysis

The computer code to describe this six-component model was written in MATLAB. MATLAB was chosen due to its user friendliness and good graphical representation of model output. To simultaneously solve the system of six non-linear differential equations that comprise the model the ordinary differential equation solver 'ODE45' provided with the standard MATLAB toolbox was implemented. This is an initial value problem that requires input of a column vector specifying the initial conditions at the initial time (t_0), and a vector of time values [t_0:t_{final}] over which the solver was required to integrate. By determining the time rate of change for each state variable over the time frame specified, the ODE solver effectively calculates their time series solutions. To determine if the time series solutions of the six non-linear equations, as calculated by the ODE solver, were approaching a steady solution, *i.e.,*

$$\left(\frac{dN_1}{dt} = \frac{dN_2}{dt} = \frac{dP_1}{dt} = \frac{dP_2}{dt} = \frac{dZ_1}{dt} = \frac{dZ_2}{dt} = 0 \right) \qquad \text{Eq. 2.24}$$

the MATLAB optimization function 'fsolve', which attempts to find the root (zero) of a system of nonlinear equations was employed. To save time and increase the chances of finding the global rather than a local minimum, the vertical concentration profiles from the last day (t_{final}) of the time series solution generated by ODE45 were used as an initial guess to the solution.

Following Edwards *et al.* (2000), model solutions were deemed to have a steady equilibrium if the time derivative term (fval) calculated by fsolve were smaller than 10^{-4} μM N day^{-1}. Any solution which could not be classified as steady was manually examined, at the 25 meter depth which was well within the mixed layer, to determine if behavior was periodic (limit cycles). If a model's classification was unclear, the ODE solver was used to extend the time series' solution; then the vertical concentration

profiles for each of the state variables at the new t_{final} were used as input to fsolve. Initially, stability of equilibrium solutions was determined by calculating the eigenvalues of the solution, although it was later determined that this method was not very helpful with regards to furthering our understanding on the models non-linear dynamics (Chapter 3). Further details on the method of analysis can be found in subsequent chapters. A flow diagram of pseudocode for this method can be seen below (Figure 2-4).

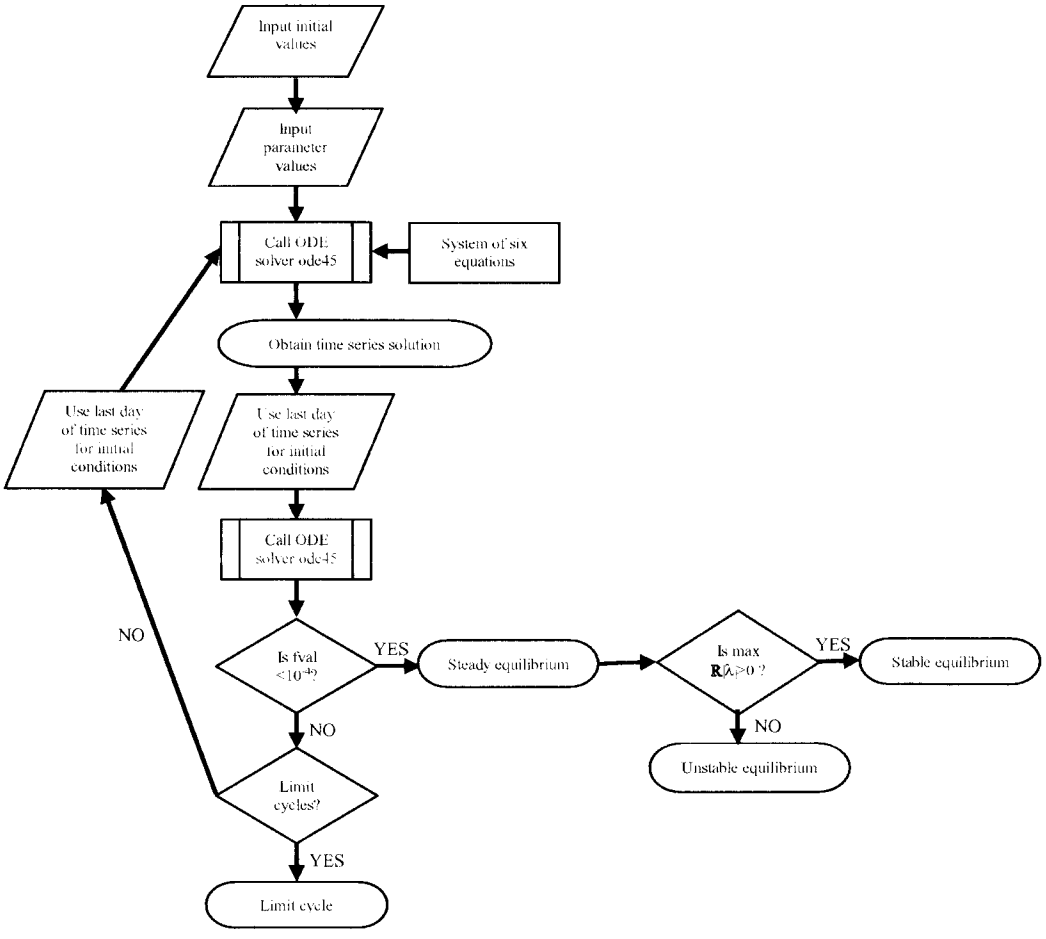

Figure 2-4 Flow diagram of approach followed to and seek equilibrium solutions. fval is the time derivative term, and $\mathbb{R}|\lambda|$ is the real portion of the eigenvalue.

2.4 Testing the NPZ model code

Before using the computer code written to describe the behavior of the six-component model to perform analysis of the model dynamics, it was necessary to ensure that it was functioning correctly. The code's performance was tested by attempting to reproduce published results for the three component model (Edwards *et al.*, 2000). An adequate match of model output was required to be confident of the model's functionality prior to using the code to test dynamics of the more complex model.

Method

The six-component model had to be parameterized (Table 2-1) with values equivalent to those used in the three-component model parameterized for mesozooplankton and with non-zero diffusion (Edwards *et al.*, 2000). The parameter values corresponding to small phytoplankton, microzooplankton and ammonium were set so that these model components experienced no change in concentration with time. Initial conditions equivalent to those used in the three component model were implemented (P_1=0, P_2=1, Z_1=0, Z_2=1, N_2=0, N_2=8), microzooplankton, small phytoplankton and ammonium had initial concentrations of zero. All inputs to the ammonium component (due to mortality etc.) were assumed to be instantaneously remineralized to nitrate (r=100).

For the model comparison grazing function I was implemented in the model. This grazing function has roots in the single resource 'Michaelis-Menten' grazing equation described in Chapter 1. This grazing function was selected due to its similarity in form to the Ivlev function used in the original three-component model, *i.e.*, an initial linear increase before approaching saturation. Grazing function I (Table 4-3) extends the prey field available to a zooplankton grazer to contain the sum of multiple prey items. However, assuming that small phytoplankton and microzooplankton have zero concentrations and that

mesozooplankton are able to eat all of the available large phytoplankton (e_{22}=1), the functional form for mesozooplankton grazing on large phytoplankton simplifies to:

$$i_{max} Z_2 \cdot \frac{P_2}{k_{32} + P_2} \qquad \text{Eq. 2.25}$$

Using this notation, the Ivlev grazing function used by Edwards *et al.* (2000) is expressed as:

$$i_{max} Z_2 (1 - e^{-\Lambda P_2}) \qquad \text{Eq. 2.26}$$

where i_{max}=0.5, Λ=0.2, Z_2=1, and P_2=0-1

Intuitively, it would appear that equivalent parameter values implemented in grazing function I would provide the best match to the Ivlev function, *i.e.*, i_{max}=0.5. However, the Ivlev function did not reach saturation, even at the maximum scaled prey concentration of 1, and a higher i_{max} was required in function I to get a best fit to the Ivlev curve (Figure 2-5). The Ivlev constant Λ=0.2 determines the steepness of the initial increase in grazing rate with prey concentration. The half-saturation constant (k_{32}) in grazing function I performs the same role. A half-saturation constant of 6 μM N combined with an i_{max} of 0.7 day^{-1} was required in order for grazing function I to have a satisfactory fit to the Ivlev curve (Figure 2-5d).

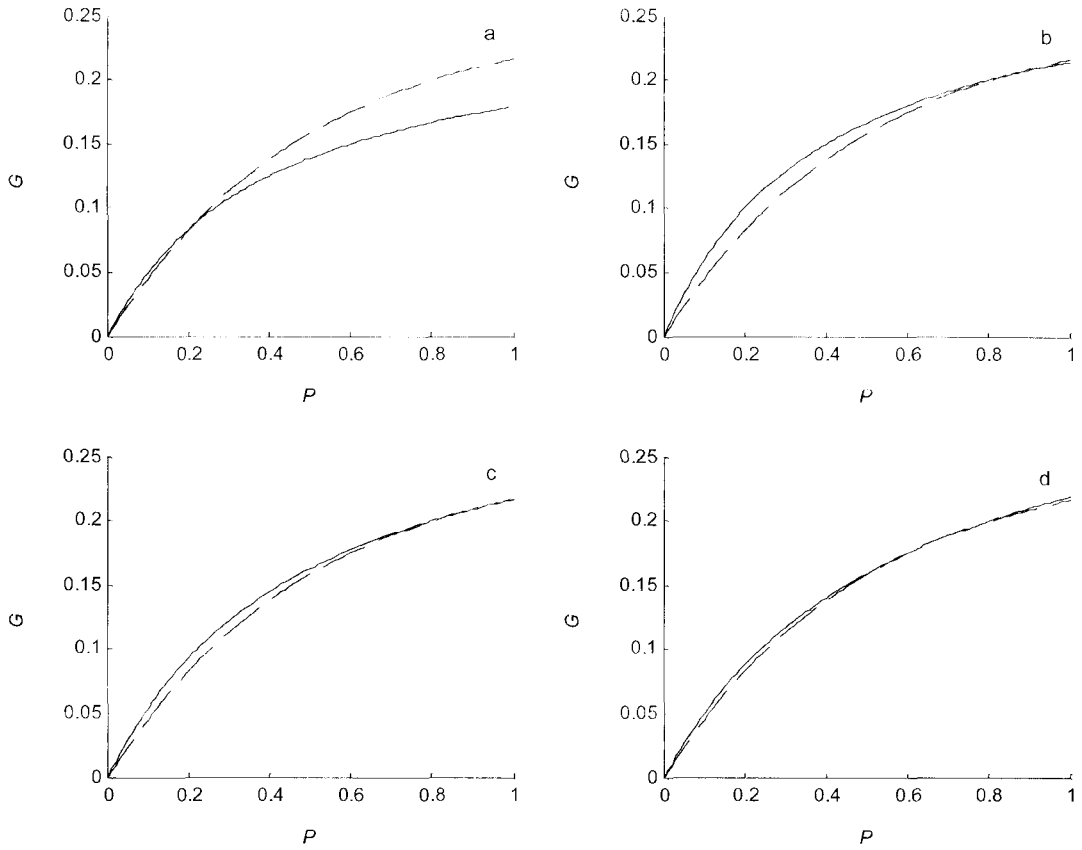

Figure 2-5 Matching grazing function I to the Ivlev formulation for grazing.
The Ivlev curve (dashed line) with i_{max}=0.5, Λ=0.2 and the grazing curves produced by grazing function I when (a) k_{32}=4μM N, i_{max} =0.5day^{-1}, (b) k_{32}=4 μM N, i_{max}=0.6day^{-1}, (c) k_{32}=5 μM N, i_{max}=0.65day^{-1}, and (d) k_{32}=6 μM N, i_{max} =0.7day^{-1}. G and P are the non-dimensional grazing rate and phytoplankton concentration respectively.

Table 2-1 Parameter values used to test functionality of model code

Parameter	Symbol	Values		Units
		$X=1$	$X=2$	
maximum growth rate of P_X	$P_{\max X}$	0	2	day^{-1}
P_X half-saturation constant for N_1	k_{1X}	0	.1	µM N
P_X half-saturation constant for N_2	k_{2X}	0	0	µM N
inhibition parameter for U_1 by N_2	ψ	0		$[\mu M\ N]^{-1}$
nitrification rate	r	100		day^{-1}
light extinction coefficient	k_{ext}	0.06		m^{-1}
		$Y=1$	$Y=2$	
maximum ingestion rate	$i_{\max Y}$	0	0.7	day^{-1}
assimilation efficiency of Z_Y	γ_Y	0	0.7	-
half-saturation coefficient for Z_Y grazing	k_{3Y}	0	3	µM N

Z_Y capture efficiency for P_X — e_{YX}

X \ Y	1	2	
1	0	0	-
2	0	1	-

Z_2 capture efficiency for Z_1	e_{ZZ}	0		
		$X=1$	$X=2$	
natural mortality rate of P_X	m_X	0	0.2	day^{-1}
natural mortality rate of Z_1	m_Z	0		day^{-1}
specific predation rate	h	0.2		$(gCm^{-3})^{1-q}$ day^{-1}
predation exponent	q	1		-

Results and Discussion

Using $Kv_m=Kv_b=10^{-5}$ m^2 s^{-1}, the six-component model code produced a time series solution (Figure 2-6) which bore a striking resemblance to the time series solution for the three-component model (Figure 2-7) presented by Edwards *et al.* (2000). There are slight differences between the two figures which are due to the slight difference in grazing function and because the solutions of the three-component model are presented for 5.5 m, 25.5 m etc., whereas solutions for the six-component model were calculated for every whole meter (5 m, 25 m etc.). In spite of these slight differences, which are due to differences in coding, it can be concluded that the six-component model was functioning satisfactorily.

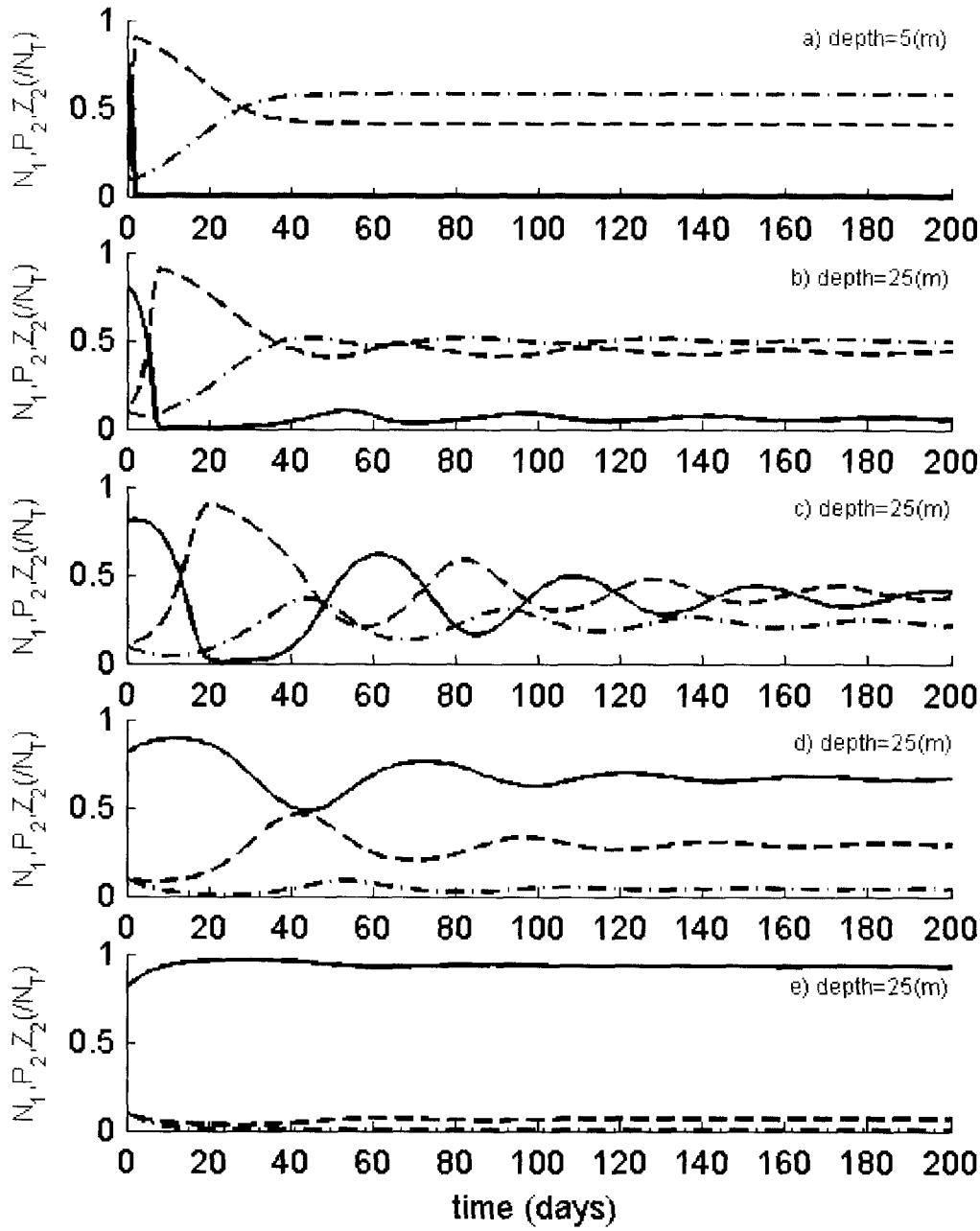

Figure 2-6 Time-series solution for six-component NPZ model.
Model was parameterized following Table 2-1 and $K\nu_m=K\nu_b= 10^{-5}$ m^2 s^{-1}. The lines represent phytoplankton (dashed), zooplankton (dash-dot) and nutrient (solid).

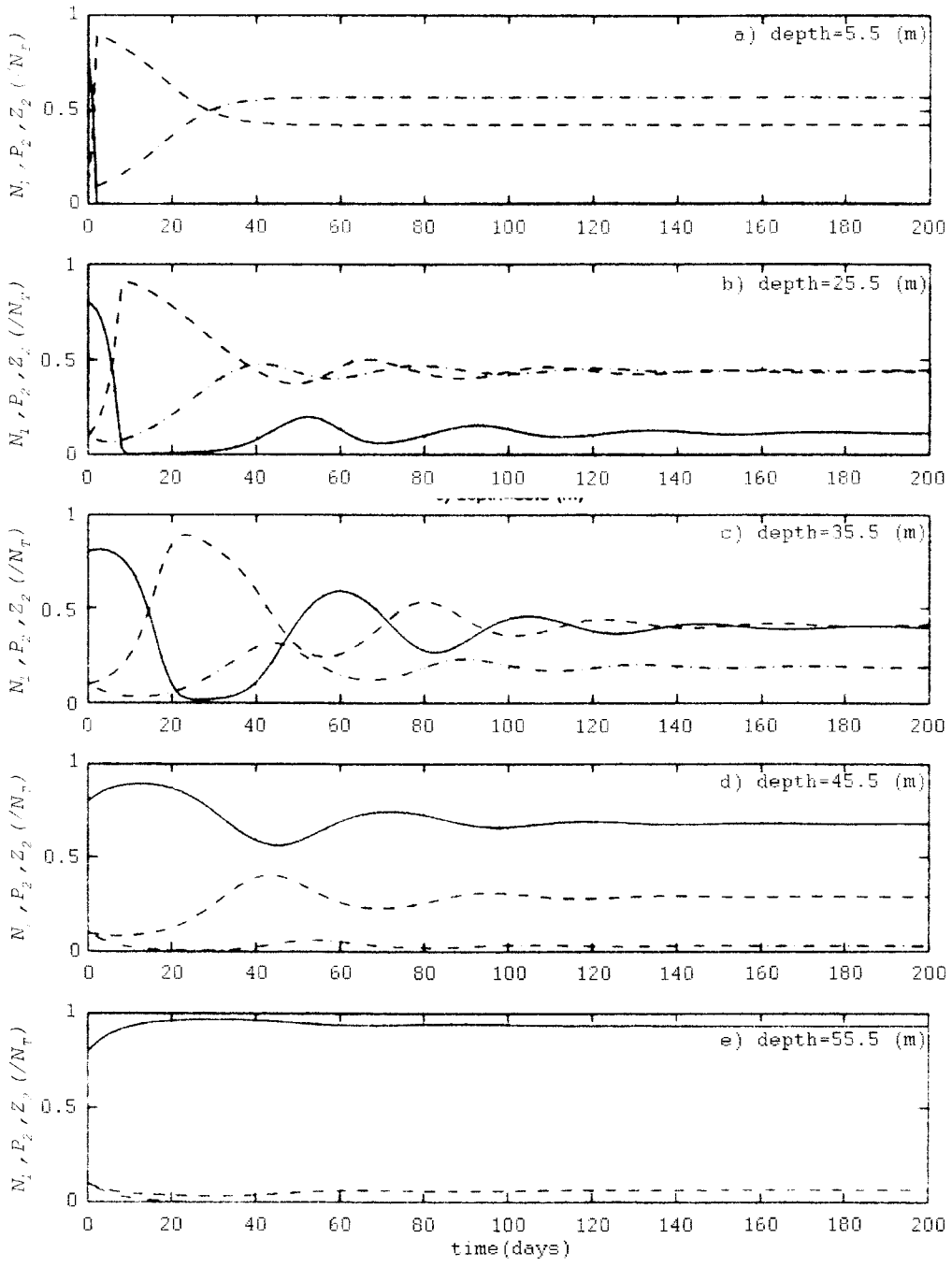

Figure 2-7 Time-series solution for three-component NPZ model.
Reproduced from Figure 6 in Edwards *et al.* (2000). Model was parameterized for macrozooplankton and $Kv=10^{-5}$ m^2 s^{-1}. The lines represent phytoplankton (dashed), zooplankton (dash-dot) and nutrient (solid).

2.5 References

Ambler, J. W. (1986) Formulation of an ingestion function for a population of Paracalanus feeding on mixtures of phytoplankton. *J. Plankton Res.*, **8**, 957-972.

Chifflet, M., Andersen, V., Prieur, L. and Dekeyser, I. (2001) One-dimensional model of short-term dynamics of the pelagic ecosystem in the NW Mediterranean Sea: effects of wind events. *J. Mar. Syst.*, **30**, 89-114.

Dagg, M. (1993) Grazing by the copepod community does not control phytoplankton production in the Subarctic Pacific Ocean. *Prog. Oceanogr.*, **32**, 163-183.

Dagg, M. (1995) Ingestion of phytoplankton by the micro- and mesozooplankton communities in a productive subtropical estuary. *J. Plankton Res.*, **17**, 845-857.

Denman, K. L. and Peña, M. A. (2002) The response of two coupled one-dimensional mixed layer/planktonic ecosystem models to climate change in the NE subarctic Pacific Ocean. *Deep-Sea Res. II*, **49**, 5739-5757.

Dugdale, R. C. and Goering, J. J. (1967) Uptake of new and regenerated forms of nitrogen in primary productivity. *Limnol. Oceanogr.*, **12**, 196-206.

Edwards, A. M. (2001) Adding detritus to a Nutrient Phytoplankton Zooplankton model: A dynamical-systems approach. *J. Plankton Res.*, **23**, 389-413.

Edwards, A. M. and Bees, M. A. (2001) Generic dynamics of a simple plankton population model with a non-integer exponent of closure. *Chaos, Solutions and Fractals*, **12**, 289-300.

Edwards, A. M. and Brindley, J. (1996) Oscillatory behaviour in a three-component plankton population model. *Dynamics and Stability of Systems*, **11**, 347-370.

Edwards, A. M. and Brindley, J. (1999) Zooplankton mortality and the dynamical behaviour of plankton population models. *Bulletin of Mathematical Biology*, **61**, 303-339.

Edwards, A. M. and Yool, A. (2000) The role of higher predation in plankton population models. *J. Plankton Res.*, **22**, 1085-1112.

Edwards, C. A., Powell, T. A. and Batchelder, H. P. (2000) The stability of an NPZ model subject to realistic levels of vertical mixing. *J. Mar. Res.*, **58**, 37-60.

Eppley, R. W. and Peterson, B. J. (1979) Particulate organic matter flux and planktonic new production in the deep ocean. *Nature,* **282**, 677-680.

Evans, G. T. and Parslow, J. S. (1985) A model of annual plankton cycles. *Biol. Oceanogr.*, **3**, 327-347.

Fasham, M. J. R., Ducklow, H. W. and McKelvie, S. M. (1990) A nitrogen-based model of plankton dynamics in the oceanic mixed layer. *J. Mar. Res.*, **48**, 591-639.

Fasham, M. J. R., Sarmiento, J. L., Slater, R. D., Ducklow, H. W. and Williams, R. (1993) Ecosystem behaviour at Bermuda Station "S" and ocean weather station "India": a general circulation model and observational analysis. *Global Biogeochem. Cycles,* **7**, 379-415.

Franks, P. J. S., Wroblewski, J. S. and Flierl, G. R. (1986) Behavior of a simple plankton model with food-level acclimation by herbivores. *Mar. Biol.,* **91**, 121-129.

Frost, B. W. (1972) Effects of size and concentration of food particles on the feeding behavior of the marine planktonic copepod *Calanus pacificus. Limnol. Oceanogr.,* **17,** 805-815.

Gifford D. J. and Dagg M. J. (1988) Feeding of the estuarine copepod Acartia tonsa Dana: Carnivory vs. herbivory in natural microplankton assemblages. *Bull. Mar. Sci.*, **43**, 458-468.

Landry, M. R. and Hassett, R. P. (1982) Estimating the grazing impact of marine micro-zooplankton. *Mar. Biol.*, **67**, 283-288.

Legendre, L. and Rassoulzadegan, F. (1995) Plankton and nutrient dynamics in marine waters. *Ophelia,* **41**, 153-172.

Lomas, M. W. and Glibert, P. M. (1999) Temperature regulation of nitrate uptake: A novel hypothesis about nitrate uptake reduction in cool-water diatoms. *Limnol. Oceanogr.*, **44**, 556-572.

Malchow, H. (1994) Non equilibrium structures in plankton dynamics. *Ecol. Model.*, **75/76**, 123-134.

May, R. M. (1972) Limit cycles in predator-prey communities. *Science,* **177**, 900-902.

Oaten, A. and Murdoch, W. W. (1975) Switching, functional response, and stability in predator-prey systems. *The American Naturalist,* **109**, 299-318.

Ryabchenko, V. A., Fasham, M. J. R., Kagan, B. A. and Popova, E. E. (1997) What causes short-term oscillations in ecosystem models of the ocean mixed layer? *J. Mar. Res.,* **13**, 33-50.

Strom, S. L. and Welschmeyer, N. A. (1991) Pigment-specific rates of phytoplankton growth and microzoopalnkton grazing in the open subarctic Pacific Ocean. *Limnol. Oceanogr.,* **36**, 50-63.

Strom, S. L., Brainard, M. A., Holmes, J. L. and Olson, M. B. (2001) Phytoplankton blooms are strongly impacted by microzooplankton grazing in coastal North Pacific waters. *Mar. Biol.,* **138**, 355-368.

Wroblewski, J. S. (1977) A model of phytoplankton plume formation during variable Oregon upwelling. *J. Mar. Res.,* **35**, 357-394.

Chapter 3 . Linear stability analysis of an NPZ model with multiple prey types

3.1 Introduction

The objective of this experiment was to test hypothesis 1 and 2 by determining if the *stability* of an NPZ model, in which zooplankton could graze on multiple prey types, was impacted by the formulation chosen for the grazing or predation functions.

Hypothesis 1: The dynamics of an NPZ model in which multiple grazers could feed on multiple prey types is uninfluenced by the functional form for grazing.

Hypothesis 2: The dynamics of a NPZ model in which multiple grazers could feed on multiple prey types is uninfluenced by the form of the predation function (the model closure term).

Following the approach used by Edwards *et al.* (2000), the linear stability of the depth dependent six-component model (Eq. 2.4-2.9) was sought. This approach requires that Eq. 2.4-2.9 have a steady state equilibrium solutions where $\frac{dC_i}{dt} = 0$. In the absence of diffusive coupling, Eq. 2.1-2.3 remain depth dependent because of the light levels given by $e^{-k_{ext}z}$. However, Franks *et al.* (1986) were able to analytically calculate the steady solution for the three component model (Eq. 2.1-2.3) and Edwards *et al.* (2000) were able to examine the stability at the steady state for each depth in his model. No analytical solution could be found when there was diffusive coupling ($Kv \neq 0$), however, the model was robust enough to numerically solve the diffusive steady-state on which the stability analysis was performed.

In the work presented in this chapter, a similar approach is outlined Eq. 2.4-2.9. Attempts at using the approach failed in many cases, because the model did not have a steady solution from which a linear stability analysis could be performed. Nonetheless, this work is included here because it provides a sequence between Edwards' stability analysis on 2.1-2.3, and the work on dynamic behavior of equations that is presented subsequently (Chapters 4 and 5).

The stability characteristics of the NPZ model, in the local neighborhood of the equilibrium where the time dependency terms on the LHS of Eq. 2.4-2.9 are zero, can be evaluated using the eigenvalue approach. By calculating the eigenvalues, a parameter that characterizes the overall dynamics of the system (Haefner 1996), it is possible to determine the stability of a set of linear equations. For example, for a linear model that comprises a set of n state variables:

$$C_i = [C_1, C_2 ... C_n] \qquad \text{Eq. 3.1}$$

whose time tendency term $\frac{d}{dt}$ is given as a linear function of the n state variables:

$$\frac{dC_i}{dt} = AC_i \qquad \text{Eq. 3.2}$$

where A may be a function of time, but not of C_i.

Then the equilibrium steady state

$$\frac{dC_i}{dt} = 0 \qquad \text{Eq. 3.3}$$

is given by

$$AC_i^* = 0 \qquad \text{Eq. 3.4}$$

where C_i^* represents the equilibrium solution.

We then ask if this solution tends to return to the equilibrium state if perturbed.

If the perturbed population is expressed as:

$$C_i = C_i^* + C_i' \qquad \text{Eq. 3.5}$$

Eq.3.2 can be written as

$$\frac{d(C_i^* + C_i')}{dt} = A(C_i^* + C_i') \qquad \text{Eq. 3.6}$$

and since

$$\frac{dC_i^*}{dt} = AC_i^* = 0 \qquad \text{Eq. 3.7}$$

we get

$$\frac{dC_i'}{dt} = AC_i' \qquad \text{Eq. 3.8}$$

which is similar to Eq. 3-2 except that C_i is replaced with the perturbed solution C_i'

To solve the set of differential equations in Eq. 3-8 it is assumed that the answer is the form:

$$C_i' = B_i e^{\lambda t} \qquad \text{Eq. 3.9}$$

where the behavior of the system is dependent on the sign of its eigenvalues λ.

In general, λ may be complex, *i.e.*,

$$\lambda = \alpha + i\beta \qquad \text{Eq. 3.10}$$

where β is the imaginary part of λ and describes the oscillatory part of C_i' and α is the real portion of λ and describes the secular trend. The classification of the model as stable or unstable depends on the sign of the real part of the eigenvalues (λ_n). The dynamics of the system are dominated by the largest real eigenvalue (α). If all eigenvalues of a system have negative real parts ($\mathbb{R}|\lambda| \leq 0$) the steady-state (equilibrium) solution is classified as stable. This means that following a perturbation the system will return to the steady state solution. Conversely, the existence of one or more eigenvalues with a positive real part ($\mathbb{R}|\lambda| > 0$) indicates that small perturbations from the steady state solution will grow without bound away from the equilibrium (Edwards *et al.*, 2000), and

for that reason the model is classified as unstable. If the imaginary portion of the eigenvalue is zero ($\beta=0$) then the approach towards or away from equilibrium is monotonic (Figure 3-1a). However, if the eigenvalues comprise an imaginary portion ($\beta\neq0$) then the dynamical behavior will be oscillatory in nature (Figure 3-1b and c). If $\alpha<0$ and $\beta\neq0$ following the perturbation oscillations are damped and the solution is stable (Figure 3-1b). If $\alpha=0$ and $\beta\neq0$ following the perturbation the solution enters undamped oscillations, this is known as neutral stability (Figure 3-1c). If $\alpha>0$ and $\beta\neq0$ following the perturbation oscillations will grow exponentially and the solution is said to be unstable. Due to the closed system nature of the model under investigation here this type of behavior was not possible.

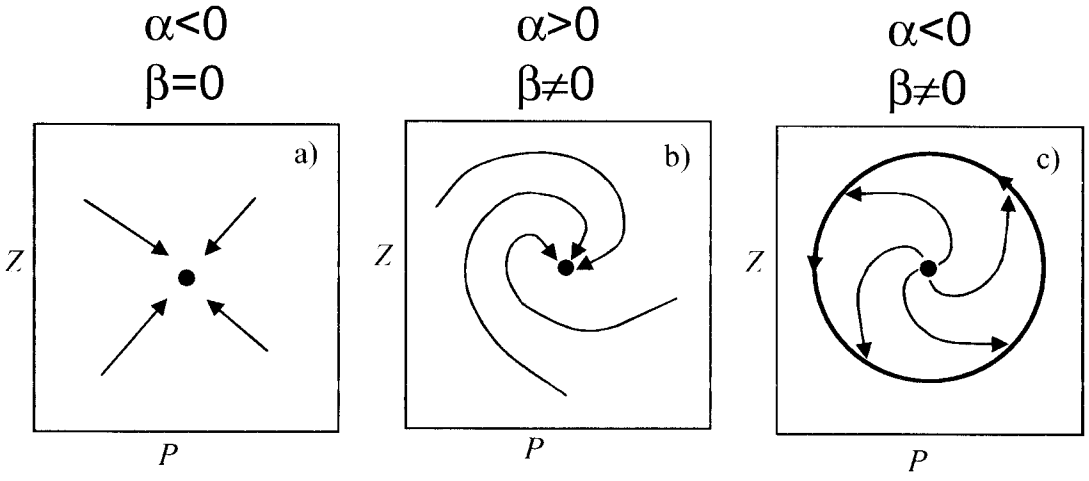

Figure 3-1 Some possible responses of a two component model to perturbations. (a) $\alpha<0$, $\beta=0$, (b) $\alpha>0$ and $\beta\neq0$ and (c) $\alpha<0$ and $\beta\neq0$. *P* and *Z* represent phytoplankton and zooplankton concentration respectively.

Due to the complexities of natural systems it is quite unusual to find linear equations in biology. Indeed, the six differential equations that comprise the NPZ models are non-linear. It is therefore necessary to convert this system of equations to linear equations in order to perform stability analysis. It is important to realize that the linearization of the equations effectively transforms the problem from studying dynamics of the state

variables (model components) to studying the dynamics of deviations from the equilibrium. Therefore, the eigenvalue can only reveal information regarding the system behavior in the neighborhood of an equilibrium if it exists.

3.2 Method

To determine the stability of the six-component NPZ model a standard procedure for model linearization and eigenvalue determination, used previously on simple NPZ models, was followed (May, 1973; Edwards *et al.*, 2000). The biological system under investigation here comprised six non-linear differential equations at each of the 100 depth levels in the model, therefore, a total of six-hundred eigenvalues were examined for each model simulation.

3.2.1 Calculating the equilibrium solution

Simple NPZ models with zero diffusivity can be solved analytically to find the steady state (equilibrium) solution. Edwards (2000) followed this approach in his analysis of the three component model. He then used the zero diffusivity solution as a starting 'guess' at the solution with non-zero diffusivity, which he sought using a MATLAB function, fsolve, which is a multi-dimensional equation solver. Due to the spatially explicit diffusive coupling of each layer within the model, and the additional complexity of the model equations, it was not practical (or possible) to solve the system of equations analytically, in order to find the steady state solution. Instead, the steady solution of the non-linear system of six equations, if it exists, was approached iteratively by time-stepping the model for 100 days using the MATLAB ode45 solver, an automatic step-size Runge-Kutta-Fehlberg integration method. The resulting solutions were employed as the initial starting guess for the MATLAB numerical solver fsolve.

3.2.2 *Determination of Eigenvalues*

Having found a steady state equilibrium solution, the eigenvalues of the system can be calculated and thus the local stability of the model determined. To proceed, the equilibrium population $C_i^*(z) = \left[P_1^*(z), P_2^*(z), Z_1^*(z), Z_2^*(z), N_1^*(z), N_2^*(z)\right]$ was perturbed by a small amount $C_i'(z,t)$, which is assumed to be initially very small. The perturbed population is then expressed as:

$$\underbrace{C_i(z,t)}_{\substack{\text{Concentration}\\ \text{at any depth}\\ \text{and time}}} = \underbrace{C_i^*(z)}_{\substack{\text{Depth specific}\\ \text{equilibrium}\\ \text{concentration}}} + \underbrace{C_i'(z,t)}_{\substack{\text{Perturbation about}\\ \text{equilibrium concentration}\\ \text{-depends on depth and time}}} \qquad \text{Eq. 3.11}$$

Therefore, the system of equations that include the affects of biological interactions and the action of diffusion on the six model components can be expressed as:

$$\frac{\partial(C^* + C')}{\partial t} = F_{C_i}(C_i^* + C_i') + \frac{\partial}{\partial z}\left(Kv\frac{\partial(C_i^* + C_i')}{\partial z}\right) \qquad \text{Eq. 3.12}$$

Where F_{C_i} is the net source/sink term for each state variable C_i

I had to approximate the function with a first-order Taylor series because F_{Ci} is non-linear, thus the Taylor series expansion of F_{C_i} around about the equilibrium point C_i^* is given by:

$$F_{Ci}(C_i^* + C_i') = \underbrace{F^*{}_{C_i} + \sum_j C_j' \frac{\partial F^*{}_{C_i}}{\partial C_j}}_{\text{LINEAR}} + \underbrace{\textit{HIGHER OREDR TERMS}}_{\text{NON-LINEAR}} \qquad \text{Eq. 3.13}$$

Where

$$F^*_{C_i} = F_{C_i}(C_i^*) \qquad \text{Eq. 3.14}$$

Since the perturbations are assumed to be small the terms of second order or higher were ignored. Eq. 3.12 can then be written as:

$$\frac{\partial(C_i^* + C_i')}{\partial t} = F^*_{C_i} + \sum_j C_j' \frac{\partial F^*_{C_i}}{\partial C_j'} + \frac{\partial}{\partial z}\left(Kv \frac{\partial(C_i^* + C_i')}{\partial z} \right) \qquad \text{Eq. 3.15}$$

I then let $\frac{\partial F^*_{C_i}}{\partial C_j'} = a_{ij}$ where the elements a_{ij} constitute the $i \times j$ Jacobian, or community matrix, which is a measure of the per capita population growth rate in the immediate neighborhood of the equilibrium point. Each element a_{ij} describes the effect of species j upon species i near the equilibrium, and depends both on the details of the original equations and on the values of the equilibrium populations.

At equilibrium, by definition, $C_i' = 0$ and $\frac{\partial C_i^*}{\partial t} = 0$

therefore

$$F^*_{C_i} + \frac{\partial}{\partial z}\left(Kv \frac{\partial C_i^*}{\partial z} \right) = 0 \qquad \text{Eq. 3.16}$$

and

$$\frac{\partial C_i'}{\partial t} = a_{ij} \cdot \sum_j C_j' + \frac{\partial}{\partial z}\left(Kv \frac{\partial C_i'}{\partial z} \right) \qquad \text{Eq. 3.17}$$

Introducing $C_i' = \hat{C}_i e^{\lambda t}$ Eq. 3.17 becomes:

$$\frac{\partial \hat{C}_i e^{\lambda t}}{\partial t} = a_{ij} \cdot \sum_j \hat{C}_j e^{\lambda t} + \frac{\partial}{\partial z}\left(Kv \frac{\partial \hat{C}_i e^{\lambda t}}{\partial z} \right) \qquad \text{Eq. 3.18}$$

Which simplifies to

$$\lambda \hat{C}_i = a_{ij} \cdot \sum_j \hat{C}_j + \frac{\partial}{\partial z}\left(Kv \frac{\partial \hat{C}_i}{\partial z} \right)$$

This can be written out more fully in matrix form as:

$$\lambda \begin{bmatrix} P_1 \\ P_2 \\ Z_1 \\ Z_2 \\ N_1 \\ N_2 \end{bmatrix} = \begin{bmatrix} \frac{\partial F_{P_1}}{\partial P_1} + Kv\frac{\partial^2}{\partial z^2} & \frac{\partial F_{P_1}}{\partial P_2} & \frac{\partial F_{P_1}}{\partial Z_1} & \frac{\partial F_{P_1}}{\partial Z_2} & \frac{\partial F_{P_1}}{\partial N_1} & \frac{\partial F_{P_1}}{\partial N_2} \\ \frac{\partial F_{P_2}}{\partial P_1} & \frac{\partial F_{P_2}}{\partial P_2} + Kv\frac{\partial^2}{\partial z^2} & \frac{\partial F_{P_2}}{\partial Z_1} & \frac{\partial F_{P_2}}{\partial Z_2} & \frac{\partial F_{P_2}}{\partial N_1} & \frac{\partial F_{P_2}}{\partial N_2} \\ \frac{\partial F_{Z_1}}{\partial P_1} & \frac{\partial F_{Z_1}}{\partial P_2} & \frac{\partial F_{Z_1}}{\partial Z_1} + Kv\frac{\partial^2}{\partial z^2} & \frac{\partial F_{Z_1}}{\partial Z_2} & \frac{\partial F_{Z_1}}{\partial N_1} & \frac{\partial F_{Z_1}}{\partial N_2} \\ \frac{\partial F_{Z_2}}{\partial P_1} & \frac{\partial F_{Z_2}}{\partial P_2} & \frac{\partial F_{Z_2}}{\partial Z_1} & \frac{\partial F_{Z_2}}{\partial Z_2} + Kv\frac{\partial^2}{\partial z^2} & \frac{\partial F_{Z_2}}{\partial N_1} & \frac{\partial F_{Z_2}}{\partial N_2} \\ \frac{\partial F_{N_1}}{\partial P_1} & \frac{\partial F_{N_1}}{\partial P_2} & \frac{\partial F_{N_1}}{\partial Z_1} & \frac{\partial F_{N_1}}{\partial Z_2} & \frac{\partial F_{N_1}}{\partial N_1} + Kv\frac{\partial^2}{\partial z^2} & \frac{\partial F_{N_1}}{\partial N_2} \\ \frac{\partial F_{N_2}}{\partial P_1} & \frac{\partial F_{N_2}}{\partial P_2} & \frac{\partial F_{N_2}}{\partial Z_1} & \frac{\partial F_{N_2}}{\partial Z_2} & \frac{\partial F_{N_2}}{\partial N_1} & \frac{\partial F_{N_2}}{\partial N_2} + Kv\frac{\partial^2}{\partial z^2} \end{bmatrix} \bullet \begin{bmatrix} P_1 \\ P_2 \\ Z_1 \\ Z_2 \\ N_1 \\ N_2 \end{bmatrix}$$

The 6x6 finite difference Jacobian matrix can be computed at steady state ($P_1^*, P_2^*, Z_1^*, Z_2^*, N_3^*, N_4^*$), therefore the above equation can be solved to determine the eigenvalues (λ) of the system. For each steady solution a set of 600 eigenvalues, corresponding to the six state equation and 100 depth levels in the model, can be determined. The biological interactions at each depth level cannot be considered independent dynamical systems because vertical diffusion effectively coupled the layers within the model. It was, therefore, impossible to associate any given eigenvalue with any given depth level. This meant that if even one of the six-hundred eigenvalues has a positive real portion, the associated model possesses dynamic instabilities. Thus, the modulus of the largest real eigenvalue ($\mathbb{R}|\lambda^*|>0$) determines the systems stability.

3.2.3 *Model setup*

I used initial conditions (Figure 3-2) that were based on observational results from the Long Term Observational Program (Weingartner *et al.*, 2002) and the Plankton Process Program (Strom *et al.*, 2001), the two components of the GLOBEC coastal Gulf of Alaska program. By letting $N_2 = 15-(P_1+P_2+Z_1+Z_2+N_1)$ μM N the total nitrogen (N_T) in the system was constant with depth. These values were considered reasonable representations of conditions in the coastal Gulf of Alaska during spring.

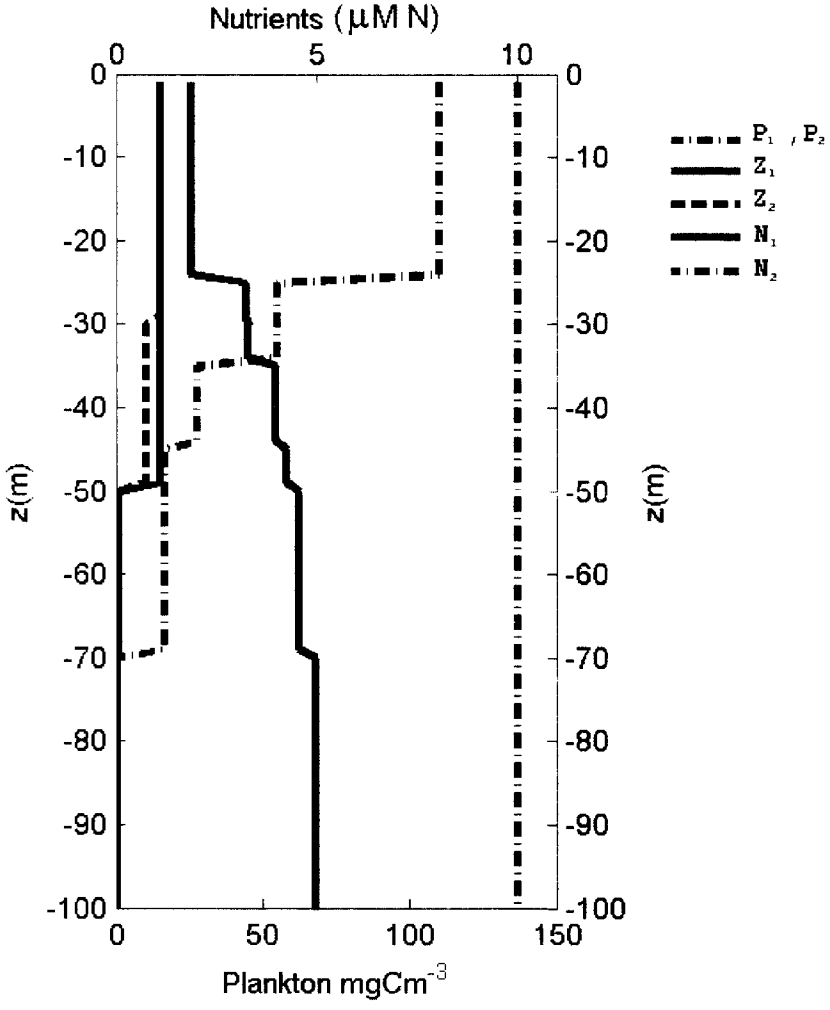

Figure 3-2 Profile of Initial Conditions used to determine model stability.

In order to non-dimensionalize the model, parameters were scaled according to the transformations presented in Table 3-1 with the suit of parameter values used is presented in Table 3-2. These values are very similar, although not identical to those used subsequently in Chapter 4. A detailed explanation of why these values were selected is provided in Chapter 4 so not repeated here.

Table 3-1 Transformations used to make model non-dimensional.
Primes denote the non-dimensional quantities.

Symbol		Transformation
C'	=	C / N_T
$P'_{\max X}$	=	$P_{\max X} / P_{\max 2}$
k'_{1X}	=	k_{1X} / N_T
k'_{2X}	=	k_{2X} / N_T
ψ'	=	$\psi \cdot N_T$
r'	=	$r / P_{\max 2}$
$i'_{\max Y}$	=	$i_{\max Y} / P_{\max 2}$
γ'_Y	=	$\gamma_Y / P_{\max 2}$
k'_{3Y}	=	k_{3Y} / N_T
e'_{YX}	=	e_{YX}
e'_{ZZ}	=	e_{ZZ}
θ'	=	θ / N_T
m'_X	=	$m_X / P_{\max 2}$
m'_Z	=	$m_Z / P_{\max 2}$
h'	=	$h \cdot / P_{\max 2}$
Kv'	=	$Kv \cdot k_{ext}^2 / P_{\max 2}$
z'	=	$z \cdot k_{ext}$

Table 3-2. Parameter values used in the NPZ model.
X and Y can be 1 or 2 to represent the two classes of phytoplankton and zooplankton, respectively.

Symbol	Definition	Parameter Values		Units
Phytoplankton growth parameters				
		X		
		1	*2*	
$P_{\max X}$	maximum growth rate	1	1	day^{-1}
k_{1X}	half-saturation constant for N_1	.75	.5	μM N
k_{2X}	half-saturation constant for N_2	.5	.75	μM N
ψ	Ammonium inhibition parameter X	1.5		$[\mu M\ N]^{-1}$
r	Nitrification of N_2 to N_1	0.05		day^{-1}
k_{ext}	Light extinction coefficient	0.06		m^{-1}
Zooplankton ingestion parameters				
		Y		
		1	*2*	
$i_{\max Y}$	maximum ingestion rate	1.4	1.0	day^{-1}
γ_Y	assimilation efficiency	0.4	0.3	-
k_{3Y}	light extinction coefficient	1.2	.7	$\mu g\ C\ l^{-1}$
θ	feeding threshold concentration	0.05		$\mu g\ C\ l^{-1}$
Mortality Parameters				
		X		
		1	*2*	
m_X	natural mortality rate P_X	0.2	0.3	day^{-1}
m_Z	natural mortality rate Z_Y	0.75		
h	specific predation rate	0.01 or 0.1		day^{-1}
q	predation exponent	1 or 2		
Diffusion Parameters				
Kv_m	mixed layer vertical diffusivity	10^{-3}		$m^2 s^{-1}$
Kv_b	background vertical diffusivity	10^{-5}		$m^2 s^{-1}$
Φ	Shape parameters for diffusion profile	$z-40$		-
ω		5		-

3.2.4 Analysis

The stability of the model was examined when using the five alternative functional forms for zooplankton grazing (grazing functions I-V) for the case of both linear (q=1) and quadratic predation (q=2); the specific predation rate was also varied (h=0.1 or 0.01). Two alternative parameter sets (A and B) were implemented to represent zooplankton capture efficiency for each prey type (e). Set 'A' represents an ecosystem in which, due to size restrictions, micro-zooplankton capture small phytoplankton with a greater efficiency (e_{11}=1.0) than large phytoplankton (e_{12}=0.7) and mesozooplankton capture microzooplankton (e_{ZZ}=1.0), large phytoplankton (e_{22}=0.7) and small phytoplankton (e_{21}=0.2) with a decreasing order of efficiency. Set 'B' represents an alternative ecosystem in which microzooplankton can feed on the two size classes of phytoplankton with equal efficiency (e_{11}=e_{12}=1.0), but mesozooplankton's 'capture efficiency' for large phytoplankton (e_{22}=0.4) is reduced. A synopsis of each model run is provided in Table 3-3.

3.3 Results

The trivial (and uninteresting) solution for the model is considered to be a system containing only nitrate, with zero concentrations of the other five model components (N_1,N_2,P_1,P_2,Z_1,Z_2,)=(1,0,0,0,0,0). This is because there is a rapid return of the system to nitrate if the light dependent photosynthetic process that drives the model is halted. It was not common to have all six model components simultaneously comprising the model solution. In fact, solutions comprising all model components were only found when grazing function V was implemented. In the majority of the remaining model simulations large phytoplankton was reduced to negligible concentrations as was one of the zooplankton components. Generally, the choice of predation function (linear or quadratic) determined which zooplankton size group thrived. With functions I, II and III simulations in which predation was linear (q=1) and the specific predation rate was high (0.1)

mesozooplankton were quickly reduced to concentrations several orders of magnitude less than the microzooplankton. With this parameterization, the constant specific predation rate exerted on the mesozooplankton, regardless of rarity, kept their concentrations low. The reduction of the mesozooplankton population effectively relieved the microzooplankton of any grazing pressure. Limited now only by prey availability microzooplankton were able to flourish and became the only significant source of grazing pressure on the phytoplankton. Thus, the dynamics of the six-component model were effectively controlled by the behavior of only five components; small and large phytoplankton, microzooplankton, nitrate and ammonium. Decreasing the specific predation rate or using a quadratic predation function (q=2) effectively reduced the specific predation rate experienced by the mesozooplankton. The resulting balance between biological process rates meant that mesozooplankton were able to achieve net population growth but grazing pressure on the microzooplankton by the mesozooplankton meant that the microzooplankton population was reduced to negligible concentrations.

Eigenvalues were determined only for those solutions that were found to be steady and non-trivial, *i.e.*,, those solutions obtained when implementing grazing functions IV and V. The absence of a steady solution when grazing functions I, II and III were implemented meant that linear stability analysis could not be used to reveal information of the non-steady solutions. For each steady equilibrium solution, the largest real, stability determining eigenvalue was very small in magnitude. Some of the eigenvalues were slightly positive, while others were slightly negative. In practice, due to the small magnitude of the eigenvalues (both positive and negative), the time that it would take a perturbed solution to explode or return to the equilibrium solution is insignificant (thousands of years) with respect to time scales of concern for the biological populations, *i.e.,* months and years. Over the timescales of concern, model solutions can be considered to possess neutral stability. This means that following a perturbation, populations of each model component will not return to the equilibrium solution, nor will they move further away than the initial perturbation. Examining the complete set of real eigenvalues (Figure

3-3) for simulation 20, although the largest real eigenvalue is positive (2.32×10^{-4}) all remaining eigenvalues were negative and many were large in magnitude, indicating a series of decaying modes with very large amplitude. A similar profile of eigenvalues occurred for each of the other models that reached a steady equilibrium.

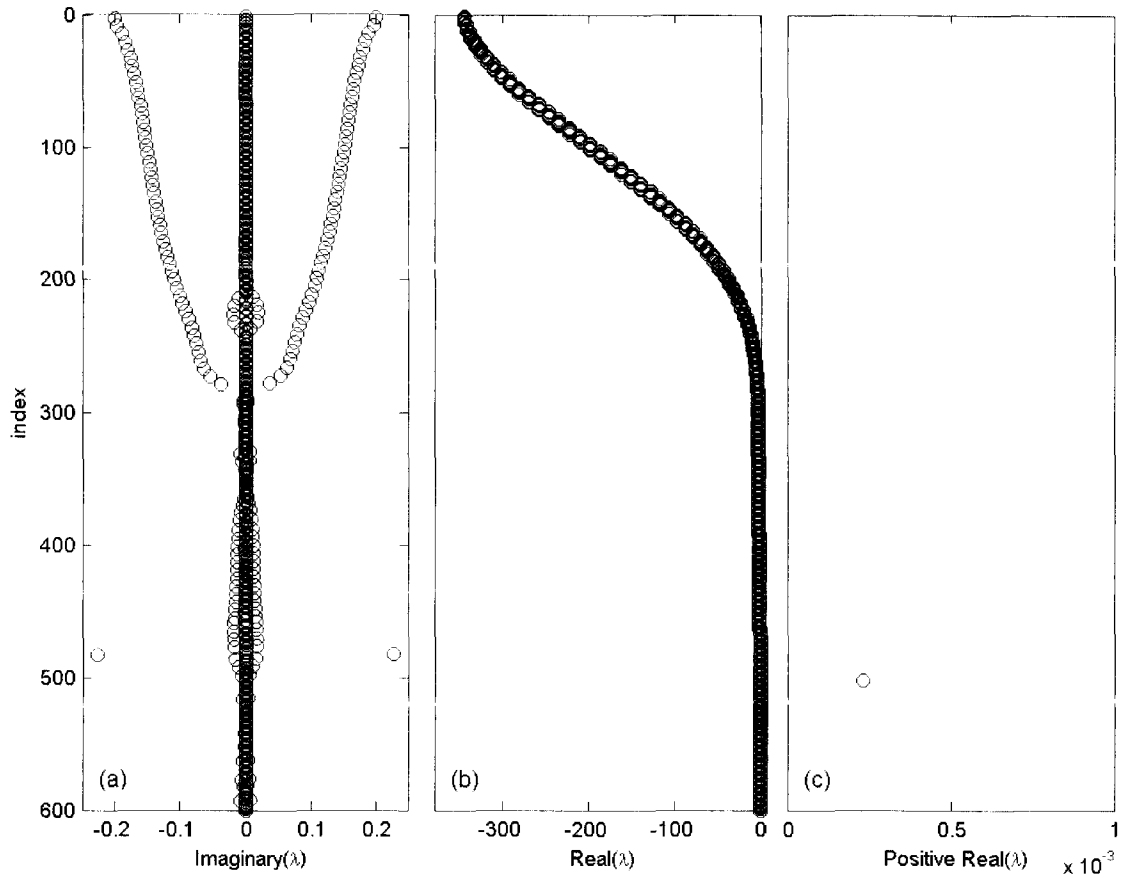

Figure 3-3 Example of a suite of eigenvalues for six-component model.
(a) imaginary portion of eigenvalues, (b) real portion of eigenvalues, (c) positive real eigenvalues. Eigenvalues shown were obtained for simulation 20. *i.e.*, grazing function V, parameter set 'B', h=0.01, q=2simulations. The index serves to order the six-hundred eigenvalues based on the size of $\mathbb{R}(\lambda)$.

Table 3-3 Maximum real and imaginary eigenvalues for each model simulation.
Note, it was only possible to perform eigenvalue analysis for those models which possessed a steady equilibrium solution. The maximum time derivative term for each model component was required to be smaller than $1x10^{-4}$ for a model solution to be designated as a steady equilibrium. Steady equilibrium solutions are indicated by a *.

Run	Parameter	q	h	Grazing	Max. time derivative	max(λ)	Trivial components
1	B	1	0.1	I	0.1568	-	P_2, Z_2
2				II	0.002	-	P_2, Z_2
3				III	0.0113	-	P_2, Z_2
4				IV	$5.24x10^{-6*}$	$-1.30x10^{-14}$	P_2, Z_2
5				V	$3.23x10^{-5*}$	$-1.44x10^{-14}$	Z_2
6			0.01	I	0.0039	-	P_2, Z_1
7				II	0.045	-	P_2
8				III	0.0034	-	P_2, Z_1
9				IV	$4.71x10^{-6*}$	$-2.20x10^{-14}$	P_2
10				V	$2.74x10^{-5*}$	$-1.21x10^{-14}$	none
11		2	0.1	I	0.0054	-	P_2, Z_1
12				II	0.367	-	P_2, Z_1
13				III	$2.84x10^{-4}$	-	P_2, Z_1
14				IV	$5.03x10^{-6*}$	$4.55x10^{-15}$	P_2
15				V	$2.60x10^{-5*}$	$8.09x10^{-5}$	none
16			0.01	I	0.1044	-	P_2, Z_1
17				II	0.012	-	P_2, Z_1
18				III	$1.88x10^{-4}$	-	P_2, Z_1
19				IV	$9.34x10^{-6*}$	$1.19x10^{-4}$	P_2
20				V	$2.60x10^{-5*}$	$2.32x10^{-4}$	none
21	A	1	0.1	I	0.0189	-	P_2, Z_2
22				II	0.002	-	P_2, Z_2
23				III	0.0403	-	P_2, Z_2
24				IV	$5.70x10^{-6*}$	$-1.18x10^{-14}$	P_2, Z_2
25				V	$3.31x10^{-5*}$	$7.58x10^{-15}$	Z_2
26			0.01	I	0.0049	-	P_2, Z_1
27				II	0.0177	-	P_2
28				III	0.0181	-	P_2, Z_1
29				IV	$6.41x10^{-6*}$	$-1.52x10^{-14}$	P_2
30				V	$2.87x10^{-5*}$	$8.36x10^{-15}$	none
31		2	0.1	I	0.0046	-	P_2, Z_1
32				II	0.0359	-	P_2, Z_1
33				III	$2.71x10^{-4}$	-	P_2, Z_1
34				IV	$8.73x10^{-6*}$	$-7.24x10^{-15}$	P_2
35				V	$2.76x10^{-5*}$	$7.83x10^{-5}$	none
36			0.01	I	0.0344	-	P_2, Z_1
37				II	0.0116	-	P_2, Z_1
38				III	$2.25x10^{-4}$	-	P_2, Z_1
39				IV	$8.69x10^{-6*}$	$1.18x10^{-4}$	P_2
40				V	$2.75x10^{-5*}$	$2.33x10^{-4}$	none

3.4 Discussion

The work presented in this chapter constitutes a preliminary investigation into the impact of varying the zooplankton grazing and higher predation (model closure) formulations on the dynamical behavior of a six-component NPZ model developed for the coastal Gulf of Alaska. The model had two phytoplankton components, two zooplankton components and two nutrient components. Stationary physical forcing, representative of the coastal Gulf of Alaska in spring, was used to force the model.

This work builds on several previous works which have shown that the choice of functional form for grazing (Oaten and Murdoch, 1975; Armstrong, 1976; Franks, *et al.* 1986) and the form for higher predation on zooplankton (Steele and Henderson, 1992; Edwards and Brindley, 1999; Edwards and Yool, 2000; Edwards and Bees, 2001) can have a large impact on the non-linear dynamics of simple three component NPZ models. Here it was shown that the choice of formulation for undefined predation and zooplankton grazing also impacts the non-linear model dynamics and structural stability of a more complex six-component ecosystem model in which zooplankton can graze on multiple prey types. More importantly, however, the traditional eigenvalue approach to examine model dynamics is shown to be inappropriate for intermediately complex NPZ models that cannot be solved analytically. Stability analysis of simpler models (Edwards *et al.* 2000; May, 1973) relied on finding equilibrium solutions analytically. Solutions found in this manner could potentially be stable, unstable or neutrally stable, as would be revealed by the eigenvalue analysis. Due to the additional complexity in the six-component model, solutions could not be found analytically, requiring use of an alternative approach to finding the equilibrium solutions by time-stepping the model with stationary forcing. Herein the problem lies: if the time series solution approached a steady equilibrium it was likely to be stable – or at least not unstable - otherwise the solution would not remain at the equilibrium. Conversely, if a model trajectory was oscillatory in nature, although it could be oscillating about an

unstable node (equilibrium point), this cannot be determined through our approach because I no steady solution existed from which to determine the eigenvalues. Thus, only those models that had a steady equilibrium solution could have their eigenvalues and their stability determined. No conclusion could be drawn with respect to the stability of the non-steady (oscillatory) model solutions.

This experiment revealed the interesting point that it was difficult to find solutions that were steady and comprised all model components. The form of the grazing function, the value of the specific predation rate (h) and the form of the predation function (as determined by q=1 or q=2) all had an influence on the composition of model solutions. Interestingly, a model with linear predation was found to have very similar dynamics to a model with quadratic predation but with a higher specific predation rate. This indicates that it will be necessary to look over a broad range of values for h and q, with each of the five grazing functions, in order to get a clear picture of model behavior with respect to the existence of the six-model components.

The two alternative parameter sets implemented to simulate zooplankton capture efficiency did not have any impact on the model dynamics or on the model structure, with respect to the existence of model components. It is likely that comparison of more diverse parameter sets for zooplankton capture efficiency will yield a different result. However, to focus the exploration on model behavior over a finer resolution of q-h parameter space, in subsequent experiment only capture efficiency parameter set A is considered.

3.5 Experiment Redesign

The results from this experiment led me to re-design the experiment in order to better address hypothesis 1 and 2. Below is an outline of the revisions made to the method used in this experiment; the complete outline of methods for this experiment is presented in Chapter 4 and so is not repeated here. Initial results presented above suggest that the non-

linear dynamics of the model were heavily dependent on both h and q. Therefore, in subsequent experiments model dynamics were explored over a finer resolution q-h parameter space. For example, in Chapter 4 model behavior is investigated for eleven values of the predation exponent (q=1.1,1.2,1.3...2.0) and nineteen values of the specific predation exponent (h=0.05-2.24). The resolution of h varied, becoming finer as h declined, because during the experiment it became apparent that in this region of parameter space a higher resolution of h was required in order to adequately capture patterns of dynamical behavior; the oscillatory region bounded by the Hopf bifurcations was very narrow in this region and would be missed by a coarse resolution investigation. For each parameter set the dynamics of the NPZ model were compared when the five alternative functional forms for zooplankton grazing were implemented. A total of 1045 individual model runs comprised this experiment.

Rather than attempting to determine the stability of the system through eigenvalues analysis, which was only possible when a steady equilibrium solution can be found, the focus was shifted to classifying the form of the nature of the solution with respect to its time series behavior when subjected to stationary forcing. For example, model solutions can be classified as, steady equilibrium, periodic limit cycles, chaotic etc. From the above experiment, it became apparent that with each model run there was an initial period of transitory behavior before the equilibrium solution (be it steady or oscillatory) is reached. This suggests that it would be prudent to time-step the models for longer than the 100 days used above. This would ensure that a solution would have the opportunity to come within adequate proximity to a steady equilibrium. Insufficient time stepping of the model could mean that the optimization function (fsolve) would be provided with an inadequate initial guess of a potentially steady solution and subsequently could fail to find the root (zero) of a system of nonlinear equations that did exist. In the new experiment, each model was initially run for 300 time steps (days), and the resulting solution provided as a starting guess to a numerical solver of the steady state solution (equations 1–6 with the left hand sides set to zero). Following Edwards *et al.* (Edwards *et*

al., 2000), for a model to be classified as steady, the associated time derivative terms were required to be smaller than 10^{-4} μM N/day. Models that failed to converge to a steady solution were run for a further 700 days, and the time series solution on the one-thousandth day was provided to the numerical solver. These solutions were then reclassified. Any solution which could not be classified as steady was manually examined at the 25 meter depth, which was considered to be well within the mixed layer, to determine if behavior was periodic (limit cycles) or something more complex. This process of time stepping solutions for 1,000 days followed by examination of the solution trajectory was repeated until it could be determined that the solutions were indeed limit cycles and not anything more complex.

A few changes were made to the parameter values and initial conditions used in the above experiment. Most notably, because the large phytoplankton group was frequently reduced to negligible concentrations the maximum photosynthetic rate for phytoplankton (P_{max}) was increased to 2 day^{-1}. The full suite of parameter values and justification for using them is presented in Chapter 4 so not repeated here. Due to the additional complexity that a full exploration of q-h parameter space will add to the experiment, to simplify things somewhat initial conditions that had a constant vertical profile were used in place of the non-homogeneous initial conditions used previously.

Subsequent to the above experiment, it became apparent that the scaling used for h require modification in the case of $q>1$. This is because in order for the predation term ($H = h \cdot Z_2^q$) to have constant units (day^{-1}) as q changes, the units of h must change accordingly. For example, when $q=1$ the specific predation rate is constant and not dependent on the size of the zooplankton population units of h are therefore day^{-1}. However if $q=2$ the rate of predation is dependent upon the size of the zooplankton population and units of h are $(gCm^{-3})^{-1}$ day^{-1}. The units of h will vary in a continuum as q increases from 1 to 2. In general terms, $h=(gCm^{-3})^{1-q}$ day^{-1}. Therefore, in order to non-dimensionalize this parameter a scaling factor that is also dependent on q is required. *i.e.*,

$$h' = h \cdot N_T^{(q-1)} / P_{\max 2}$$

Scaling of all other parameters was the same as presented in Table 3-1.

A similar correction had to be made when converting the parameter h into units on nitrogen, the currency in the model. When q=1, h is constant and not dependent on the amount of carbon so no conversion is required. However, when q=2, h is specified as a rate per quantity of carbon, per day and so must be multiplied by a conversion factor (η) to convert to units of nitrogen (μM N)$^{-1}$ day^{-1}. Assuming the Redfield ratio of 106 C:16 N η is given by:

$$\eta = \frac{12gC}{l} \cdot \frac{1000l}{m^3} \cdot \frac{106molC}{16molN} = \frac{12}{1000} \cdot \frac{106}{16} \qquad \text{Eq. 3.19}$$

Therefore, in general:

$$(gCm^{-3})^{1-q} \cdot d^{-1} \cdot \eta = (mmolNm^{-3})^{1-q} d^{-1} = (\mu M\ N)^{1-q} d^{-1} \qquad \text{Eq. 3.20}$$

The modified experiment formed the basis of a manuscript which was submitted in its original form to Journal of Plankton Research on May 24th 2004. Comments were received from two anonymous reviewers on July 17th 2004. The manuscript was modified to address reviewers concerns and the resubmitted on September 28th 2004. The resubmitted version of the manuscript constitutes Chapter 4.

3.6 References

Armstrong, R. A. (1976) The Effects of Predator Functional Response and Prey productivity on Predator-prey Stability: A Graphical Approach. *Ecology,* **57,** 609-612.

Edwards, A. M. and Yool, A. (2000) The role of higher predation in plankton population models. *J. Plankton Res.*, **22**, 1085-1112.

Edwards, C. A., Powell, T. A. and Batchelder, H. P. (2000) The stability of an NPZ model subject to realistic levels of vertical mixing. *J. Mar. Res.*, **58**, 37-60.

Edwards, A. M. and Bees, M. A. (2001) Generic dynamics of a simple plankton population model with a non-integer exponent of closure. *Chaos, Solutions and Fractals,* **12**, 289-300.

Edwards, A. M. and Brindley, J. (1999) Zooplankton mortality and the dynamical behaviour of plankton population models. *Bulletin of Mathematical Biology,* **61**, 303-339.

Franks, P. J. S., Wroblewski, J. S. and Flierl, G. R. (1986) Behavior of a simple plankton model with food-level acclimation by herbivores. *Mar. Biol.*, **91**, 121-129.

Haefner, J. W. (1996) *Modeling Biological Systems: Principles and Applications.* Chapman and Hall, New York.

May, R. M. (1973). Stability and Complexity in Model Ecosystems, *Princeton University Press.*

Oaten, A. and Murdoch, W. W. (1975) Switching, functional response, and stability in predator-prey systems. *The American Naturalist,* **109**, 299-318.

Steele, J. H. and Henderson, E. W. (1992) The role of predation in plankton models. *J. Plankton Res.*, **14**, 157-172.

Strom, S. L., Brainard, M. A., Holmes, J. L. and Olson, M. B. (2001) Phytoplankton blooms are strongly impacted by microzooplankton grazing in coastal North Pacific waters. *Mar. Biol.*, **138**, 355-368.

Weingartner, T., Coyle, K., Finney, B., Hopcroft, R., Whitledge, T., Brodeur, R., Dagg, M., Farley, E., Haidvogel, D., Haldorson, L., Hermann, A., Hinckley, S., Napp, J., Stabeno, P., Kline, T., Lee, C., Lessard, E., Royer, T. and Strom, S. (2002) The Northeast Pacific GLOBEC Program: Coastal Gulf of Alaska. *Oceanography,* **15**, 48-63.

Chapter 4 . Non-linear dynamics of a pelagic ecosystem model with multiple predator and prey types[1]

4.1 Abstract

Using numerical techniques we explored the dynamics of a one-dimensional, six-component Nutrient-Phytoplankton-Zooplankton model in which zooplankton grazed on a mixed prey field. Five alternative functional forms were implemented to describe zooplankton grazing, and the form for predation on mesozooplankton was prescribed by a product of a specific predation rate (h) and the mesozooplankton concentration raised to a power (q) which we varied between one and two. With all five grazing functions, Hopf bifurcations, where the form of the solution transitioned between steady equilibrium and periodic limit cycles, persisted across the q-h parameter space. Regardless of the values of h and q, with some forms of the grazing function we were unable to find steady equilibrium solutions that simultaneously comprised non-zero concentrations for all six model components. Extensions of Michaelis-Menten-based single resource grazing formulations to multiple resources resulted in periodic solutions for a large portion of the q-h space. Conversely, extensions of the sigmoidal grazing formulation to multiple resources resulted in steady solutions for a large portion of q-h parameter space.

4.2 Introduction

Since the historical works of Riley (Riley, 1946) and Steele (Steele, 1974), the use of Nutrient-Phytoplankton-Zooplankton (NPZ) models as tools to understand temporal and spatial dynamics of marine ecosystems has become common practice. Despite the many gross generalizations these models embody, they provide useful research tools to test understanding of marine ecosystem functionality. Reflecting our increased understanding

[1] Gibson, G.A., Musgrave, D.L., and Hinckley, S. Non-Linear Dynamics of a Pelagic Ecosystem Model with Multiple Predator and Prey Types. Submitted to *Journal of Plankton Research*.

of the marine ecosystem, and in an effort to simulate observed dynamics left unexplained by simple three-component NPZ models, there has been a trend toward developing more sophisticated NPZ models with an increasing number of components and associated interactions. The ever-increasing availability of computational power has enabled the development of high-resolution, three-dimensional, coupled NPZ physical models that can perform realistic simulations of a marine ecosystem. Such coupled models are now frequently an integral part of research programs geared to understand ecosystem dynamics, for example, the Global Ocean Ecosystem Dynamics Experiment (Franks and Chen, 2001), the Joint Global Ocean Flux Study (Loukos *et al.,* 1997), and the North Pacific Marine Organization (Aita *et al.,* 2003).

Our conceptual view of the minimum complexity required to replicate observations constantly shifts, reflecting the continual refinement of our understanding of marine ecosystems. The early, simple, zero- or one-dimensional, three-component NPZ models reflected the understanding of the ecosystem at the time and were generally considered to represent nitrate, microphytoplankton, and herbivorous mesozooplankton. Phytoplankton are now known to utilize both new (nitrate) and regenerated (ammonium) forms of inorganic nitrogen (Dugdale and Goering, 1967; Eppley and Peterson, 1979). Pico- and nanophytoplankton have been found to frequently contribute a large percentage of the total primary production (Johnson and Sieburth, 1979, 1982; Strom *et al.,* 2001). Microzooplankton, with their ability to feed on these small, phytoplankton size fractions, are now thought to be the primary grazers (Dagg, 1993) controlling the chlorophyll standing stock in many regions (Landry and Hassett, 1982; Gifford, 1988; Strom and Welschmeyer, 1991; Dagg, 1995).

Although the numerous variations of complex ecosystem models presented in the literature frequently share the same roots, they often differ substantially in the formulation of biological processes. It is widely accepted that phytoplankton nutrient uptake is best represented by the hyperbolic function first introduced by Monod (Monod, 1942). Conversely, there is not yet such a general agreement on which functional forms

are most appropriate for simulating grazing, defined here as zooplankton grazing on phytoplankton and smaller zooplankton, or 'predation', defined as mesozooplankton mortality due to consumption by undefined higher trophic levels. Predation is often simulated using either a linear formulation, that represents a predator whose biomass does not fluctuate (Evans and Parslow, 1985; Fasham *et al.*, 1990), or a quadratic formulation, that represents a predator whose biomass is proportional to that of the zooplankton (Fasham, 1995; Edwards, 2001). Hyperbolic (Frost, 1987; Fasham *et al.*, 1993) and sigmoidal formulations (Malchow, 1994) have also been used to simulate predation, although not as commonly, perhaps due to the additional parameters and associated assumptions these formulations require. Historically, the formulation for zooplankton grazing has also taken several different forms. The hyperbolic formulation (Ivlev, 1961; Frost, 1987) was once a common choice. However, in an effort to prevent complete prey elimination due to zooplankton grazing, formulations were developed to provide rare prey with a refuge from grazing pressure. The most notable of the prey refuge functions are the 'threshold' function (Steele, 1974; Mullin and Fuglister, 1975; Wroblewski, 1977), which incorporates a critical prey concentration below which grazing ceases, and the sigmoidal function, in which the grazing rate is reduced at low prey concentrations (Evans and Parslow, 1985; Steele and Henderson, 1992; Denman and Peña, 1999). There is evidence that at least some species of zooplankton exhibit behavior consistent with this concept (Frost, 1972, 1975; Strom, 1991; Gismervik and Andersen, 1997). Such observations are, however, usually made on individual species that are fed known prey types, and do not necessarily reflect the behavior of the zooplankton community at large. Nevertheless, the addition of a grazing refuge to a grazing function is popular with the modeling community because it often overcomes the problem of prey elimination. With the advent of multiple prey NPZ models it is becoming increasingly common to see extensions of the single resource grazing functions in order to simulate zooplankton grazing on a mixed prey field (Ambler, 1986; Fasham *et al.*, 1990; Ryabchenko *et al.*, 1997; Chifflet *et al.*, 2001; Denman and Peña, 2002). A comprehensive review of the grazing functional response for zooplankton grazing on

single and multiple nutritional resources (prey items) is provided by Gentleman *et al.* (Gentleman *et al.*, 2003).

Despite a rapid trend towards more realistic NPZ models, in which zooplankton are presented with multiple nutritional resources, investigations into the fundamental dynamics of these newer models have been limited (Armstrong, 1994; Ryabchenko *et al.*, 1997; Yool, 1998). Over the past few decades, the application of non-linear systems dynamics has provided a basis for understanding the behavior of NPZ models (May, 1973; Oaten and Murdoch, 1975; Edwards and Brindley, 1996; Edwards *et al.*, 2000). The formulations for both zooplankton grazing (Franks *et al.*, 1986) and predation on zooplankton (Steele and Henderson, 1992; Edwards and Yool, 2000) have been found to influence the fundamental dynamics of simple NPZ model, determining whether a model's time-dependent behavior will approach steady state or exhibit oscillatory behavior, such as periodic limit cycles. Furthermore, incorporating moderate levels of vertical diffusion into a purely biological NPZ model has been shown to impart model stability (Edwards *et al.*, 2000), an important consideration for the realm of coupled biophysical models. Without a good understanding of the fundamental behavior of the more complex NPZ models now commonly employed in ecosystem studies, time-dependent behavior simulated with coupled biological-physical models, as in periodic or chaotic solutions, could be interpreted as due to variable physical forcing rather than as an inherent property of an ecosystem model. It is important that we extend our understanding of NPZ system dynamics to these more complex models and develop an appreciation of how choices of formulations for simulating biological processes can affect their behavior.

Here we explore the fundamental non-linear dynamics of an intermediately complex NPZ model in which zooplankton grazers can feed on multiple prey types. Time series solutions are examined and their behavior classified with respect to their non-linear dynamics and structural stability as steady, limit cycle (periodic), or chaotic. Our analysis is based on a six-component model, subjected to stationary physical forcing (vertical light

and mixing profiles). One of our long-term interests is to include our NPZ model into a simulation with realistic three-dimensional physics in the coastal Gulf of Alaska. Therefore, where possible, we have used biological and physical parameter values that are realistic for that region. We compare model behavior with alternative functional forms for zooplankton grazing over a realistic range of specific predation rates (h = 0-2.4 $[gCm^{-3}]^{1-q}$ day^{-1}) and predation exponents ($1 \leq q \leq 2$).

4.3 Method

4.3.1 Model Structure

To investigate the influence on model dynamics of alternative grazing and mortality functions when zooplankton are able to graze on a mixed prey field, we developed a six-component model (Figure 4-1) that simulated the exchange of nitrogen (μM N) between two classes of phytoplankton, small (< 8μm, P_1) and large (> 8μm, P_2); two classes of zooplankton, microzooplankton (Z_1) and mesozooplankton (Z_2); and two types of dissolved inorganic nitrogen, nitrate (N_1) and ammonium (N_2). Both size classes of zooplankton were allowed to graze on multiple prey types. This model was developed from the three-component NPZ model whose stability has previously been investigated (Edwards *et al.,* 2000). We selected this model due to the simplicity of its functional forms. We increased model complexity by adding a second phytoplankton and zooplankton component and splitting the nutrient component into nitrate and ammonium. The one-dimensional model was spatially explicit in the vertical, with a resolution of one meter and an extent of one hundred meters (z_i=[1m, 2m, 3m, ... 100m). The model was a closed system with no net inputs or outputs; therefore, the total nitrogen content, summed over all depths, was constant at all times ($N_T=P_1+P_2+Z_1+Z_2+N_1+N_2$). We feel that this is not an unrealistic assumption to make considering the vertical extent of the model. Potential losses from the system (*i.e.,* mortality, predation, and egestion) were treated as inputs to the ammonium pool; no detrital pool was explicitly modeled. Initial

concentrations for all model components were taken to be vertically homogeneous at 2 μg Chl-a L^{-1} for both phytoplankton groups, 15μg C L^{-1} for both zooplankton groups, 10 μM N for nitrate, and 1μM N for ammonium. Based on observational results from the GLOBEC coastal Gulf of Alaska program (Strom *et al.*, 2001; Weingartner *et al.*, 2002), these values were considered reasonable representations of conditions in the coastal Gulf of Alaska during spring (May). To enable material flow between the phytoplankton, zooplankton, and nutrient components we used a common currency of nitrogen and assumed a C:N ratio of 106:16 (Redfield *et al.*, 1963) and a C:Chl-a ratio of 55:1 (Frost, 1987). This gave initial phytoplankton and zooplankton concentrations of 1.386 μM N and 0.189 μM N respectively.

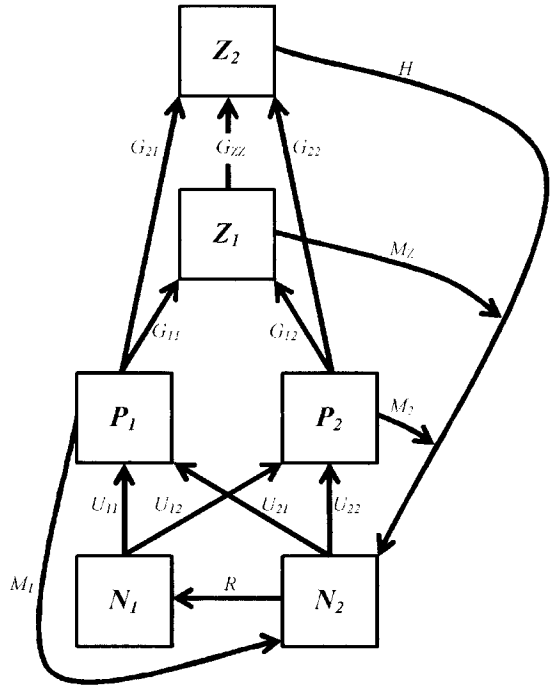

Figure 4-1 Interactions within the six-component NPZ model.
Nitrate (N_1), ammonium (N_2), small phytoplankton (P_1), large phytoplankton (P_2), microzooplankton (Z_1) and mesozooplankton (Z_2). Arrows indicate the direction of material flow. Biological processes, *i.e.*, grazing (G), nutrient uptake (U), mortality (M), predation (H), and nitrification (R) associated with each arrow are indicated. See Table 4-2 for explanation of suffixes. Note that for simplicity, zooplankton assimilation efficiencies have been omitted.

4.3.2 Formulation

The purely biological dynamics are shown below in Eq. 4.1 – 4.6. As discussed later, these biological dynamics are also subjected to vertical mixing within the model (Eq. 4.7). During computation the biological equations were transformed to non-dimensional forms. To non-dimensionalize, the parameters were rescaled (Table 4-1) and the new (primed) values were substituted in place of the original parameters in Table 4-2. For the reader's convenience, we have re-dimensionalized all results and presented them in this form.

Table 4-1 Transformations used to non-dimensionalize the model.

Symbol		Transformation
C'	=	C / N_T
$P'_{\max X}$	=	$P_{\max X} / P_{\max 2}$
k'_{1X}	=	k_{1X} / N_T
k'_{2X}	=	k_{2X} / N_T
ψ'	=	$\psi \cdot N_T$
r'	=	$r / P_{\max 2}$
$i'_{\max Y}$	=	$i_{\max Y} / P_{\max 2}$
γ'_Y	=	$\gamma_Y / P_{\max 2}$
k'_{3Y}	=	k_{3Y} / N_T
e'_{YX}	=	e_{YX}
e'_{ZZ}	=	e_{ZZ}
θ'	=	θ / N_T
m'_X	=	$m_X / P_{\max 2}$
m'_Z	=	$m_Z / P_{\max 2}$
h'	=	$h \cdot N_T^{(q-1)} / P_{\max 2}$
Kv'	=	$Kv \cdot k_{ext}^2 / P_{\max 2}$
z'	=	$z \cdot k_{ext}$

Nutrient Equations

Nitrate (N_1) and ammonium (N_2) dynamics were described by

$$\frac{dN_1}{dt} = -U_{11} - U_{12} + R \qquad \text{Eq. 4.1}$$

$$\frac{dN_2}{dt} = -U_{21} - U_{22} + M_1 + M_2 + M_Z + H + (1-\gamma_1)\cdot(G_{11} + G_{12}) + (1-\gamma_2)\cdot(G_{21} + G_{22} + G_{ZZ}) - R \qquad \text{Eq. 4.2}$$

Where γ_1 and γ_2 represent zooplankton grazing efficiency for microzooplankton and mesozooplankton, respectively. In these and the following equations, *U, M, G, H,* and *R* represent transformation rates of nitrogen due to nutrient uptake, mortality, grazing, predation, and the nitrification of ammonium to nitrate, respectively. Details of the formulations for the transformation rates and definitions of the subscripts are presented in Table III, and parameter values associated with the formulations are given in Table II. Uptake of both of nitrate and ammonium was modeled using a Monod (Monod, 1942) formulation, the classic saturation response with increased concentration of resource. The inhibition of nitrate uptake due to the presence of ammonium was simulated using the exponential function introduced by Wroblewski (Wroblewski, 1977). Following similar studies of this nature (Edwards *et al.*, 2000; Edwards and Brindley, 1999) no detrital component was explicitly modeled. This may have little consequence since Edwards (Edwards, 2001) found that if zooplankton were unable to graze on detritus, the addition of a detrital component to the model made little difference to the observed dynamics. Losses from the phytoplankton and zooplankton model components were assumed to be instantaneously remineralized back to ammonium. Nitrification then occurs at a specific constant rate (*r*). Parameter values (Table 4-2I) most representative of the coastal Gulf of Alaska ecosystem were selected; however, knowledge of parameter values in this region is limited. Where possible, observational values were used, but in their absence, values were selected that fell within the range presented in the marine ecosystem modeling literature.

Table 4-2 Parameter values used in the NPZ model.

X and Y can be 1 or 2 to represent the two classes of phytoplankton and zooplankton, respectively.

Parameter	Symbol	Values		Units
		$X=1$	$X=2$	
maximum growth rate of P_X	$P_{\max X}$	2	2	day^{-1}
P_X half-saturation constant for N_1	k_{1X}	.75	.5	μM N
P_X half-saturation constant for N_2	k_{2X}	.5	1	μM N
inhibition parameter for U_1 by N_2	ψ	1.462		$[\mu M\ N]^{-1}$
nitrification rate	r	0.05		day^{-1}
light extinction coefficient	k_{ext}	0.07		m^{-1}
		$Y=1$	$Y=2$	
maximum ingestion rate	$i_{\max Y}$	1.2	.7	day^{-1}
assimilation efficiency of Z_Y	γ_Y	0.4	0.3	-
Z_Y half-saturation grazing coefficient	k_{3Y}	30	60	$\mu g\ C\ L^{-1}$
Z_Y capture efficiency for P_X	e_{YX}	$Y=1$: $X=1$: 1; $X=2$: .7	$Y=2$: $X=1$: .2; $X=2$: .7	- -
Z_2 capture efficiency for Z_1	e_{ZZ}	1		
Variable Z_Y capture efficiency for P_X	ε_{YX}	$Y=1$: $\frac{e_{YX} \cdot P_X}{\sum_{X=1,2} e_{YX} P_Y}$	$Y=2$: $\frac{e_{YX} \cdot P_X}{e_{ZZ} \cdot Z_1 + \sum_{X=1,2} e_{YX} P_X}$	
Variable Z_2 capture efficiency for Z_1	ε_{ZZ}	$\frac{e_{ZZ} \cdot Z_1}{e_{ZZ} \cdot Z_1 + \sum_{X=1,2} e_{YX} P_X}$		
feeding threshold concentration	θ	0.05		$\mu g\ C\ L^{-1}$
		$X=1$	$X=2$	
natural mortality rate of P_X	m_X	0.2	0.1	day^{-1}
natural mortality rate of Z_1	m_z	0.08		day^{-1}
specific predation rate	h	0.05-2.4		$(gCm^{-3})^{1-q}\ day^{-1}$
predation exponent	q	1 - 2		-

Table 4-3 Biological processes used in the six-component NPZ model .

Parameter definitions and values are given in Table 4-2. X and Y can be 1 or 2 to represent the two classes of phytoplankton and zooplankton, respectively.

Process	Symbol	Formulation
P_X uptake of N_1	U_{1X}	$P_X \cdot P_{\max X} \cdot e^{-z \cdot k_{ex}} \cdot \frac{N_1 \cdot e^{-\psi \cdot N_2}}{k_{1X} + N_1}$
P_X uptake of N_2	U_{2X}	$P_X \cdot P_{\max X} \cdot e^{-z \cdot k_{ex}} \cdot \frac{N_2}{k_{2X} + N_2}$
natural mortality of P_X	M_X	$m_X \cdot P_X$
natural mortality of Z_1	M_Z	$m_Z \cdot Z_1$
higher predation on Z_2	H	$h \cdot Z_2^q$
$N_2 \xrightarrow{regeneration} N_1$	R	$r \cdot N_2$
Zooplankton Grazing	G	See below

Grazing function	Capture efficiency	Z_1 grazing on P_X (G_{YX})	Z_2 grazing on Z_1 (G_{ZZ})	Literature Example
I	*Constant*	$i_{\max} Z_1 \cdot \frac{\sum_{X=1,2} e_{1X} P_X}{k_{31} + \sum_{X=1,2} e_{1X} P_X} \cdot \frac{e_{1X} P_X}{\sum_{X=1,2} e_{1X} P_X}$	$i_{\max} Z_2 \cdot \frac{\sum_{X=1,2} e_{2X} P_X + e_{ZZ} \cdot Z_1}{k_{32} + \sum_{X=1,2} e_{2X} P_X + e_{ZZ} \cdot Z_1} \cdot \frac{e_{ZZ} Z_1}{\sum_{X=1,2} e_{2X} P_X + e_{ZZ} \cdot Z_1}$	Murdoch (1973) Frost (1987)
II	*Constant*	$i_{\max} Z_{1Y} \cdot \frac{\left[\sum_{X=1,2} e_{1X} P_X\right] - \theta}{k_{31} + \left[\sum_{X=1,2} e_{1X} P_X\right] - \theta} \cdot \frac{e_{1X} P_X}{\sum_{X=1,2} e_{1X} P_X}$	$i_{\max} Z_2 \cdot \frac{\left[\sum_{X=1,2} e_{2X} P_X + e_{ZZ} \cdot Z_1\right] - \theta}{k_{32} + \left[\sum_{X=1,2} e_{2X} P_X + e_{ZZ} \cdot Z_1\right] - \theta} \cdot \frac{e_{ZZ} \cdot Z_1}{\sum_{X=1,2} e_{2X} P_X + e_{ZZ} \cdot Z_1}$	Lancelot *et al.* (2000) Chifflet *et al.* (2001)
III	*Variable*	$i_{\max} Z_{1Y} \cdot \frac{\sum_{X=1,2} \varepsilon_{1X} P_X}{k_{31} + \sum_{X=1,2} \varepsilon_{1X} P_X} \cdot \frac{\varepsilon_{1X} P_X}{\sum_{X=1,2} \varepsilon_{1X} P_X}$	$i_{\max} Z_2 \cdot \frac{\sum_{X=1,2} \varepsilon_{2X} P_X + \varepsilon_{ZZ} Z_1}{k_{32} + \sum_{X=1,2} \varepsilon_{2X} P_X + \varepsilon_{ZZ} Z_1} \cdot \frac{\varepsilon_{ZZ} Z_1}{\sum_{X=1,2} \varepsilon_{2X} P_X + \varepsilon_{ZZ} Z_1}$	Fasham *et al.* (1990) Strom and Loukos (1998)
IV	*Constant*	$i_{\max} Z_1 \cdot \frac{\left[\sum_{X=1,2} e_{1X} P_X\right]^2}{k_{31}^2 + \left[\sum_{X=1,2} e_{1X} P_X\right]^2} \cdot \frac{e_{1X} P_X}{\sum_{X=1,2} e_{1X} P_X}$	$i_{\max} Z_2 \cdot \frac{(\sum_{X=1,2} e_{2X} P_X + e_{ZZ} Z_1)^2}{k_{32}^2 + (\sum_{X=1,2} e_{2X} P_X + e_{ZZ} Z_1)^2} \cdot \frac{e_{ZZ} Z_1}{\sum_{X=1,2} e_{2X} P_X + e_{ZZ} Z_1}$	Denman and Peña (2002)
V	*Constant*	$i_{\max} Z_1 \cdot \frac{\sum_{X=1,2} e_{1X} P_X^2}{k_{31}^2 + \sum_{X=1,2} e_{1X} P_X^2} \cdot \frac{e_{1X} P_X^2}{\sum_{X=1,2} e_{1X} P_X^2}$	$i_{\max} Z_2 \cdot \frac{\sum_{X=1,2} e_{2X} P_X^2 + e_{ZZ} Z_1^2}{k_{32}^2 + \sum_{X=1,2} e_{2X} P_X^2 + e_{ZZ} Z_1^2} \cdot \frac{e_{ZZ} Z_1^2}{\sum_{X=1,2} e_{2X} P_X^2 + e_{ZZ} Z_1^2}$	Ryabchenko *et al.*(1997)

Phytoplankton Equations

Phytoplankton dynamics were described by:

$$\frac{dP_1}{dt} = U_{11} + U_{21} - M_1 - G_{11} - G_{21} \qquad \text{Eq. 4.3}$$

$$\frac{dP_2}{dt} = U_{12} + U_{22} - M_2 - G_{12} - G_{22} \qquad \text{Eq. 4.4}$$

The phytoplankton size division (P_1<8μm<P_2) was chosen to mimic that selected by Strom *et al.* (Strom *et al.*, 2001), who have conducted the majority of the limited work on phytoplankton and microzooplankton processes in the coastal Gulf of Alaska. Reflecting observations in this ecosystem (Strom *et al.*, 2001) no significant difference between the maximum growth rate of the two phytoplankton size groups was assumed. A P_{max} of 2 day^{-1} was assigned to both size classes, which seems appropriate given the ranges (0.54-2.21 day^{-1}) found for the total chlorophyll size fraction in this region during spring (Strom *et al.*, 2001). Daily average phytoplankton growth was assumed to be simultaneously limited by the availability of nutrients and Photosynthetically Active Radiation (PAR). The attenuation of PAR below the sea surface was simulated using the exponential decay function ($e^{-z \cdot k_{ext}}$) after Edwards *et al.* (Edwards *et al.*, 2000). A light extinction coefficient (k_{ext} = 0.07 m^{-1}) was chosen which gave an e-folding depth ($1/k_{ext}$) of 14.3 meters and put the midpoint of the euphotic zone ($2.3/k_{ext}$) at 33m (Figure 4-2). As discussed above, the dependence of phytoplankton growth on nitrate and ammonium availability was simulated with the saturating Monod function and the ammonium inhibition function (Wroblewski, 1977). Following Wroblewski (Wroblewski, 1977), and most ecosystem models since, we assigned the inhibition parameter (ψ) a value of 1.462 $[\mu M\ N]^{-1}$. Reflected in their half-saturation constants, the two phytoplankton size fractions were assumed to have different preferences for the two nitrogen pools. Small

phytoplankton, generally more proficient at utilizing low levels of nutrients (Evans and Parslow, 1985), had a smaller half-saturation uptake for ammonium than large phytoplankton. Small phytoplankton's half saturation uptake for nitrate was considered larger than for ammonium, reflecting a general preference for ammonium (Legendre and Rassoulzadegan, 1995). Large phytoplankton had a smaller half-saturation uptake for nitrate than ammonium because in cold water this size class preferentially takes up nitrate even when ammonium is present (Lomas and Glibert, 1999).

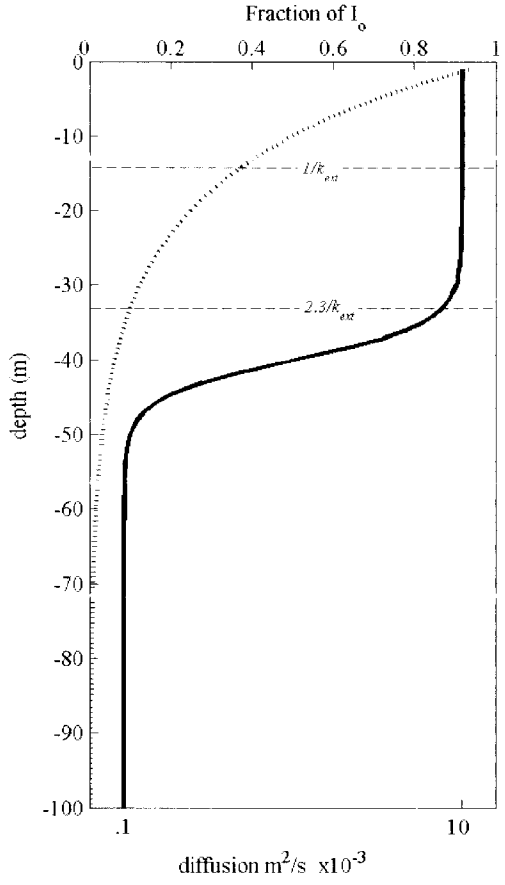

Figure 4-2 Vertical diffusion and light extinction profiles used in the model.
The solid line represents the diffusion profile and the dotted line represents the light profile. The important depths associated with these stationary forcing functions are the e-folding depth ($1/k_{ext}$) for the light extinction, the midpoint of the euphotic zone ($2.3/k_{ext}$), the top of the pycnocline at approximately 30 meters, and the bottom of the pycnocline at approximately 50 meters.

Both phytoplankton size fractions suffered losses due to natural mortality and zooplankton grazing. Mortality of each phytoplankton size class was taken to be a constant fraction of the standing stock and was assumed to be higher for the smaller cells. Both size fractions could potentially be grazed by either of the zooplankton size fractions. The form of the grazing function varied and is discussed further below.

Zooplankton Equations.

The dynamics of the two zooplankton components were described by

$$\frac{dZ_1}{dt} = \gamma_1 \cdot (G_{11} + G_{12}) - G_{ZZ} - M_Z \qquad \text{Eq. 4.5}$$

$$\frac{dZ_2}{dt} = \gamma_2 \cdot (G_{21} + G_{22} + G_{ZZ}) - H \qquad \text{Eq. 4.6}$$

The mesozooplankton fraction (Z_2) was considered to represent mainly coastal copepods common in the coastal Gulf of Alaska, while the microzooplankton fraction (Z_1) was considered to consist of mainly heterotrophic dinoflagellates and ciliates. The diet of copepods is known to be very diverse (Kleppel, 1993) and members of this group can potentially feed on microzooplankton (Gifford and Dagg, 1988; Jonsson and Tiselius, 1990), large phytoplankton such as diatoms (Corkett and McLaren, 1978; Dagg and Walser, 1987; Dagg, 1995) and even nanoplankton (Kleppel, 1993; Kleppel *et al.*, 1996). Microzooplankton are also able to consume a wide range of particle sizes. Observational studies in the coastal Gulf of Alaska (Strom *et al.*, 2001) have found that microzooplankton were just as effective at feeding on large plankton (>8μm) as they were at feeding on small plankton (<8μm). To reflect our understanding of this ecosystem, mesozooplankton were assumed capable of grazing on both small and large phytoplankton and microzooplankton. Microzooplankton were assumed able to graze on

both phytoplankton size fractions. Capture efficiency parameters were chosen to represent an ecosystem in which, due to size restrictions, microzooplankton could capture small phytoplankton with a greater efficiency than large phytoplankton, and mesozooplankton could capture microzooplankton, large phytoplankton and small phytoplankton with a decreasing order of efficiency. Microzooplankton were assigned a maximum grazing rate of 1.2 day^{-1}, which was the maximum found for this size class in the coastal Gulf of Alaska in May (Strom *et al.*, 2001). This was higher than the maximum grazing rate (0.7 day^{-1}) assigned to the mesozooplankton. The microzooplankton were also able to respond more rapidly (smaller half-saturation constant) to increases in phytoplankton biomass than the mesozooplankton, whose growth was assumed to be not as tightly coupled to the phytoplankton.

Five different functional forms for zooplankton grazing on multiple prey types were implemented, all of which had previously been used in ecosystem modeling studies. The formulations for each grazing function are presented in Table III. Schematics to illustrate the essential differences between each of these functions are presented in Figure 4-3. Grazing functions I, II and III are extensions of the 'Michaelis-Menten' and 'Threshold' single resource functional responses curves to multiple nutritional resources (prey items). Functions IV and V are two alternative extensions of the single resource sigmoidal function to multiple prey types. Function I never provides rare prey with a reprise from grazing. Functions II and IV provide prey with a reprise from zooplankton grazing pressure only if the combined concentration of all prey resources is sufficiently small. Functions III and V permit scarce prey with a reprise from grazing pressure even if concentrations of alternative prey items are high. With function V, this prey refuge persists even when only one prey type remains. With function III, once the prey field has been reduced to a single nutritional resource, the functional form for grazing is similar to function I.

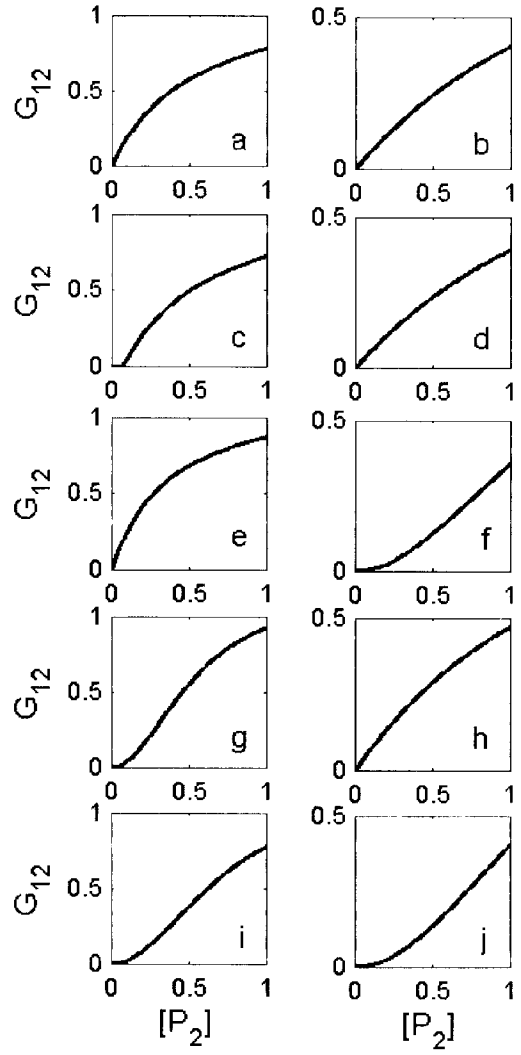

Figure 4-3 Schematic of the key differences between the five grazing functions. Grazing by Z_1 on P_2 when P_1=0 and when P_1=1 with grazing function I (a and b), function II (c and d), function III (e and f), function IV (g and h), and function V (i and j).

Grazing functions I and II used in this research have been categorized as 'Class 1 multiple functional responses' by Gentleman *et al.* (Gentleman *et al.*, 2003) because they assume passive selection and no switching. Grazing function III is also an extension of

the 'Michaelis-Menten' curve; however, this function incorporates 'capture efficiencies' (or preferences) that vary with prey ratios. This function is categorized as a 'Class 3 (proportion based) multiple functional response' (Gentleman *et al.*, 2003) because the capture efficiencies are density dependent, varying with the densities of other resources. Function V is a 'Class 2 (Sigmoidal I) multiple functional response' (Gentleman *et al.*, 2003). Grazing function IV has not been classified under this scheme, however its nutritional intake behavior is similar to grazing function II.

In addition to grazing pressure by mesozooplankton, microzooplankton experienced natural mortality at a constant specific rate. In reality, mesozooplankton also suffer losses due to natural mortality and predation by higher trophic levels. However, due to the uncertainty associated with both of these terms, we combined them into a single term ($H=h\cdot Z_2^q$), which is referred to throughout as 'predation'. H is effectively the model closure term. Common choices for the predation exponent are $q=1$ (Evans and Parslow, 1985; Fasham *et al.*, 1990) or $q=2$ (Denman and Gargett, 1995; Fasham, 1995). The former parameterization represents a predator that exhibits a constant response to zooplankton prey numbers (linear closure), this could be thought of as a simple filter feeding strategy. The later parameterization (quadratic closure) is thought to represent a predator that exhibits an ambush feeding strategy, being attracted to large concentration of zooplankton and less inclined to feed at low concentrations. It is thought, however (Edwards and Bees, 2001), that because a predators' effective reaction distance varies with the turbulent energy dissipation rate, the proportion of predators adopting each strategy will vary in a continuous fashion depending on the environmental and physical conditions. Non-steady model solutions are not necessarily eliminated with the use of quadratic closure, as was once thought (Steel and Henderson, 1992). Rather much of an NPZ model's dynamical behavior is generic, occurring for any exponent of closure between one and two (Edwards and Bees, 2001). In light of this finding, we chose to explore the dynamics of our model with a non-integer predation exponent that was varied from linear to quadratic ($1\leq q \leq 2$) while the specific predation rate (h) was varied over a biologically realistic range (0.05-2.4 $[gCm^{-3}]^{1-q}$ day^{-1}).

Diffusion

Within the model, the purely biological dynamics (equations 1–6) were subjected to vertical mixing. This physical forcing was represented by the addition of a term (equation 7) to each of the six biological equations.

$$\frac{\partial}{\partial z}\left(Kv\frac{\partial C_i}{\partial z}\right) \qquad \text{Eq. 4.7}$$

where z is depth, Kv is the vertical diffusion coefficient, and C_i represents each of the model components P_1, P_2, Z_1, Z_2, N_1, and N_2.

It is known that the magnitude of diffusion can modify the non-linear dynamics of an NPZ model (Edwards *et al.*, 2000). Therefore, to best understand the NPZ model dynamics without the complications of temporally varying physical forcing, model behavior was explored in the presence of stationary but spatially varying levels of diffusion. The vertical diffusion profile was described by

$$Kv(z) = Kv_b - \left(\frac{Kv_b - Kv_m}{\tanh(\Phi_{100}) - \tanh(\Phi_1)}\right) - \left(\frac{Kv_b - Kv_m}{\tanh(\Phi_{100}) - \tanh(\Phi_1)}\right) \cdot \tanh\left(\frac{-\Phi(z)}{\psi}\right) \qquad \text{Eq. 4.8}$$

Although simplified, this approach provided a somewhat realistic structure, with a smooth transition between the higher coefficient of diffusion (Kv_m=1x10^{-3} m^2 s^{-1}) in the surface mixed layer and the smaller background value (Kv_b=1x10^{-5} m^2 s^{-1}) below (Figure 4-2). The shape parameters, $\Phi(z) = z - 40$ (where z=[1,2,3,...100]) and $\psi = 5$, which respectively define the position and thickness of the pycnocline, were used to give a mixed layer of about 40 meters and a pycnocline about 20 meters thick, appropriate conditions for the coastal Gulf of Alaska in spring (Luick *et al.*, 1987). No flux boundary conditions were enforced at the upper and lower boundaries, *i.e.*,

At z=0 and 100m

$$Kv\frac{\partial P_1}{\partial z} = Kv\frac{\partial P_2}{\partial z} = Kv\frac{\partial Z_1}{dz} = Kv\frac{\partial Z_2}{\partial z} = Kv\frac{\partial N_1}{\partial z} = Kv\frac{\partial N_2}{\partial z} = 0 \qquad \text{Eq. 4.9}$$

4.3.3 Analysis

The dynamics of our NPZ model were compared when five alternative functional forms for zooplankton grazing (G) were implemented, and the predation exponent (q) and the specific predation rate (h) in the predation term (H) were systematically varied over a biologically realistic range. For each model simulation, we attempted to find the steady solutions of the non-linear system of six equations iteratively. Each model was initially run for 300 time steps (days), and the resulting solution provided as a starting guess to a numerical solver of the steady state solution (equations 4.1–4.6 with the left hand sides set to zero). Following Edwards *et al.* (Edwards *et al.*, 2000), for a model to be classified as steady, the associated time derivative terms were required to be smaller than 10^{-4}. Models that failed to converge to a steady solution were run for a further 700 days, and the time series solution on the one-thousandth day was provided to the numerical solver. These solutions were then reclassified. Any solution which could not be classified as steady was manually examined, at the 25 meter depth, to determine if behavior was periodic (limit cycles) or something more complex. This process of time stepping solutions for 1,000 days followed by examination of the solution trajectory was repeated until we were confident that the solutions were indeed limit cycles and not anything more complex. The last 500 days of all non-steady solutions were used to determine the period of oscillations. In order that the model makes biological sense, concentrations of all model components were restricted to positive finite or zero values.

4.4 Results

Model behavior was dependent on the total predation experienced by the mesozooplankton ($H=h\cdot Z_2^q$), rather than just on the predation exponent (q) or the specific predation rate (h) (Figure 4-4). The relationship between the predation rate and the two predation parameters was dependent on the concentration of Z_2. As the concentration of

Z_2 increased, H became more dependent on h than q. Relatively high predation on mesozooplankton resulted when the predation exponent (q) was close to one (linear predation) or when the specific predation rate (h) was large. Conversely, relatively low predation resulted when the predation exponent approached two (quadratic predation) or the specific predation rate was small.

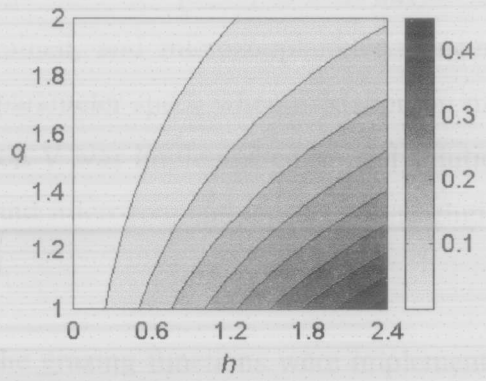

Figure 4-4 Predation on mesozooplankton ($H=h\cdot Z_2^q$) over h and q parameter space. Non-dimensional mesozooplankton concentration (Z_2) was set to 0.1. Note that as the concentration of Z_2 is increased H will become more dependent on h than q.

With some of the grazing functions (I, II, and IV) it was not common to have all six model components existing simultaneously; solutions often comprised negligible concentrations (scaled concentrations $< 10^{-6}$) of at least one model component (Figure 4-5). The structural composition of model solutions was largely dependent on the choice of grazing function. For all grazing functions, when predation on mesozooplankton was high, the mesozooplankton component had negligible concentrations, and microzooplankton became the dominant grazer in the system. When implementing grazing functions I, II, and IV, the maximum concentrations of each plankton component were similar throughout q and h parameter space. In each case, there was a clear boundary between two predominant forms. When predation on mesozooplankton was

medium to high, solutions predominantly comprised large phytoplankton, microzooplankton, nitrate, and ammonium. When the predation on mesozooplankton was low, solutions were dominated by small phytoplankton, mesozooplankton, nitrate, and ammonium. It was rare for both phytoplankton size classes to simultaneously have non-negligible concentrations. As such, there was only a narrow region, corresponding to intermediate predation, where all six model components could simultaneously coexist. With function III, both large and small phytoplankton thrived simultaneously throughout the parameter space examined, and microzooplankton concentrations were negligible only in a small region of parameter space when predation on mesozooplankton was very low. When grazing function V was implemented, model solutions comprised both small and large phytoplankton and microzooplankton, in non-negligible concentrations for all parameter space examined.

Irrespective of which of the grazing functions were implemented, steady state solutions could not be found for some regions of the q-h parameter space examined (Figure 4-6a–e). With each grazing function, as q and h were varied there was at least one clear Hopf bifurcation, where the qualitative form of the solution shifted between attraction to a steady equilibrium (see Figure 4-7a-d for example) and a periodic limit cycle (see Figure 4-7e-h for example). With grazing functions I, II, and III, steady solutions could not be found for the majority of the parameter space (Figure 4-6a–c). With each of these model variants, when the total predation on mesozooplankton (H) was medium to high, model trajectories were oscillatory. As predation became relatively small, there was a Hopf bifurcation with a transition to steady solutions. In the case of grazing function III, at very low predation a second bifurcation returned solutions to an oscillatory regime (Figure 4-6c). With grazing functions IV and V, model solutions reached a steady state for much of the parameter space examined (Figure 4-6d and e). In both cases, there were, however, still two clear Hopf bifurcations as q and h were varied. With these two model variants, we found model solutions to be steady at high predation, to undergo a bifurcation to oscillatory behavior in the region of intermediate predation, and to undergo a second bifurcation back to a steady regime at low predation.

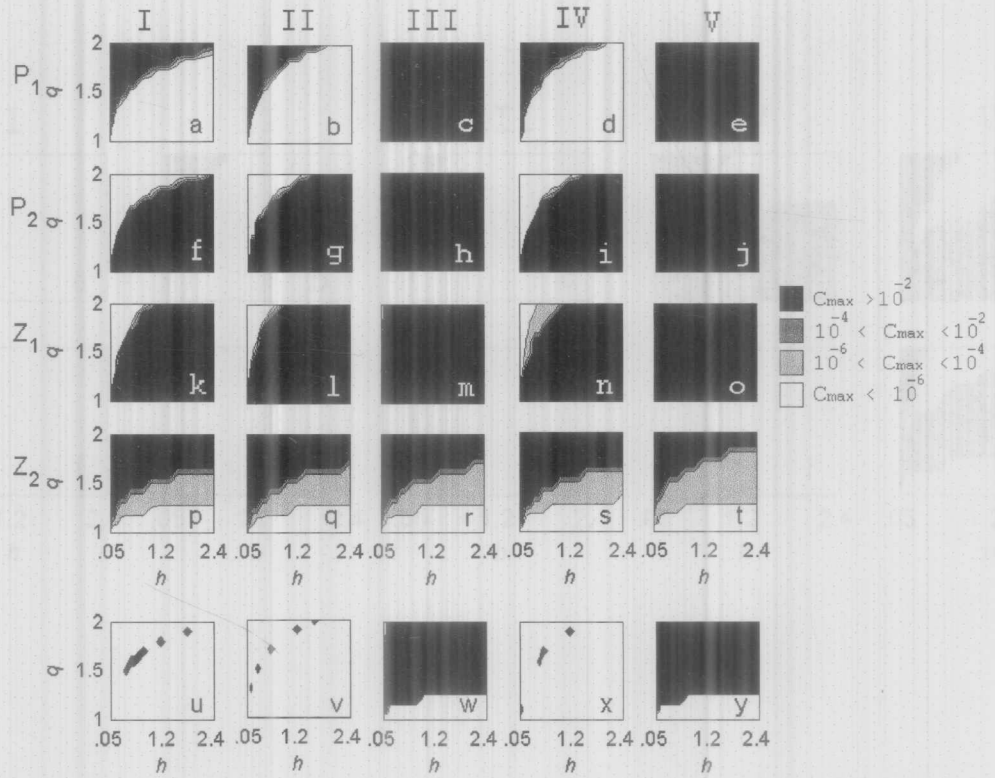

Figure 4-5 Maximum non-dimensional concentration of the four plankton components.
If solutions were steady, maximum plankton concentrations over all depths at equilibrium were used. If solutions were oscillatory, maximum plankton concentrations over all depths, over the last 200 days of a simulation were used. C_{max} represents the maximum concentration of each of the plankton components (P_1, P_2, Z_1, Z_2). For the five grazing functions as indicated; (a-e) P_{1max}, (f-j) P_{2max}, (k-o) Z_{1max}, (p-t) Z_{2max}. The region of q-h parameter space for which all model components had non-negligible concentrations simultaneously is also indicated (u-y). Note that N_1 and N_2 had non-negligible concentrations throughout q-h parameter space with every simulation.

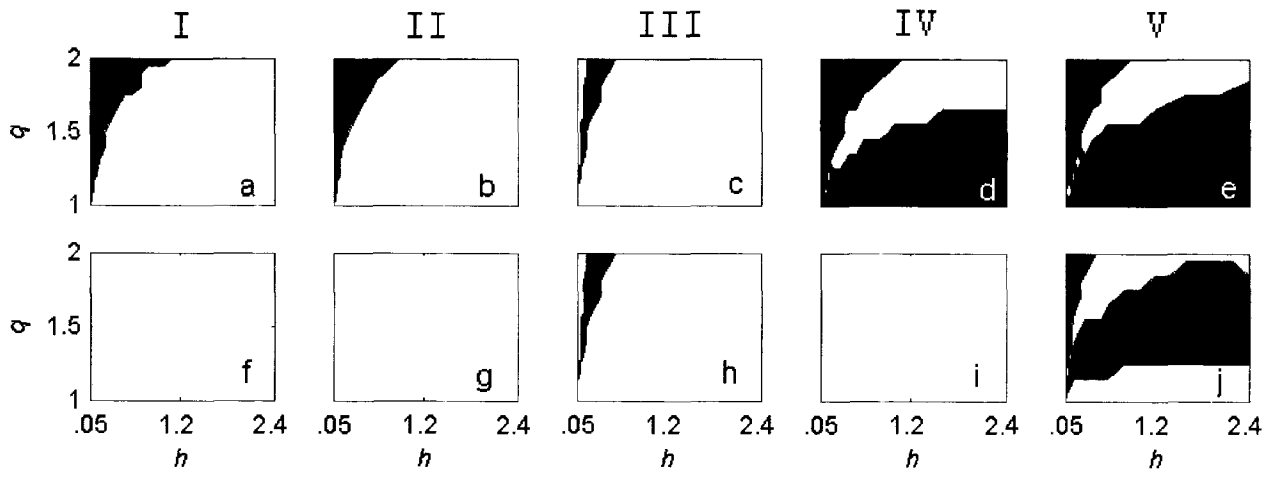

Figure 4-6 Classification of model solutions over q and h parameter space.
Regions of q-h space where model solutions were at steady equilibrium (shaded black) and were limit cycles (white) for each of the five grazing functions (a) function I, (b) function II, (c) function III, (d) function IV, (e) function V. Regions of q-h space where model solutions reached a steady equilibrium and all six model components were simultaneously non-negligible are also shown (shaded black) (f) function I, (g) function II, (h) function III, (i) function IV, (j) function V.

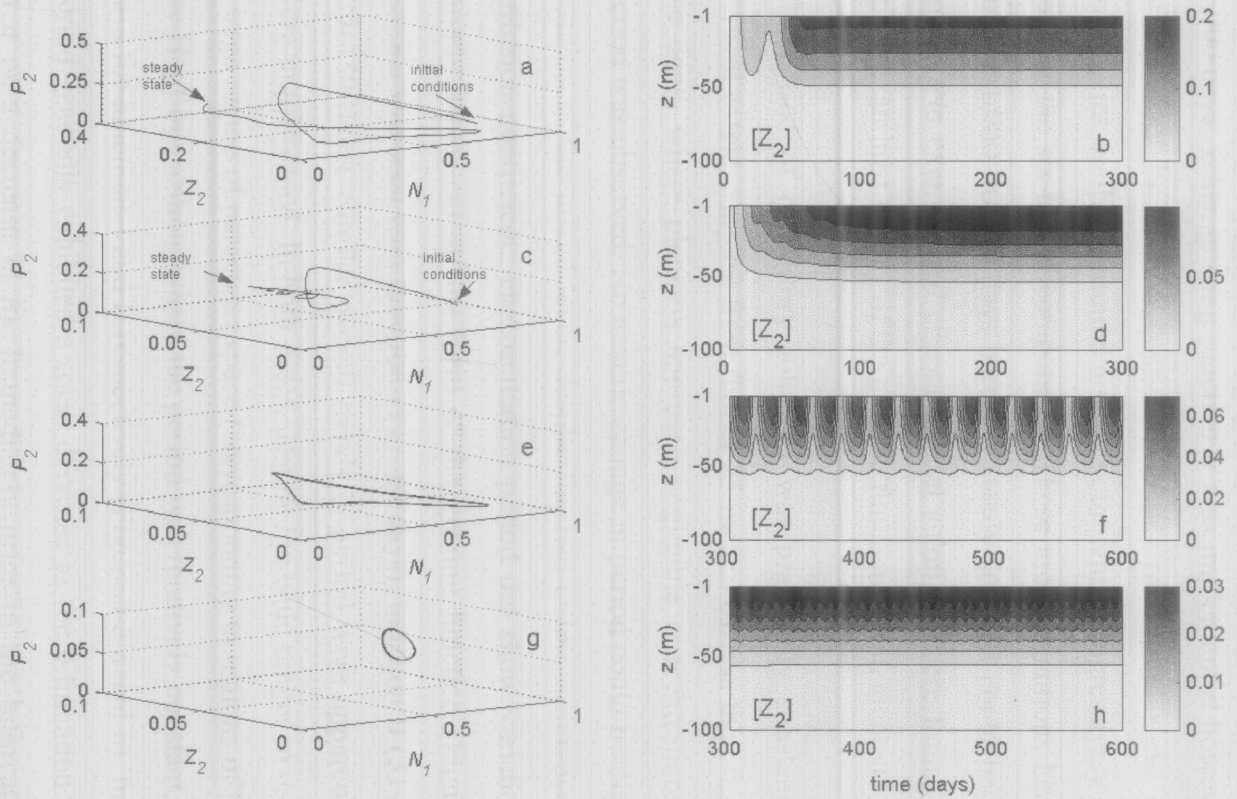

Figure 4-7 Examples of steady and non-steady solutions.
Illustrated with three dimensional (N_1, P_2 ,Z_2) phase space diagrams and corresponding time series solution for Z_2. (a) steady solution when grazing function=III, q=2, h=.4, (b) steady solution when grazing function=V, q=2, h=.4, (c) limit cycle solution when grazing function=III, q=2, h=1.4, (d) limit cycle solution when grazing function=V, q=2, h=1.4. Note that in the case of limit cycle solutions the transient behavior is not shown.

Model trajectories that did not reach a steady equilibrium solution described closed limit cycles wherein the population numbers underwent well-defined cyclic changes in time. Most oscillatory solutions had settled into a limit cycle trajectory at 25 meters depth after 1,000 days. When grazing function V was implemented however, several solutions close to the Hopf bifurcation continued to describe spiral sinks at this time, wherein the trajectories oscillated around a fixed point while progressively decreasing in amplitude of each of the six model components. These model solutions had to be time stepped for a further 1,000–10,000 days before a steady solution could be found with the numerical solver. No examples of chaotic model solutions were found throughout the parameter space examined for any of the grazing functions implemented.

The period of oscillatory solutions was practically constant throughout the model's vertical extent, varying from that at 25 meters by less than 0.3% at most depths. Below the depth where plankton approach negligible concentrations, more variability in the period was observed. No notable change in period could be discerned with respect to the position of the mixed layer, despite the two orders difference in the magnitude of the diffusion coefficient. The oscillation period did show variation with q and h, but was largely dependent on the form of the grazing function (Figure 4-8). A wide range in periods was seen with function I (37–97 days), function II (31–86 days), and function III (29–159 days). Similar overall trends in period were apparent when functions I and II were implemented. In both cases, despite the wide ranges in oscillation period, there was a large region of parameter space (corresponding to regions of high predation) away from the Hopf bifurcation, where the period was relatively constant, approximately 65 and 39 days for functions I and II respectively (Figure 4-8 a and b). In both cases the oscillation period generally exhibited a small decrease as the bifurcation was approached (increase in q or a decrease in h). Immediately prior to the bifurcation, however, the period increased rapidly, approaching infinity in the region of steady solutions. When grazing function III was implemented, in addition to the large difference in the oscillation period on either side of the Hopf bifurcation, no region of constant period was found (Figure

4-8 c). Rather, there was a notable decline in period approaching either of the Hopf bifurcations. The oscillation period was lower in the region of medium to high predation compared to the region of 'low' predation. The period of oscillation covered only a narrow range (30–40) days with function IV (Figure 4-8d), while with function V, the period, at approximately 16 days, was short and practically constant with variations in h and q (Figure 4-8e).

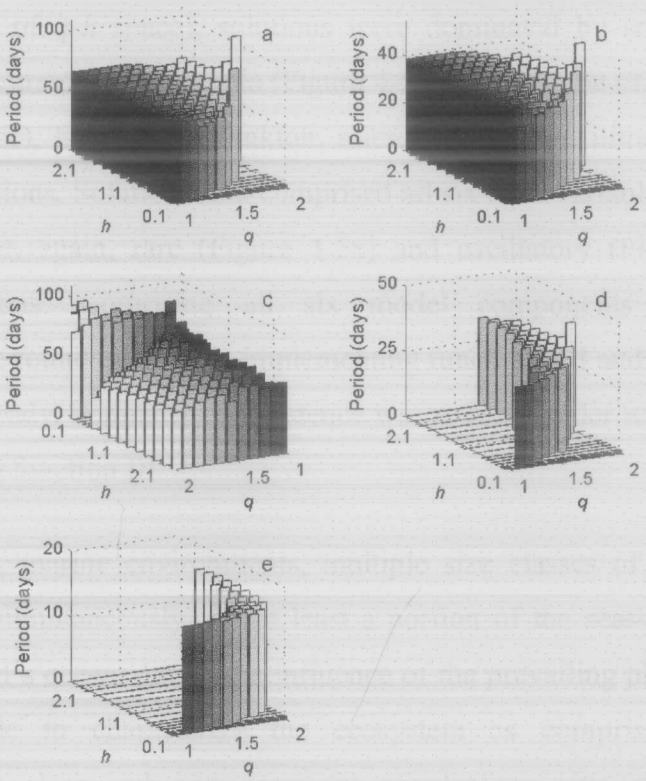

Figure 4-8 Variation in period of oscillation over q and h parameter space.
When implementing the five alternate grazing functions. (a) function I, (b) function II, (c) function III, (d) function IV, and (e) function V. The oscillation periods shown were calculated from the final 500 days of time series data at 25 meters; however, these values are representative of the period throughout the mixed layer. For clarity, the scale of the axis in each plot varies and the x and y axis in (c) have been permuted. Note that in the region of steady solutions the period of solution goes to infinity, and not zero as shown.

The non-linear dynamics of model solutions correlated well to their structural composition. With grazing functions I and II, equilibrium solutions that comprised only small phytoplankton, mesozooplankton, nitrate, and ammonia were generally steady, while equilibrium solutions that predominantly comprised large phytoplankton and microzooplankton, nitrate, and ammonium were oscillatory. The narrow regions of parameter space that did comprise all model components in non-negligible concentrations (Figure 4-5u and v) were non-steady (Figure 4-6f and g). Models with grazing function IV had steady equilibrium solutions at both high and low H. In the region of low H (upper left portion of q-h space), solutions were dominated by small phytoplankton, mesozooplankton, nitrate, and ammonia (Figure 4-5). In the region of high H (lower right portion of q-h space), large phytoplankton, microzooplankton, nitrate, and ammonium dominated the solutions. Solutions that comprised all six state variables in non-negligible concentrations were, again, rare (Figure 4-5x) and oscillatory (Figure 4-6d). Steady equilibrium solutions comprising all six model components in non-negligible concentrations were found only when implementing functions III and V (Figure 4-6h and j). The region of steady, permanent coexistence was much broader with grazing function V than with grazing function III.

In most, if not all, marine environments, multiple size classes of phytoplankton and zooplankton exist simultaneously, for at least a portion of the seasonal cycle. In some regions of the world's ocean, due to the influence of the prevailing physical dynamics, it becomes acceptable to characterize the ecosystem as comprising one dominant phytoplankton size class and one dominant zooplankton size class. For example, upwelling systems are generally dominated by large phytoplankton and mesozooplankton. However, we believe that a successful model should be capable of simulating an ecosystem in which multiple size classes can prevail, and it should be the prescribed forcing to which the ecosystem model is subjected that determines the final composition of the model solution. In general, although individual species do disappear over a seasonal cycle, we do not expect the aggregate to disappear. Additionally, for the sake of modeling convenience, the elimination of a trophic level is generally considered

highly undesirable. As we were only able find solutions which comprised all model components for a narrow region of parameter space when implementing grazing functions I, II, and IV, we did not consider these model variants further in this investigation. We focus on comparing and contrasting solutions obtained when implementing grazing functions III and V because these model variants are capable of producing solutions comprising all model components for the majority of parameter space examined.

All steady equilibrium solutions obtained when implementing grazing functions III and V had vertical profiles that shared many features (see Figure 4-9 for examples). In each case nitrate concentration was low in the surface mixed layer but increased with depth to dominate the system below the bottom of the mixed layer. Conversely, the concentration of all plankton components decreased with depth from maximum values at the surface. Ammonium always exhibited a sub-surface maximum close to the midpoint of the euphotic zone ($2.3/k_{ext}$). Although small and large phytoplankton and microzooplankton did not persist much below the bottom of the mixed layer, mesozooplankton, when present at steady state, persisted well below this.

Despite these general commonalities, the vertical profiles as q and h space was traversed differed quite markedly with the two grazing functions. Rather than presenting the full vertical profile for each steady solution, the change in concentration of each model component with q and h at 10 meters depth was used to illustrate changes to the complete vertical profile with these parameters. Changes to the concentration of model components at this depth were representative of the trends exhibited at all depths. With both grazing functions III and V, when mesozooplankton concentrations were negligible (q close to 1), variations in h had little influence on model solutions. With grazing function III, there was only a small region of parameter space where the model produced steady equilibrium solutions (Figure 4-10). There was nowhere within this region that the vertical profiles could be considered to remain constant with h. With this grazing function, there were no steady solutions when predation was linear (q=1), but as q was increased and the Hopf

bifurcation traversed, the vertical concentration profiles for each steady solution varied smoothly but markedly as h varied. Within this steady region, increasing h resulted in an increase followed by a decrease in P_1, an overall increase in P_2 and Z_1, a decrease in Z_2, and a slight decrease followed by a slight increase in N_1 and N_2. With grazing function V, there were two regions of parameter space, on either side of the Hopf bifurcation, where the model had steady solutions. Within the first region (high total predation), concentrations of each model component varied very little with q or h, even approaching the first Hopf bifurcation (Figure 4-11). As mentioned previously, this was in large part due to the low concentrations of mesozooplankton in this region. Throughout this region the vertical profile closely resembled those shown in Figures 4-9a and b. Both phytoplankton size fractions had similar vertical profiles, although the concentration of P_2 exceeded that of P_1 at every depth. Concentrations of Z_1 were approximately twice that of the phytoplankton at every depth. Z_2 had negligible concentrations throughout the water column. Following the second Hopf bifurcation, moving into the region of low predation, model components reached alternative steady states. Within this second region of steady solutions, the vertical profiles of each model component changed smoothly but rapidly with q and h. Moving away from the bifurcation (increasing q, decreasing h), there was an overall decrease in P_2, Z_1, N_1, and N_2, and an overall increase in P_1 and Z_2 at each depth within the mixed layer.

The non-steady solutions obtained with both grazing functions III and V also provided an insight into the fundamental dynamics of the two model variants. With function V, the maximum and minimum concentrations of each model component reached during a limit cycle varied smoothly and continuously with h and q as the Hopf bifurcation was traversed (Figure 4-11). With function III, in the region of medium to low predation, away from the Hopf bifurcation, the maximum concentrations of each of the model components reached during the limit cycles remained relatively constant as h was increased (Figure 4-10). The amplitude of limit cycles obtained with function III tended to be much greater than those obtained with function V. In the former case (function III), the concentrations of model components tended to oscillate between a maximum

(approaching 1 in the case of nitrate) and negligible concentrations. In the latter case (function V), the maximum concentration attained by any of the model components was smaller than the equivalent model with grazing function III, and the minimum values were always non-negligible. This difference in oscillation amplitude can also clearly be seen in the phase space plots of limit cycle solutions (Figure 4-7c and d).

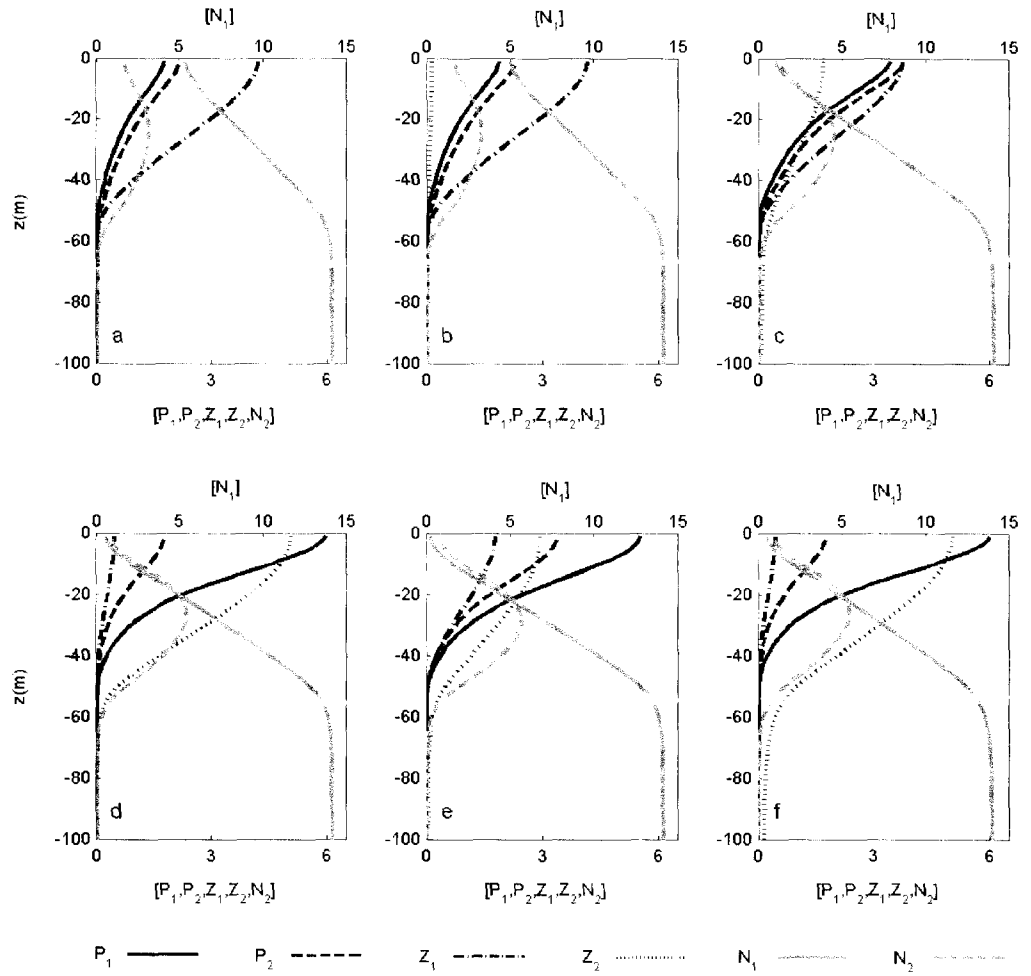

Figure 4-9 Equilibrium profiles of scaled concentration for the six model components. When implementing grazing function V with (a) h=.06, q=1, (b) h=.06, q=1.5, (c) h=.06, q=2, and when implementing grazing function III with (d) h=.06, q=1.5, (e) h=.1, q=1.5 and (f) h=.1, q=2. Note that the nitrate (N_1) profile is plotted on a different scale for clarity.

Sensitivity to parameter values and initial conditions

Past studies have shown that model dynamics can be sensitive to both parameterization and initial conditions (Popova *et al.,* 1997; Edwards and Yool, 2000). In the Gulf of Alaska, the maximum photosynthetic growth P_{max} was found to be equivalent for both phytoplankton size fractions (Strom *et al.*, 2001). With an alternate size division, or in other ecosystems, this may not be the case. To see how the model dynamics presented above would be impacted by a change in this parameter, we held the initial conditions and all other parameter values constant, but reduced the maximum photosynthetic growth for large phytoplankton (P_{max2}) to 1 day^{-1}, half that for the small phytoplankton. We explored the model dynamics over a course resolution *q-h* parameter space for the structurally most dissimilar grazing functions, I and V. Patterns of dynamical model behavior were found to be similar to those presented above. Model solutions generally came to oscillatory limit cycle solutions with grazing function I and steady equilibrium solutions with function V. The locations of the Hopf bifurcations, in both cases, were similar to those found with the original model parameterization. With grazing function V, the structural composition of model solutions was also similar to that arising with the original parameterization. With grazing function I and the alternative parameterization of P_{max} model solutions comprised small phytoplankton throughout *q-h* space, while large phytoplankton had negligible concentrations.

To test the sensitivity of our model to initial conditions we doubled the initial nitrate concentration from 10 μM to 20 μM. All other initial concentrations and parameter values were as for the original model. Again, with grazing functions I and V, the patterns of model behavior were little changed to those presented for the original model. The notable difference was the presence of a second Hopf bifurcation at low total predation (*H*) when implementing grazing function I. With both grazing functions I and V, the structural composition of model solutions, with respect to survivorship of model components, was little different to that presented for the original initial conditions.

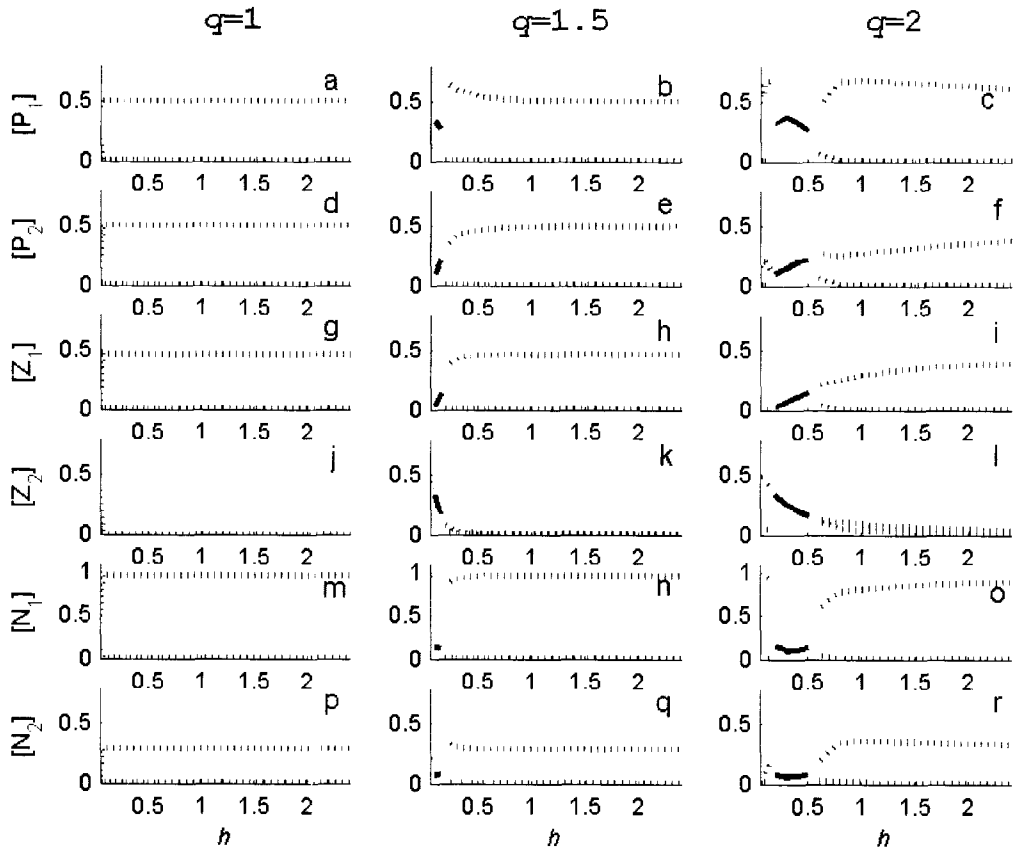

Figure 4-10 Bifurcation diagrams when grazing function III is implemented.
For $q=1$, 1.5, and 2 as indicated. (a-c) P_1, (d-f) P_2, (g-i) Z_1, (j-l) Z_2, (m-o) N_1 and (p-r) N_2. The dotted lines indicate the maximum and minimum and concentrations reached during the cycle of an oscillatory solution. The solid line indicates the equilibrium concentration reached in steady solutions. Data shown is for the 10 meter depth level.

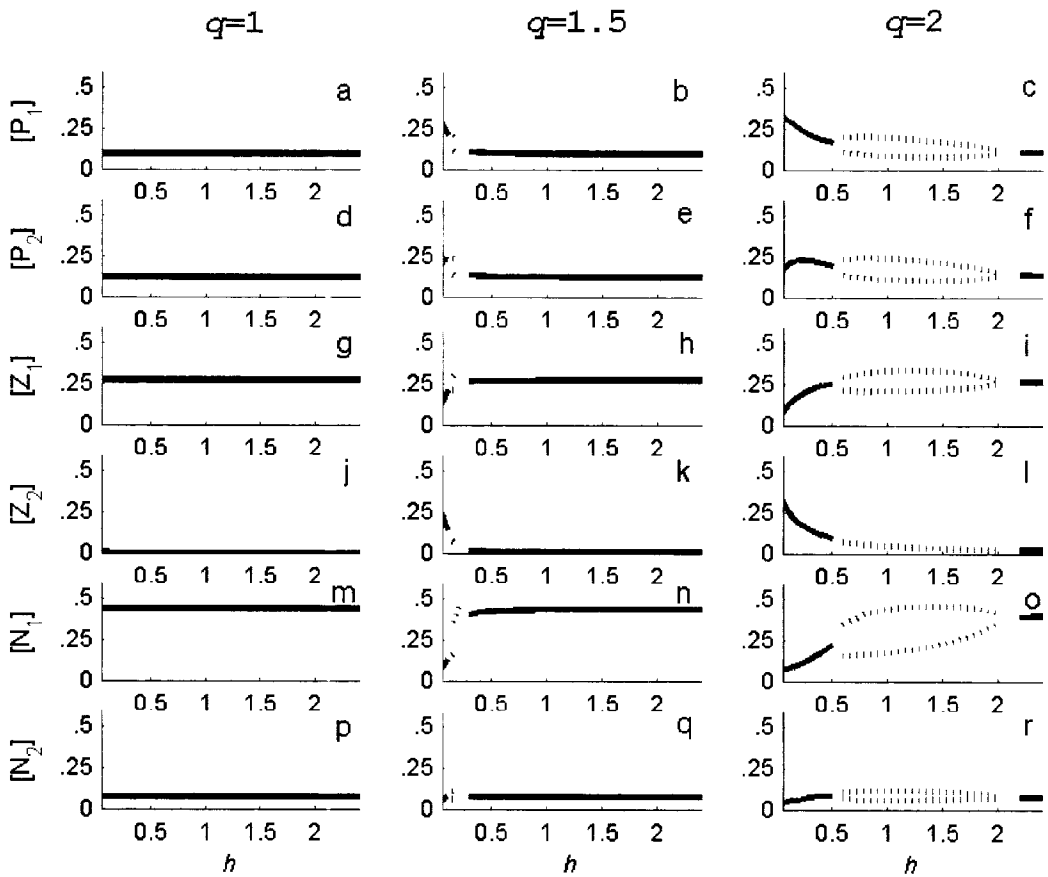

Figure 4-11 Bifurcation diagrams when grazing function V is implemented.
For $q=1$, 1.5, and 2 as indicated. (a-c) P_1, (d-f) P_2, (g-i) Z_1, (j-l) Z_2, (m-o) N_1 and (p-r) N_2. The dotted lines indicate the maximum and minimum concentrations reached during the cycle of an oscillatory solution. The solid line indicates the equilibrium concentration reached in steady solutions. Data shown is for the

4.5 Discussion

This investigation explored the equilibrium dynamics of a depth-explicit, one-dimensional, six-component NPZ model in which zooplankton could graze on multiple nutritional resources. The model was parameterized for the coastal Gulf of Alaska ecosystem, and was subjected to stationary physical forcing. We systematically varied the specific predation rate (h=0.05-2.4 [g C m^{-3}]$^{1-q}$ day^{-1}), the form of the predation function ($1 \leq q \leq 2$), and the form of the grazing function.

Classic stability analysis has been used to investigate the dynamical behavior of simple NPZ models (Franks *et al.*, 1986; Edwards and Brindley, 1999; Edwards *et al.*, 2000), and more complex models that retain the assumption of a homogeneous mixed layer (Ryabchenko *et al.*, 1997; Armstrong, 1999). Such studies have provided the foundation for understanding NPZ model dynamics. However, it is essential that we extend this knowledge to the more complex NPZ models now commonly used in ecosystem studies. It is not possible to find an analytical solution to our intermediately complex, spatially explicit model. Therefore, the classic approach to stability analysis, determination of the eigenvalues of the Jacobian (community) matrix, was of limited use for classifying model behavior. Despite this obstacle, it is important to gain an appreciation of the dynamics of such complex systems. Therefore, we examined model trajectories in time and space, numerically seeking and classifying the equilibrium solutions. This analysis provides a useful insight into behavior of models where zooplankton grazers, subjected to a depth-explicit mixing profile, can feed on a mixed prey field.

The total predation ($H=hZ_2^q$) experienced by the mesozooplankton and the form of the grazing function played an important role in governing the non-linear dynamics of this intermediately complex ecosystem model. In agreement with past investigations using simpler NPZ models (Edwards and Bees, 2001), we found that limit cycles can be found for all predation exponents and are not exclusively a result of using a linear ($q=1$) form of predation. With each of the five grazing functions, we found Hopf bifurcations spanning

the q and h parameter space, where the form of the solution transitioned between steady equilibrium and periodic limit cycles. A three-component, one-predator, one-prey model with a sigmoidal grazing function has been shown to have two Hopf bifurcations that span q and h space bounding a region of limit cycle behavior (Edwards and Bees, 2001). We have shown that sigmoidal grazing functions extended to multiple nutritional resources (functions IV and V) give rise to similar patterns of bifurcations in our more complex model (Figure 4-6 d and e). Additionally, we have shown that Hopf bifurcations also exist when implementing alternative extensions of the Michaelis-Menten grazing function to multiple nutritional resources (functions I, II, and III). With these functional forms, however, limit cycle behavior was found to be the more prevalent form for model solutions. Only in a narrow region of parameter space did these grazing functions give rise to steady equilibrium solutions. This pattern of behavior, with a region of stable steady states surrounded by two regions of oscillations, is interesting because it is opposite to that found previously (Edwards and Bees, 2001). It is interesting to note that while we found Fasham's switching grazing model (grazing function III) to only rarely produce models that were dynamically stable, Armstrong (Armstrong, 1999) found that a model with 'distributed grazing' being modeled at a community level for a single zooplankton species was dynamically stable under a wide range of conditions.

The period of the limit cycle solutions depended predominantly on the form of the grazing function. When either variants of the sigmoidal grazing function were implemented (functions IV and V), the period of oscillation remained relatively constant over q and h space. The period of limit cycles produced by a three-component NPZ model with sigmoidal grazing has also been found to be about constant at 34–35 days (Steele and Henderson, 1992; Edwards and Brindley, 1996). This is well within the range of 30 to 40 days that we found when implementing grazing function IV. This investigation brings to light the fact that alternative forms of the grazing function can result in very different oscillation periods, and regions of near constant period may not exist. The existence of chaos in NPZ models has been well documented (Popova *et al.*, 1997; Edwards and Bees, 2001). For a one-predator, two-prey ecosystem, with a grazing

function equivalent to function V, model solutions have been shown to exhibit chaotic behavior when forced externally with an annual physical cycle (Popova *et al.*, 1997). With the stationary physical forcing (light level and mixing curve) used in this investigation, we did not find any examples of chaotic solutions for any of the grazing functions tested. Implementation of seasonally varying physical forcing, or a finer resolution exploration of q-h parameter space, could reveal a different result.

Permanent coexistence of model components at equilibrium was strongly influenced by the choice of grazing function. It was rare for all predators and prey to exist simultaneously when implementing I, II, and IV. This is in line with the conclusions by Armstrong (Armstrong, 1994), that such concave down functions tend to promote prey elimination. Although functions II and IV do have regions that will reduce or prevent entirely the elimination of rare prey, these reprises from zooplankton grazing do not come into effect until the total prey concentration has been reduced below a critical level. With all three of these grazing functions, the system typically purges itself until only one predator and one prey remain. Generally, if mesozooplankton were able to thrive (low total predation), microzooplankton and large phytoplankton were eliminated through competitive exclusion (mesozooplankton had higher affinity for these prey items), whereas if mesozooplankton succumbed to predation, microzooplankton became the dominant grazer and small phytoplankton were eliminated through competitive exclusion (microzooplankton had a higher affinity for this phytoplankton size class). The non-linear dynamics of the remaining four-component system was determined by the efficiency of the remaining grazer to capture the remaining prey. If the grazer was able to eat a large proportion of the prey (*i.e.*, microzooplankton grazing on large phytoplankton), the resulting solution tended to be periodic. Conversely, if the grazer could eat only a small proportion of the prey (*i.e.*, mesozooplankton grazing on small phytoplankton), a steady equilibrium was generally reached. With all three of these grazing functions, all six model components were able to coexist only in a narrow region defined by an intermediate level of total predation (H) on the mesozooplankton. Grazing functions III and V allow 'prey switching', with zooplankton eating a disproportional amount of the

abundant prey. When multiple nutritional resources were present, both of these functional response curves have regions where rare prey experience a reprise from grazing, even if the concentration of other available prey sources is relatively high. This ability of the zooplankton grazers to 'switch' prey enhances the likelihood that all plankton components will survive simultaneously (Hutson, 1984; Strom and Loukos, 1998) and so reduces the likelihood of prey elimination through competitive exclusion.

Our investigation focused on grazing functions III and IV because they produced solutions that comprised all model components and were steady, for at least some of the *q-h* parameter space examined. Balancing the best form of a grazing function from a modeler's point of view and from an observationalist's point of view can present a challenge. An observationalist may seek a form that appears to best describe the grazer under investigation. However, usually only one, or a few, species are considered at a time. Conversely, due to the necessary aggregation that modelers perform when seeking to describe an ecosystem, such a functional form may not be appropriate. Often, trophic levels rather than individual species are considered, and so certain functional forms may not make sense from a biological point of view. Additionally, the elimination of model components or the production of oscillatory model solutions are generally considered undesirable traits, and a grazing function that promotes such behavior would be less favored, although we stress that this may be due purely to modeling convenience. It could be argued that potentially, oscillatory solutions are just as realistic as steady solutions. Short-term oscillations in plankton have been observed for a few marine and freshwater ecosystems (Edwards, 2000; Ryabchenko *et al.,* 1997). However, due to inadequate sampling resolution we do not have a clear understanding of whether components of the coastal Gulf of Alaska ecosystem exhibit unforced oscillations in biomass. As with most observational studies, observational data in this region are not of a sufficiently high temporal resolution that they would capture short-term oscillations in ecosystem components such as those described above. Model solutions exhibiting unforced oscillations are, however, often considered undesirable because it makes it more difficult to discern any longer term periodicity (seasonal signal, annual, etc.).

There is much discussion in the literature with regard to the realism of different forms of grazing function. For example, there are many instances of switching reported (Kiørboe *et al.*, 1996; Gismervik and Andersen, 1997; Martin-Cereceda *et al.*, 2003), however, although microzooplankton have been shown to exhibit selective feeding, they do not necessarily alter their feeding behavior in response to a changing prey field, so stable prey trajectories are not necessarily observed under experimental conditions (Strom and Loukos, 1998). It is important to carefully consider the inherent assumptions behind a grazing function, particularly with functions that describe grazing on multiple nutritional resources, as they are not always obvious at first glance (Gentleman *et al.*, 2003). In fact, some of the most popular grazing functions, which include active selection of abundant prey (Class 3 multiple functional responses), are advised against because they have been found to produce wide regions of anomalous dynamics such as a decrease in total nutritional intake with an increase in resource density (Gentleman *et al.*, 2003). Function III investigated here falls within this class, although with our model parameterization we did not see any anomalous behavior.

Model dynamics are known to be sensitive to both parameterization and initial conditions (Popova *et al.*, 1997; Edwards and Yool, 2000). Here we investigated the influence of varying the predation parameters in some detail for a specified set of initial conditions. However, it is important to consider that variation in other parameters or a change to the initial conditions may result in dynamics different to those presented here. Our preliminary investigation into the influence of varying the maximum photosynthetic growth rate (P_{max}) for large phytoplankton revealed that the structure of the model solutions (*i.e.*, the coexistence of model components) was impacted by variation in this parameter but the location of Hopf bifurcations across q-h space went virtually unchanged. Additionally, we have shown that similar patterns of dynamics persisted even when doubling the initial nitrate concentration. From these results it is difficult to draw any conclusions regarding the model's sensitivity to variations in other parameter values, or to initial conditions very different to those used here. It has been shown, however, that a three-component, one-predator, one-prey model with sigmoidal grazing has Hopf

curves that remain fairly similar as many of the other model parameters are varied (Edwards and Brindley, 1999). This suggests, but remains for further study, that varying additional model parameters within our six-component model would result in a similar pattern of dynamical behavior.

In an effort to keep our model as simple as possible while allowing zooplankton to graze on multiple nutritional resources, we used the simplest form of many of the biological process functions that were not directly under investigation here. Inclusion or exclusion of model processes other than those under investigation here could also potentially enhance the dynamical behavior of the model. For example, within our model the rapid regeneration of organic material to a nutrient source that the phytoplankton can utilize ensures a continual nutrient supply; this could potentially enhance the excitability of the model (Popova *et al.*, 1997). We have shown, however, that despite our simplification of the nutrient regeneration loop our model is far more likely to exhibit limit cycle behavior with some grazing functions than with others. Self-shading of the phytoplankton was another biological process that was not included in our model but could potentially influence model dynamics. We did find, however, that both functions IV and V, multi-resource versions of the sigmoidal grazing function, produced a pattern of steady/limit cycle behavior across q-h parameter space which was very similar to that found for a three-component NPZ model that did include self-shading for the phytoplankton (Edwards and Bees, 2001). This suggests the dynamics presented here result primarily from the predator-prey interactions dictated by the alternate grazing functions, rather than from enhanced excitability due to our omission of self-shading.

It is important to note that the dynamics presented here were obtained when the model was subject to stationary physical forcing. Variations in physical forcing can have a large impact on model dynamics (Ryabchenko *et al.*, 1997; Edwards *et al.*, 2000) and it is possible that the dynamical behavior observed with stationary forcing could be damped out or enhanced with a seasonally varying forcing regime or with a model with more than one spatial dimension. It has been shown that strong upwelling or a high pycnocline,

which result in a high nutrient supply, can play an important role in oscillatory behavior (Popova *et al.*, 1997) and could potentially enhance the excitability of the model (and thus produce more limit cycles or even chaotic behavior). Within our model, nitrate is mixed into the upper mixed layer only through the action of diffusion. Hence, we have shown that even in the absence of strong upwelling, oscillatory dynamical behavior can be very prevalent with some grazing functions.

Biological dynamics in the ocean are highly transient, and capturing such transient biological behavior with an NPZ model that has a stationary physical forcing is inherently difficult. However, the focus of this study was to try to understand the dynamics of alternative forms of an NPZ model, parameterized with realistic values, in order to guide future modeling efforts, rather than replicate observational data. Our findings contribute towards the more general understanding of non-linear dynamics and structural stability of complex NPZ models in which multiple grazers can select from multiple prey types. We have provided an insight into the impact that the choice of commonly used multiple resource grazing functions and mortality functions can have on model dynamics. We are reluctant to suggest that any grazing or mortality function should be chosen over alternatives at this stage. However, if a modeler is selecting for or against a type of behavior (steady/oscillatory) our findings could provide a useful resource. For example, if the desire is to achieve a structurally stable model comprising all model components that does not exhibit unforced periodic oscillations, then using grazing function V to simulate zooplankton grazing appears most appropriate. Models in which this grazing function was implemented were also the most robust, *i.e.*, the form of the equilibrium solutions did not change significantly over a realistic range of parameter values. However, even this model structure has the ability to produce non-steady solutions for some forms of the predation function. With this grazing function models were more likely to be steady as the predation function tended towards the linear form, although mesozooplankton were often eliminated in this region of parameter space. With both of these biological process functions, as with any others used in the development of

an NPZ model, the modeler will have to ascertain if the assumptions inherent in the formulation are appropriate for the plankton community of interest. Our findings have important implications for modeling efforts in environments where multiple prey and predator classes persist simultaneously. It is hoped that this analysis will be of value during model construction of such ecosystems, and for interpreting results from biophysical model simulations in which the physical forcing is varied over a seasonal cycle.

4.6 References

Aita, M. N., Yamanaka, Y. and Kishi, M. J. (2003) Effects of ontogenetic vertical migration of zooplankton on annual primary production - using NEMURO embedded in a general circulation model. *Fish. Oceanogr.*, **12**, 284-290.

Ambler, J. W. (1986) Formulation of an ingestion function for a population of Paracalanus feeding on mixtures of phytoplankton. *J. Plankton Res.*, **8**, 957-972.

Armstrong, R. A. (1994) Grazing limitation and nutrient limitation in marine ecosystems: Steady state solutions of an ecosystem model with multiple food chains. *Limnol. Oceanogr.*, **39**, 597-608.

Armstrong, R. A. (1999) Stable model structures for representing biogeochemical diversity and size spectra in plankton communities. *J. Plankton Res.*, **21**, 445-464.

Chifflet, M., Andersen, V., Prieur, L. and Dekeyser, I. (2001) One-dimensional model of short-term dynamics of the pelagic ecosystem in the NW Mediterranean Sea: effects of wind events. *J. Mar. Syst.*, **30**, 89-114.

Corkett, C. J. and McLaren, I. A. (1978) The biology of Pseudocalanus, *Adv. Mar. Biol.*, **15**, 1-231.

Dagg M. J. and Walser W. E. (1987) Ingestion, gut passage, and egestion by the copepod Neocalanus plumchrus in the laboratory and in the subarctic Pacific Ocean. *Limnol. Oceanogr.*, **32**, 178-188.

Dagg, M. (1993) Grazing by the copepod community does not control phytoplankton production in the Subarctic Pacific Ocean. *Prog. Oceanogr.*, **32**, 163-183.

Dagg, M. (1995) Ingestion of phytoplankton by the micro- and mesozooplankton communities in a productive subtropical estuary. *J. Plankton Res.*, **17**, 845-857.

Denman, K. L. and Gargett, A. E. (1995) Biological physical interactions in the upper ocean: the role of vertical and small scale transport processes. *Annu. Rev. Fluid. Mech.*, **27**, 225-255.

Denman, K. L. and Peña, M. A. (1999) A coupled 1-D biological/ physical model of the northeast subarctic Pacific Ocean with iron limitation. *Deep-Sea Res. II*, **46**, 2877-2908.

Denman, K. L. and Peña, M. A. (2002) The response of two coupled one-dimensional mixed layer/planktonic ecosystem models to climate change in the NE subarctic Pacific Ocean. *Deep-Sea Res. II*, **49**, 5739-5757.

Dugdale, R. C. and Goering, J. J. (1967) Uptake of new and regenerated forms of nitrogen in primary productivity. *Limnol. Oceanogr.*, **12**, 196-206.

Edwards, A. M. (2001) Adding detritus to a Nutrient Phytoplankton Zooplankton model: A dynamical-systems approach. *J. Plankton Res.*, **23**, 389-413.

Edwards, A. M. and Bees, M. A. (2001) Generic dynamics of a simple plankton population model with a non-integer exponent of closure. *Chaos, Solutions & Fractals*, **12**, 289-300.

Edwards, A. M. and Brindley, J. (1996) Oscillatory behaviour in a three-component plankton population model. *Dyn. Stabil. Syst.*, **11**, 347-370.

Edwards, A. M. and Brindley, J. (1999) Zooplankton mortality and the dynamical behaviour of plankton population models. *Bull. Math. Biol.*, **61**, 303-339.

Edwards, A. M. and Yool, A. (2000) The role of higher predation in plankton population models. *J. Plankton Res.*, **22**, 1085-1112.

Edwards, C. A., Powell, T. A. and Batchelder, H. P. (2000) The stability of an NPZ model subject to realistic levels of vertical mixing. *J. Mar. Res.*, **58**, 37-60.

Eppley, R. W. and Peterson, B. J. (1979) Particulate organic matter flux and planktonic new production in the deep ocean. *Nature*, **282**, 677-680.

Evans, G. T. and Parslow, J. S. (1985) A model of annual plankton cycles. *Biol. Oceanogr.*, **3**, 327-347.

Fasham, M. J. R. (1995) Variations in the seasonal cycle of biological production in subarctic oceans: A model sensitivity analysis. *Deep-Sea Res. I,* **42**, 1111-1149.

Fasham, M. J. R., Ducklow, H. W. and McKelvie, S. M. (1990) A nitrogen-based model of plankton dynamics in the oceanic mixed layer. *J. Mar. Res.*, **48**, 591-639.

Fasham, M. J. R., Sarmiento, J. L., Slater, R. D., Ducklow, H. W. and Williams, R. (1993) Ecosystem behaviour at Bermuda Station "S" and ocean weather station "India": a general circulation model and observational analysis. *Global Biogeochem. Cycles,* **7**, 379-415.

Franks, P. J. S. and Chen, C. (2001) A 3-D prognostic numerical model study of the Georges bank ecosystem. Part II: biological-physical model. *Deep-Sea Res.*, **48**, 457-482.

Franks, P. J. S., Wroblewski, J. S. and Flierl, G. R. (1986) Behavior of a simple plankton model with food-level acclimation by herbivores. *Mar. Biol.*, **91**, 121-129.

Frost, B. W. (1972) Effects of size and concentration of food particles on the feeding behavior of the marine planktonic copepod *Calanus pacificus. Limnol. Oceanogr.,* **17,** 805-815.

Frost, B. W. (1975) A threshold feeding behavior in *Calanus pacificus. Limnol. Oceanogr.*, **20**, 263-266.

Frost, B. W. (1987) Grazing control of phytoplankton stock in the open subarctic Pacific Ocean: A model assessing the role of mesozooplankton, particularly the large calanoid copepods Neocalanus spp. *Mar. Ecol. Prog. Ser.*, **39**, 49-68.

Gentleman, W., Leising, A., Frost, B., Strom, S. and Murray, J. (2003) Functional response for zooplankton feeding on multiple resources: a review of assumptions and biological dynamics. *Deep Sea Res. II,* **50**, 2847-2875.

Gifford D. J. and Dagg M. J. (1988) Feeding of the estuarine copepod Acartia tonsa Dana: Carnivory vs. herbivory in natural microplankton assemblages. *Bull. Mar. Sci.*, **43**, 458-468.

Gismervik, I. and Andersen, A. (1997) Prey switching by Acartia clause: Experimental evidence and implications of intraguild predation assessed by a model. *Mar. Ecol. Prog. Ser.*, **157**, 247-259.

Hutson, V. (1984) Predator mediated coexistence with switching predator. *Mathematical Biosciences*, **68**, 233-246.

Ivlev, V. S. (1961). Experimental ecology of the feeding of fishes. Yale Univ. Press, New Haven, Connecticut, USA.

Johnson, P. W. and Sieburth, J. M. (1979) Chroococcoid cyanobacteria in the sea: A ubiquitous and diverse photo-trophic biomass. *Limnol. Oceanogr.*, **24**, 928-935.

Johnson, P. W. and Sieburth, J. M. (1982) In-situ morphology and occurrence of eucaryotic phototrophs of bacterial size in the picoplankton of estuarine and oceanic waters. *J. Phycol.*, **18**, 318-327.

Jonsson, P. R. and Tiselius, P. (1990) Feeding behaviour, prey detection and capture efficiency of the copepod Acartia tonsa feeding on planktonic ciliates. *Mar. Ecol. Prog. Ser.*, **60**, 35-44.

Kiørboe, T., Saiz, E. and Viitasalo, M. (1996) Prey switching behaviour in the planktonic copepod Acartia tonsa. *Mar. Ecol. Prog. Ser.*, **143**, 65-75.

Kleppel, G. S. (1993) On the diets of calanoid copepods. *Mar. Ecol. Prog. Ser.*, **99**, 183-195.

Kleppel, G. S., Burkart, C. A., Carter, K. and Tomas, C. (1996) Diets of calanoid copepods on the West Florida continental shelf: Relationships between food concentration, food composition and feeding activity. *Mar. Biol.*, **127**, 209-217.

Landry, M. R. and Hassett, R. P. (1982) Estimating the grazing impact of marine micro-zooplankton. *Mar. Biol.*, **67**, 283-288.

Legendre, L. and Rassoulzadegan, F. (1995) Plankton and nutrient dynamics in marine waters. *Ophelia*, **41**, 153-172.

Lomas, M. W. and Glibert, P. M. (1999) Temperature regulation of nitrate uptake: A novel hypothesis about nitrate uptake reduction in cool-water diatoms. *Limnol. Oceanogr.*, **44**, 556-572.

Loukos, H., Frost, B. W., Harrison, D. E. and Murray, J. W. (1997) An ecosystem model with iron limitation of primary production in the equatorial Pacific at 140°W. *Deep-Sea Res. II,* **44**, 2221-2249.

Luick, J. L., Royer, T. C. and Johnson, W. R. (1987) Coastal atmospheric forcing in the northern Gulf of Alaska. *J. Geophys. Res. (C Oceans).* **92:4**, 3841-3848.

Malchow, H. (1994) Non equilibrium structures in plankton dynamics. *Ecol. Model.,* **75/76**, 123-134.

Martin-Cereceda, M., Novarnio, G., and Young, J. R. (2003) Grazing by Prymnesium parvum on small planktonic diatoms. *Aquat. Microb. Ecol.* **33**, 191-199.

May, R. M. (1972) Limit cycles in predator-prey communities. *Science,* **177**, 900-902.

May, R. M. (1973). Stability and complexity in model ecosystems, Princeton University Press. Princeton, N.J.

Monod, J. (1942) Recherches sur la croissance des cultures bact'eriennes [studies on the growth of bacterial cultures]. *Actualities Scientifique et Industrielles,* **911**, 1-215.

Mullin, M. M. and Fuglister, F. J. (1975) Ingestion by planktonic grazers as a function of concentration of food. *Limnol. Oceanogr.,* **20**, 259-262.

Murdoch, W.W. (1973) The functional response of predators. *Journal of Applied Ecology*, **10**, 335-354.

Oaten, A. and Murdoch, W. W. (1975) Switching, functional response, and stability in predator-prey systems. *American Naturalist,* **109**, 299-318.

Popova, E. E., Fasham, M. J. R., Osipov, A. V. and Ryabchenko, V. A. (1997) Chaotic behaviour of an ocean ecosystem model under seasonal external forcing. *J. Plank. Res.,* **19**, 1495-1515.

Redfield, A. C., Ketchum, B. K. and Richards, F. A. (1963) The influence of organisms on the composition of sea-water. *The Sea,* **2**, 26-77.

Riley, G. A. (1946) Factors controlling phytoplankton populations on Georges Bank. *J. Mar. Res.,* **6**, 54-72.

Ryabchenko, V. A., Fasham, M. J. R., Kagan, B. A. and Popova, E. E. (1997) What causes short-term oscillations in ecosystem models of the ocean mixed layer? *J. Mar. Res.*, **13**, 33-50.

Steele, J. H. (1974). The structure of marine ecosystems, Harvard University Press. Cambridge.

Steele, J. H. and Henderson, E. W. (1992) The role of predation in plankton models. *J. Plankton Res.*, **14**, 157-172.

Strom, S. and Loukos, H. (1998) Selective feeding by protozoa: model and experimental behaviors and their consequences for population stability. *J. Plankton Res.*, **20**, 831-846.

Strom, S. L. (1991) Growth and grazing rates of the herbiverous dinoflagellate Gymnodinium sp. from the open subarctic Pacific Ocean. *Mar. Ecol. Prog. Ser.*, **78**, 103-113.

Strom, S. L. and Welschmeyer, N. A. (1991) Pigment-specific rates of phytoplankton growth and microzoopalnkton grazing in the open subarctic Pacific Ocean. *Limnol. Oceanogr.*, **36**, 50-63.

Strom, S. L., Brainard, M. A., Holmes, J. L. and Olson, M. B. (2001) Phytoplankton blooms are strongly impacted by microzooplankton grazing in coastal North Pacific waters. *Mar. Biol.*, **138**, 355-368.

Weingartner, T., Coyle, K., Finney, B., Hopcroft, R., Whitledge, T., Brodeur, R., Dagg, M., Farley, E., Haidvogel, D., Haldorson, L., Hermann, A., Hinckley, S., Napp, J., Stabeno, P., Kline, T., Lee, C., Lessard, E., Royer, T. and Strom, S. (2002) The Northeast Pacific GLOBEC Program: Coastal Gulf of Alaska. *Oceanography,* **15**, 48-63.

Wroblewski, J. S. (1977) A model of phytoplankton plume formation during variable Oregon upwelling. *J. Mar. Res.*, **35**, 357-394.

Yool, A. (1998). The dynamics of open-ocean plankton ecosystem models, Ph.D. diss, University of Warwick.

Chapter 5. The role of detritus in NPZ model dynamics

5.1 Introduction

In the coastal Gulf of Alaska, as in many regions of the world's ocean, plankton biomass exhibits a defined seasonal cycle that closely relates to the prevailing physical forcing in the environment. In winter, strong downwelling and vertical mixing in the coastal Gulf of Alaska weaken stratification, deepen the upper mixed layer, and entrain high concentrations of nutrients into surface waters (Weingartner *et al.*, 2002; Stabeno *et al.*, 2004). The deep mixing of phytoplankton, combined with a low solar angle, a short photo-period, and persistent cloud cover, limit primary productivity (Stabeno *et al.*, 2004) and thus chlorophyll–a concentrations in winter are relatively low (Childers *et al.*, in press). During late spring and early summer (March-May), the lengthening days, high solar angle and stratification of the upper water column, enable primary producers to take advantage of the high nutrient concentrations in the surface waters (Stabeno *et al.*, 2004; Childers *et al.*, in press) and a pronounced increase in chlorophyll across the shelf can be observed due to the spring phytoplankton bloom (Strom *et al.*, 2001; Childers *et al.*, in press). In the summer (July–August) high riverine discharge and seasonal heating lead to the development of an intense pycnocline at 25 meters (Stabeno *et al.*, 2004). The strongly stratified euphotic zone is depleted of nutrients during summer due to phytoplankton consumption and weak mixing (Childers *et al.*, in press). This results in the development of a strong sub-surface chlorophyll maximum during the summer at 20-30 meters depth (See Figure 5-1 for example) within or just above the pycnocline where nutrient concentrations are higher but photosynthetically available radiation is still sufficient for growth (Childers *et al.*, in press).

The six-component NPZ model comprising small and large phytoplankton, microzooplankton, mesozooplankton, nitrate and ammonium, parameterized for the

coastal Gulf of Alaska (cGOA) was able to simulate a surface bloom of plankton with higher concentrations in the surface mixed layer, decreasing smoothly to negligible concentrations below. However, despite implementing an array of functional forms for zooplankton grazing and mortality, the sub-surface chlorophyll maximum could not be simulated with the existing model structure and physical forcing. The depth-explicit forcing in this model was stationary in time and considered to be representative of the cGOA in spring. Capturing transient biological behavior, such as a sub-surface chlorophyll maximum, is an inherent difficulty when the model framework comprises stationary physical forcing. Simulation of such transient biological features could require seasonally varying forcing; however, the model's inability to simulate such features could also be indicative of inadequate representation of the ecosystem or associated biological processes.

In the six-component model, described in Chapter 4, losses from the phytoplankton and zooplankton due to mortality, sloppy feeding, etc., were assumed to be instantaneously remineralized back to a utilizable pool of nutrient at a constant rate. This rapid regeneration of organic material to a nutrient source that the phytoplankton can utilize ensured a continual nutrient supply in the upper mixed layer, and thus could be a factor behind the lack of development of the sub-surface chlorophyll maximum. In reality, following a phytoplankton bloom the nutrients are depleted in the surface waters due to the flux of rapidly sinking organic material out of the mixed layer. Generally, the bacterial degradation of this organic material occurs below the pycnocline, which means that the regenerated nutrients are not available to support further growth of plankton in the surface waters. It is likely that in order to adequately simulate the observed key features of the seasonal cycle in the cGOA, in addition to a net export of nutrient from the surface mixed layer, the six-component NPZ model will require physical forcing that is representative of conditions observed during the summer, *i.e.,* a shallower mixed layer depth and smaller mixed layer diffusion.

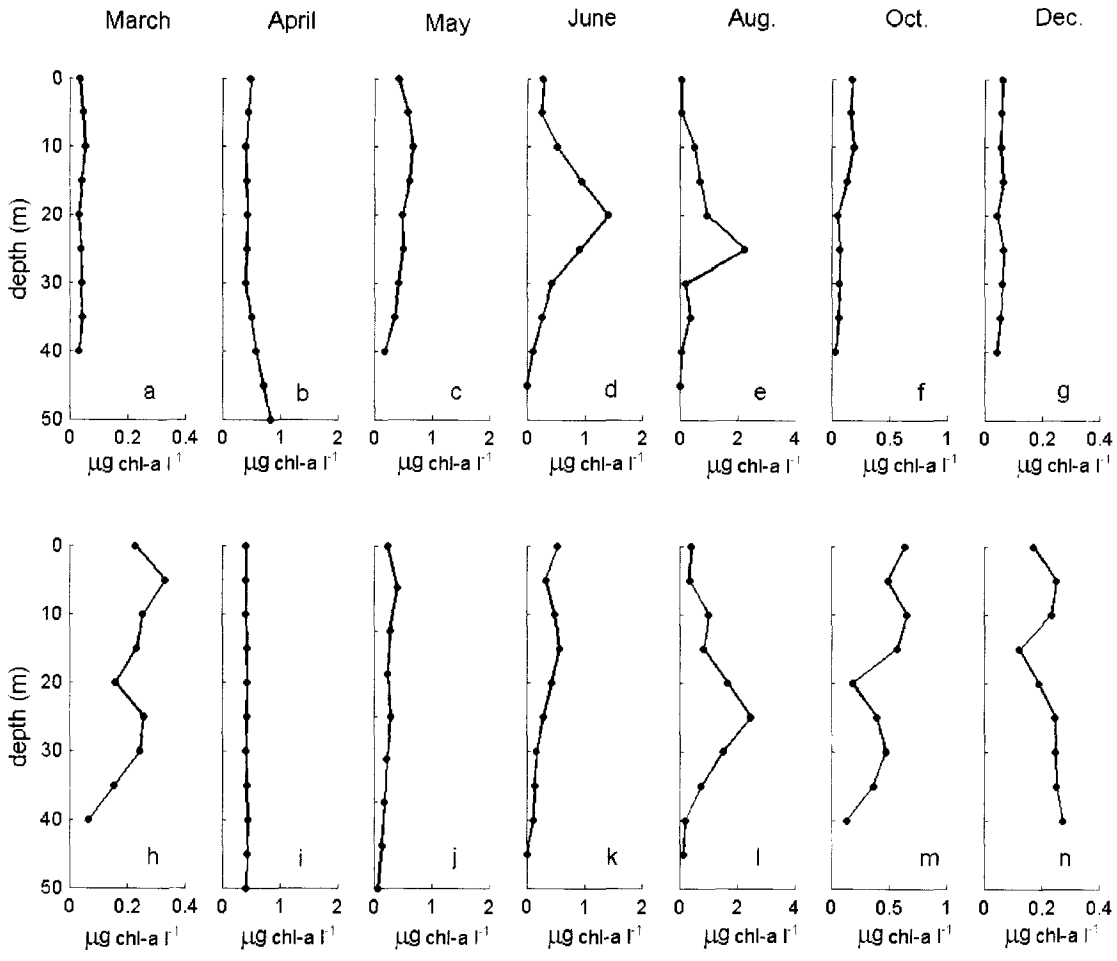

Figure 5-1 Profiles of Chl-a concentration at GAK1 in the cGOA during 2001.
GAK1 is the most inshore station on the Sewards transect line (Figure 1-1). (a-g) small size fraction (nominal pore size 0.7-5μm) and (h-n) large size fraction (nominal pore size >20μm). Data was kindly provided by T. Whitledge per. Com).

Many of the models used in ecosystem studies today incorporate more explicit representation of the regeneration loop, although the degree of detail incorporated can vary widely. More complex models include both Particulate Organic Matter (POM) and Dissolved Organic Matter (DOM) as separate state variables (Kishi, 2000) and some even specifically represent bacteria (Lancelot *et al.*, 2000). Other models have a single 'detrital' component which is assumed to comprise both POM and DOM (Loukos *et al.*, 1997; Denman and Peña, 2002).

By reducing the amount of readily available nutrient, the addition of detritus to a model could potentially act as a "brake" on the system and therefore influence model dynamics by dampening out oscillations. Detritus is effectively a nutrient store that can be exported from the mixed layer, via sinking, prior to remineralization to a utilizable form of nutrient. Thus, inclusion of detritus in an NPZ model will slow the return of organic matter to inorganic nutrients, and reduce the total nutrient available in the system. It has been shown that a high nutrient supply (caused by high entrainment into the mixed layer of high pycnocline nutrient concentrations) can enhance the susceptibility to oscillatory behavior (Popova *et al.*, 1997). This suggests that the assumption of instantaneous remineralization could be important because the continual supply of nutrient to the plankton may enhance oscillatory behavior. Edwards (2001) has shown that the addition of detritus to a three component NPZ model had little consequence for the model dynamics provided zooplankton were unable to graze on the detritus, however, the model investigated had only a single resource sigmoidal grazing function and a homogeneous mixed layer. The addition of detritus to a more complex, depth-explicit, NPZ model in which zooplankton can graze on multiple prey could have a very different influence on the model dynamics.

Changes to the physical structure of the model are also known to influence NPZ model dynamics. For example, it has been shown that incorporating moderate levels of vertical diffusion into a non-diffusive NPZ model imparts model stability (Edwards *et al.*, 2000).

However, high values of entrainment of pycnocline waters with high levels of nutrient concentrations, have also been found to play an important role in causing oscillatory behavior (Popova *et al.*, 1997), as have abrupt changes in the thickness of the upper mixed layer, such as those commonly observed in Spring or Fall, (Rybchenko *et al,*. 1997). The influence of the model's physical structure on the dynamics of the biological components is thus an important consideration for the realm of coupled bio-physical models. It is important that we understand not only how a change in physical structure can influence model solutions, with respect to replicating key features of the seasonal cycle (e.g., the sub-surface chlorophyll maximum), but also to understand how such modifications could influence the non-linear dynamics of the model.

The primary objectives of this research were to investigate if the addition of a detritus component and alternative physical forcing regimes to a six-component NPZ model significantly influenced the stability and the composition (survivorship) of model solutions, and to determine if these model modifications could yield a sub-surface chlorophyll maximum. The dynamics of a seven-component NPZ model that included detritus was explored using a systematic variation of *q*-*h* parameter space, the two parameters that govern predation on mesozooplankton (*H*). Forcing was stationary, but the influence of two alternative mixed-layer diffusion coefficients (Kv_m=1×10^{-3} m^2 s^{-1} and 1×10^{-4} m^2 s^{-1}) and two mixed layer depths (20 and 40 meters) were investigated. With each forcing scenario, model dynamics were compared with and without sinking of the detritus component. The previous investigation (Chapter 4) demonstrated that with alternative functional forms for grazing, the model may exhibit very different behavior in terms of structure and dynamics of equilibrium solutions. Therefore, the investigation was conducted with both grazing function I and function V, as these exhibited characteristics that capture the behavior of the other three grazing functions. This series of experiments effectively tests hypothesis 3 and 4 as outlined in Chapter 1.

5.2 Method

5.2.1 Model Structure

The model investigated here builds upon the six-component NPZ model whose dynamics were investigated previously (Chapter 4). Here, detritus is added to the model as a seventh state variable. The new seven-component model (Figure 5-2) thus simulates the exchange of nitrogen (μM N) between small phytoplankton (< 8μm, P_1), large phytoplankton (> 8μm, P_2), microzooplankton (Z_1), mesozooplankton (Z_2), nitrate (N_1), ammonium (N_2) and detritus (Dt). Below I outline the new system of equations, drawing attention to the new functions required to incorporate detritus into the model. The curious reader can refer to the description of the original model (Chapter 4) for a fuller explanation of the mathematical formulations selected to describe the time rate of change of the original six components.

The one-dimensional model was spatially explicit in the vertical, with a resolution of one meter and an extent of one hundred meters (z_i=[-1m, -2m, -3m, ... -100m]). The original six-component model was a closed system with no net inputs or outputs; therefore, the total nitrogen content was constant at all times ($N_T=P_1+P_2+Z_1+Z_2+N_1+N_2$). This was also true of the seven-component model when detritus had a sinking velocity of zero ($N_T=P_1+P_2+Z_1+Z_2+N_1+N_2+Dt$ =constant). In this instance no flux boundary conditions were enforced at the upper and lower boundaries (z=0 and z=100m), *i.e.,*

$$Kv\frac{\partial P_1}{\partial z}=Kv\frac{\partial P_2}{\partial z}=Kv\frac{\partial Z_1}{dz}=Kv\frac{\partial Z_2}{\partial z}=Kv\frac{\partial N_1}{\partial z}=Kv\frac{\partial N_2}{\partial z}=Kv\frac{\partial Dt}{\partial z}=0 \qquad \text{Eq. 5.1}$$

However, when detritus had a non-zero sinking velocity, to partially balance the loss of nitrogen from the system over the year, the no-flux boundary condition at the 100 meter depth level was relaxed. It was assumed that the nitrate concentration below the 100 depth level (N_{1b}) was 10μM N, concentrations of all other model components below this layer were assumed to be zero, *i.e.,* $N_{2b}=Dt_b=Z_{1b}=Z_{2b}=P_{1b}=P_{2b}=0$ μM N.

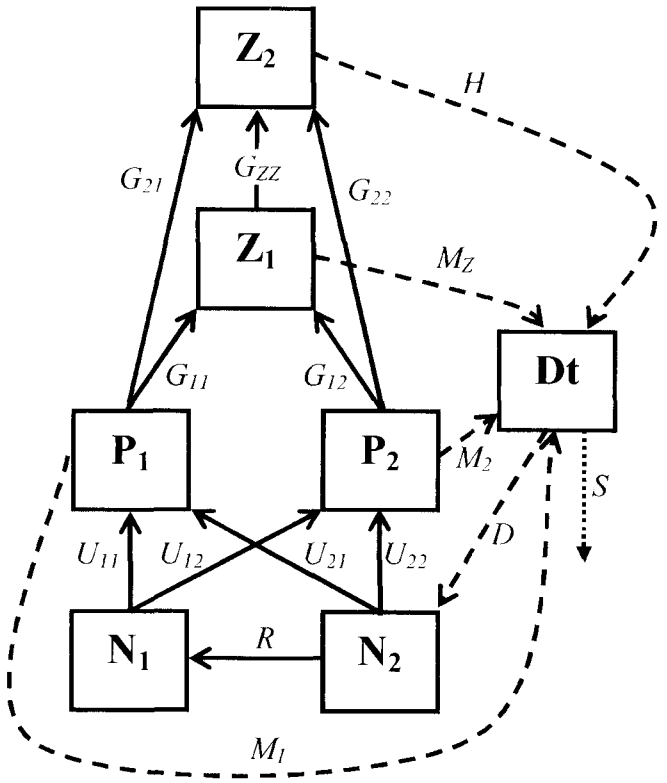

Figure 5-2 Interactions in the seven-component NPZ model.
Nitrate (N_1), ammonium (N_2), detritus (Dt), small phytoplankton (P_1), large phytoplankton (P_2), microzooplankton (Z_1) and mesozooplankton (Z_2). Arrows indicate the direction of material flow. Biological processes, *i.e.*, grazing (G), nutrient uptake (U), mortality (M), predation (H) and nitrification (R) associated with each arrow are indicated. See Table 5-1 for explanation of subscripts. Note that for simplicity, zooplankton assimilation efficiencies have been omitted.

5.2.2 *Formulation of the Biological Equations*

The equations to describe the temporal rate of change of each of the seven model components are presented below; the formulations used to describe each biological process are presented in Table 5-1.

$$\frac{dN_1}{dt} = -U_{11} - U_{12} + R \qquad \text{Eq. 5.2}$$

$$\frac{dN_2}{dt} = -U_{21} - U_{22} + \alpha_1 \cdot (G_{11} + G_{12}) + \alpha_2 \cdot (G_{21} + G_{22} + G_{ZZ}) - R + D \qquad \text{Eq. 5.3}$$

$$\frac{dP_1}{dt} = U_{11} + U_{21} - M_1 - G_{11} - G_{21} \qquad \text{Eq. 5.4}$$

$$\frac{dP_2}{dt} = U_{12} + U_{22} - M_2 - G_{12} - G_{22} \qquad \text{Eq. 5.5}$$

$$\frac{dZ_1}{dt} = \gamma_1 \cdot (G_{11} + G_{12}) - G_{ZZ} - M_Z \qquad \text{Eq. 5.6}$$

$$\frac{dZ_2}{dt} = \gamma_2 \cdot (G_{21} + G_{22} + G_{ZZ}) - H \qquad \text{Eq. 5.7}$$

$$\frac{dDt}{dt} = M_1 + M_2 + M_Z + H + (1 - \gamma_1 - \alpha_1) \cdot (G_{11} + G_{12}) + (1 - \gamma_2 - \alpha_2) \cdot (G_{21} + G_{22} + G_{ZZ}) + S - D \qquad \text{Eq. 5.8}$$

It has previously been shown that the form of the grazing function can make a large difference to the structure of model solutions and to the models dynamic behavior (Chapter 4). Therefore, the investigation outlined here was conducted with both function I and function V (Table 5-1). These alternative formulations for grazing are considered to exhibit "end-member" characteristics of the five grazing functions previously investigated, *i.e.,* the behaviors of functions II-IV were intermediate between I and V.

Rather than assuming instantaneous remineralization of organic material to ammonium, as was previously the case, particulate organic matter losses from the phytoplankton and zooplankton are now considered inputs to the detritus component. This is one of the simpler, but common, approaches to incorporating detritus into an NPZ model (Loukos *et al.,* 1997; Denman and Peña, 2000, Leonard *et al.*, 1999). Although in reality, bacteria are able to uptake and excrete ammonium (Legendre and Rassoulzadegan, 1995), the model assumed that this was a one-way process with bacterial degradation (D) converting the detritus to ammonium at a linear rate. The detrital degradation rate (d) was taken to be

0.05 day^{-1} which falls well within the range (0.03-0.1day^{-1}) of values used for this parameter in other modeling studies (Denman and Peña, 2000; Frost, 1993; Loukos *et al.*, 1997). A fraction (α) of the organic material lost from the zooplankton is considered to be dissolved and as such is treated as a direct input to ammonium rather than to detritus. Ammonium was assumed to undergo nitrification (R) back to nitrate at a constant linear rate.

The sinking of detritus (S) is also a biological process new to this model and was described by:

$$S = W_s \frac{\partial Dt}{\partial z} \qquad \text{Eq. 5.9}$$

Where W_s is the detrital sinking rate. W_s is known to be a very sensitive parameter (Sarmiento *et al.*, 1993), but within existing modeling studies is commonly given a value between 0 and 10 m day^{-1} (Loukos *et al.*, 1997; Fasham, 1990; Denman and Pena 1999). The dynamics of the seven component model will be investigated using these extremes (*i.e.*, W_s=0 and 10 m day^{-1}).

The purely biological dynamics described above were subjected to vertical mixing. This physical forcing was represented by the addition of a single term (Eq. 4.7) to each of the biological equations. In this equation C_i represents each of the seven model components P_1, P_2, Z_1, Z_2, N_1, N_2 and Dt. The stationary, but spatially varying vertical diffusion profile (Kv) was described by Eq. 4.8. Model dynamics were investigated with a constant mixed layer depth (MLD) at 40 meters, representative of spring conditions, and a constant mixed layer depth at 20 meters representative of summer conditions. Two different levels of diffusion were implemented in the surface mixed layer, Kv_m=1x10^{-3} m^2 s^{-1} and Kv_m=1x10^{-4} m^2 s^{-1}, while below the mixed layer the background diffusion was held constant at Kv_b=1x10^{-5} m^2 s^{-1}. The shape parameters $\Phi(z)$ and ω respectively defined the position and the thickness of the pycnocline.

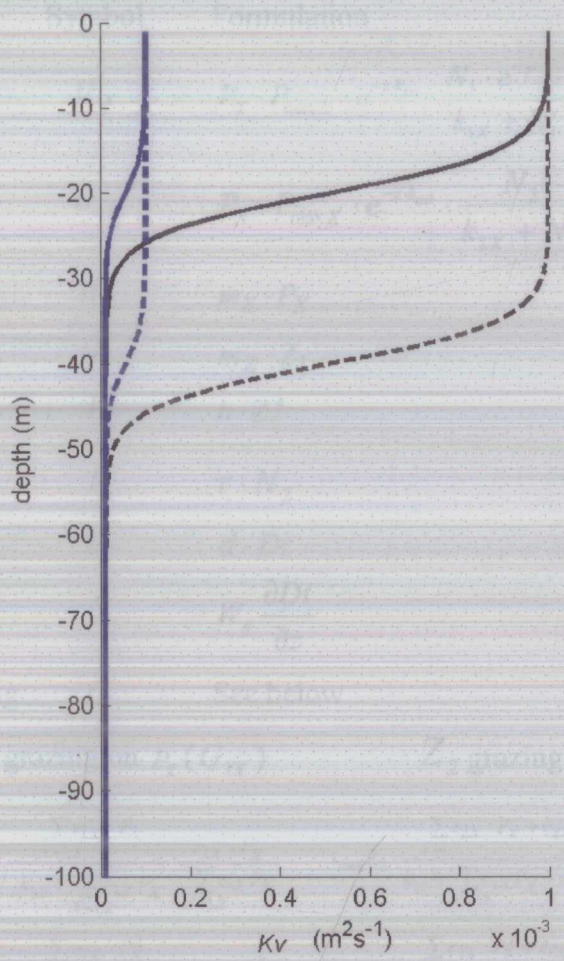

Figure 5-3 Vertical diffusion profiles used to force the seven-component NPZ model. The solid and dashed black lines represents the diffusion profile when Kv_m $=1x10^{-3} m^2 s^{-1}$ and the mixed layer depth is set to 20 and 40 meters respectively. The solid and dashed blue lines represents the diffusion profile when Kv_m= $1x10^{-4} m^2 s^{-1}$ and the mixed layer depth is set to 20 and 40 meters respectively.

Table 5-1 Biological processes used in the seven-component NPZ model. Parameter definitions and values are given in Table 5-2. X and Y can be 1 or 2 to represent the two classes of phytoplankton and zooplankton, respectively.

Process	Symbol	Formulation
P_X uptake of N_1	U_{1X}	$P_X \cdot P_{\max X} \cdot e^{z \cdot k_{ext}} \cdot \frac{N_1 \cdot e^{\psi \cdot N_2}}{k_{1X} + N_1}$
P_X uptake of N_2	U_{2X}	$P_X \cdot P_{\max X} \cdot e^{-z \cdot k_{ext}} \cdot \frac{N_2}{k_{2X} + N_2}$
natural mortality of	M_X	$m_X \cdot P_X$
natural mortality of	M_Z	$m_Z \cdot Z_1$
higher predation on	H	$h \cdot Z_2^q$
$N_2 \xrightarrow{\text{nitrification}} N_1$	R	$r \cdot N_2$
$Dt \xrightarrow{\text{degredation}} N_2$	D	$d \cdot Dt$
sinking of detritus	S	$W_s \frac{\partial Dt}{\partial z}$
Zooplankton Grazing	G	See below

Grazing Function	Z_1 grazing on P_X (G_{YX})	Z_2 grazing on Z_1 (G_{ZZ})
I	$i_{\max} Z_Y \cdot \frac{\sum_{X=1,2} e_{1X} \cdot P_X}{k_{31} + \sum_{X=1,2} e_{1X} P_X} \cdot \frac{e_{1X} \cdot P_X}{\sum_{X=1,2} e_{1X} P_X}$	$i_{\max} Z_2 \cdot \frac{\sum_{X=1,2} e_{2X} \cdot P_X + e_{ZZ} \cdot Z_1}{k_{32} + \sum_{X=1,2} e_{2X} P_X + e_{ZZ} \cdot Z_1} \cdot \frac{e_{ZZ} \cdot Z_1}{\sum_{X=1,2} e_{2X} P_X + e_{ZZ} \cdot Z_1}$
V	$i_{\max} Z_Y \cdot \frac{\sum_{X=1,2} e_{1X} \cdot P_X^2}{k_{31}^2 + \sum_{X=1,2} e_{1X} P_X^2} \cdot \frac{e_{1X} \cdot P_X^2}{\sum_{X=1,2} e_{1X} P_X^2}$	$i_{\max} Z_2 \cdot \frac{\sum_{X=1,2} e_{2X} \cdot P_X^2 + e_{ZZ} \cdot Z_1^2}{k_{32}^2 + \sum_{X=1,2} e_{2X} P_X^2 + e_{ZZ} \cdot Z_1^2} \cdot \frac{e_{ZZ} \cdot Z_1^2}{\sum_{X=1,2} e_{2X} P_X^2 + e_{ZZ} \cdot Z_1^2}$

Table 5-2 Parameter values used in the seven-component NPZ model.

X and Y can be 1 or 2 to represent the two classes of phytoplankton and zooplankton, respectively.

Parameter	Symbol	Values		Units
		$X=1$	$X=2$	
maximum growth rate of P_X	$P_{\max X}$	2	2	day^{-1}
P_X half-saturation constant for N_1	k_{1X}	.75	.5	μM N
P_X half-saturation constant for	k_{2X}	.5	1	μM N
inhibition parameter for U_1 by N_2	ψ	1.462		$[\mu M\ N]^{-1}$
nitrification rate	r	0.05		day^{-1}
detrital degredation rate	d	0.05		day^{-1}
detrital sinking rate	W_s	0 or 10		$m \cdot day^{-1}$
light extinction coefficient	k_{ext}	0.07		m^{-1}
		$Y=1$	$Y=2$	
maximum ingestion rate	$i_{\max Y}$	1.2	.7	day^{-1}
assimilation efficiency of Z_Y	γ_Y	0.4	0.3	-
Dissolved fraction of organic waste	α_Y	0.5	0.5	-
Z_Y half-saturation grazing	k_{3Y}	30	60	$\mu g\ C\ L^{-1}$

Z_Y capture efficiency for P_X	e_{YX}	X \ Y	1	2	-
		1	1	.2	-
		2	.7	.7	-

Z_2 capture efficiency for Z_1	e_{ZZ}	1			
		$X=1$	$X=2$		
natural mortality rate of P_X	m_X	0.2	0.1		day^{-1}
natural mortality rate of Z_1	m_z	0.08			day^{-1}
specific predation rate	h	0.05-2			$(gCm^{-3})^{1-q}\ day^{-1}$
predation exponent	q	1 - 2			-
Shape parameters for diffusion	ω	5			-
profile	$\Phi(z)$	$z - MLD$			-

5.2.3 *Analysis*

The dynamics of the seven-component NPZ model were compared when two alternative functional forms for zooplankton grazing (G) were implemented (I and V), and the predation exponent (q) and the specific predation rate (h) in the predation term (H) were systematically varied over a biologically realistic range, *i.e.*, $1 \leq q \leq 2$ and h=0.05-2.0 g C $m^{-3}]^{1-q}$ day^{-1}. The detrital sinking velocity was initially considered to be zero. In order that the model made biological sense, concentrations of all model components were restricted to positive finite or zero values. For each model simulation, the steady solutions of the non-linear system of seven equations were sought iteratively for thirty-six point grid in q-h parameter space; q=[1, 1.2, 1.4, 1.6, 1.8, 2.0], h=[0.05, 0.1, 0.5, 1.0, 1.5, 2.0] $[gCm^{-3}]^{1-q}$ day^{-1}. Each model was initially run for 300 time steps (days), and the resulting solution provided as a starting guess to a numerical solver of the steady state solution (Eq. 5.2-5.8 with the left hand sides set to zero). In the previous chapter, the six-component ecosystem model was required to have non-dimensional time derivative terms smaller than $1x10^{-4}$ μM N day^{-1} in order for the model to be classified as steady. The seven-component model is required to have dimensional time derivative terms smaller than $1x10^{-3}$ μM N day^{-1} in order to be classified as steady. Most steady equilibrium solutions, however, had time derivative several orders of magnitude smaller than this. Models that failed to converge to a steady solution were run for a further 600 days and the time series solution on the six hundredth day was provided to the numerical solver. These solutions were then reclassified. Any solution which could not be classified as steady was considered to be oscillatory. Visual inspection showed that the oscillatory solutions had no secular (long-term) decreases in the magnitude of oscillations.

The NPZ model behavior was subsequently analyzed assuming a detrital sinking velocity of 10 m day^{-1}. The dynamics of the NPZ model were again compared with two alternative functional forms for zooplankton grazing (I and V), for a realistic range of specific predation rates (h = 0.05-2.4 [g C $m^{-3}]^{1-q}$ day^{-1}) and predation exponents ($1 \leq q \leq 2$). Because nitrogen, in the form of detritus, could sink out of the lower boundary of the

model, the model could no longer be considered a closed system. As such, it did not make sense to seek equilibrium solutions using the numerical solver as was the case of non-sinking detritus. All solutions had to be visually inspected to determine if dynamical behavior was monotonic or oscillatory. It is not realistic to visually investigate time series solutions for all points in *q-h* space investigated with the non-sinking detritus model, however, it is clear from work in the preceding chapters (Chapters 3 and 4) that considering only a single *q-h* parameterization would not reveal a complete picture of model dynamics. Therefore, time series solutions (300 days) for a eighteen point grid in *q-h* parameter space, *i.e.*, q=[1, 1.2, 1.4, 1.6, 1.8, 2.0], h=[0.05, 1.0, 2.0], were visually inspected for each of the physical forcing regimes considered. Although coarse in resolution, this coverage of parameter space provides a good indicator of how sinking detritus impacted the NPZ model dynamics.

5.3 Results

5.3.1 Structure of equilibrium solutions

Adding non-sinking detritus to the original six-component model did not have a notable influence on the composition of model solutions with respect to the existence of model components. For ease of comparison, the maximum plankton concentration at equilibrium for the six-component NPZ model has been re-plotted at the reduced resolution *q-h* space used for the seven component model (Figure-5-4). As with the six-component model, the seven-component model produced solutions that differed markedly depending on whether grazing function I or V was implemented (Figure 5-5). In both cases, the structure of model solutions was related to the magnitude of the predation experienced by the mesozooplankton ($H=h\cdot Z_2^q$). An explanation of which regions of *q-h* parameter space correspond to low and high predation is provided in Chapter 4.4. With grazing function I there was a clear divide in the *q-h* parameter space where the composition of model solutions switched between two predominant forms (Figure 5-5 a,

c, e, g). Note that the maximum concentration of nitrate, ammonium and detritus was never negligible, therefore for brevity the maximum concentrations of these model components are not shown. When predation on mesozooplankton was high, solutions predominantly comprised large phytoplankton, microzooplankton, nitrate, ammonium, and detritus. The region of parameter space over which small and large phytoplankton persisted at equilibrium was slightly expanded with the incorporation of a detrital component [Figures (5-4 and 5-5) a and c]. This contributed to the broader region of *q-h* space for which all plankton components were found to persist simultaneously at equilibrium [Figures (5-4 and 5-5) i]. When the predation on mesozooplankton was low, solutions were dominated by small phytoplankton, mesozooplankton, nitrate, ammonium and detritus. When grazing function V was implemented, equilibrium solutions comprised both small and large phytoplankton and microzooplankton, in non-negligible concentrations for all parameter space examined (Figure 5-5 b, d, f). Mesozooplankton concentration was negligible when predation (*H*) on this component was high (Figure 5-5 h). This region of high '*H*' thus defined the only region of parameter space that did not comprise non-negligible concentrations of all model components when implementing grazing function V (Figure 5-5 j); this is very similar result to that found with the six-component model (Figure 5-4 j).

Influence of physical regime

Changing the diffusion in the surface mixed layer had a variable impact on the structure of model solutions depending on which grazing function was implemented. With grazing function I, regardless of whether the mixed layer depth was 40 or 20 meters, reducing the mixed layer diffusion by an order of magnitude had little impact on the concentrations of microzooplankton and mesozooplankton at equilibrium [Figures (5-5 – 5-8) e and g)]. However, a reduction in the vertical mixing resulted in high equilibrium concentrations of small phytoplankton ($P_1>10^{-1}$ μM N) but negligible concentrations of large phytoplankton ($P_2<1^{-5}$ μM N) for the majority of *q-h* space [Figures (5-5 – 5-8) a and c)].

When grazing function V was implemented, the only notable change to the composition of equilibrium solutions resulting from the lower mixed layer diffusion was a slightly narrower region of *q-h* parameter space over which mesozooplankton had a negligible equilibrium concentration, and the reduction of microzooplankton to negligible concentrations, when predation on mesozooplankton was very low [Figures (5-5 – 5-8) f and h)].

Holding the mixed layer diffusivity constant, reducing the mixed layer depth from 40 meters to 20 meters had little impact on the structure of equilibrium solutions. With grazing function I and V and a mixed layer diffusion of $Kv_m=10^{-3}$ m^2 s^{-1}, reducing the mixed layer depth from 40 to 20 meters did not notably impact the structure of equilibrium solutions [Figures (5-5 and 5-7)]. Similarly, with grazing function V and a mixed layer diffusion of $Kv_m=10^{-4}$ m^2 s^{-1} reducing the mixed layer depth from 40 to 20 meters did not notably impact the structure of equilibrium solutions [Figures (5-6 and 5-8) b, d, f, h]. The only notable impact of a reduction in the mixed layer depth with grazing function I and $Kv_m=10^{-4}$ m^2 $s^{-1}$was an increase in the maximum equilibrium concentration of large phytoplankton at intermediate levels of predation on mesozooplankton [Figures (5-6 and 5-8) c].

Although plotted at a coarser resolution, it can be seen that with the original physical forcing ($Kv_m=10^{-3}$ m^2 s^{-1} and MLD=40 meters) incorporation of sinking detritus did not significantly alter the composition of solutions throughout *q-h* parameter space [Figures (5-5 – 5-9)]. This was true when implementing either of the grazing functions. With the addition of sinking detritus the composition of model solutions were more robust to changes in physical forcing [Figures (5-9 - 5-12)]. The only notable change was when the mixed layer depth was shallow (20 m) and the mixed layer diffusion low ($Kv_m=10^{-4}$ $m^2 s^{-1}$). With this forcing regime, when function V was implemented, small phytoplankton and microzooplankton no longer persisted throughout *q-h* parameter space. Rather, small phytoplankton only persisted at regions of low predation (Figure 5-12b). Conversely, this

was the only region of parameter space where microzooplankton concentration was negligible (Figure 5-12f).

Existence of sub-surface Chlorophyll Maximum

The existence of a sub-surface maximum in chlorophyll ($P_1 + P_2$) was largely dependent on the magnitude of mixed layer diffusion. The depth and strength of this maximum varied with grazing function and detrital sinking velocity. With non-sinking detritus, irrespective of the mixed layer depth (40 or 20 meters) or the grazing function (I or V), with the higher mixed layer diffusion (Kv_m=10^{-3} m^2 s^{-1}) no sub-surface maximum was found throughout the entire region of q-h parameter space [Figures (5-13 and 5-14) a, c, g, i]. The same was also true in the case of sinking detritus, with the exception of a single point in parameter space (q=2, h=1.2) when the mixed layer depth is 40 meters and grazing function I was implemented [Figures (5-15 and 5-16) a, c, g, i]. Barring this exception, with high diffusion the chlorophyll concentration was maximum at the surface and decreased smoothly with depth, approaching negligible concentrations below the mixed layer [Figures (5-17 and 5-18) a and c]. Profiles of chlorophyll are shown only for the point q=1.2 and h=0.05, this point was selected for ease of comparison between model experiment because model solutions always had a steady equilibrium there. However, these profiles are considered to be representative of other steady equilibrium profiles over q-h space. Figure 5-19 illustrates how the model dynamics vary with q and h. In this example, at low predation (top left of figure) solutions are approaching a steady equilibrium and the concentration of chlorophyll at 20 meters generally exceeds that at the surface (1 meter). At high predation (bottom right of figure), solutions are oscillatory but a sub-surface maximum in chlorophyll still persists periodically. It is clear that diagnostic plots of chlorophyll concentration in this oscillatory region of q-h space are not appropriate due to the ephemeral nature of the sub-surface chlorophyll maximum.

With high mixed layer diffusivity (10^{-3} m^2 s^{-1}) the surface chlorophyll concentrations tended to be unrealistically high (>10μg chl l^{-1}) compared to observations (Figure 5-1) for large regions of parameter space. With the smaller mixed layer diffusion (10^{-4} m^2 s^{-1}), the difference between the surface chlorophyll concentration and the sub-surface chlorophyll maximum varied throughout *q-h* space. When the detritus had a zero sinking velocity the size of this difference depended on the grazing function. With function I, the maximum difference was 1.5 μg chl l^{-1} (Figure 5-13 f and l), while with function V the maximum difference was an order of magnitude smaller at 0.2 μg chl l^{-1} (Figure 5-14 f and l). With both of these functions, the subsurface maximum was more prevalent when the predation on mesozooplankton was low and there were large regions of *q-h* space where no sub-surface chlorophyll maximum was observed. When detritus could sink and the mixed layer diffusion was low (10^{-4} m^2 s^{-1}), the sub-surface maximum persisted for a much larger region of *q-h* space and the difference between the surface chlorophyll concentration and the sub-surface chlorophyll maximum was similar with both grazing function I (0-0.8) and function V (0.3-0.5) [Figures (5-16 and 5-17) d-f and j-i]. The depth of the sub-surface chlorophyll maximum varied with grazing function and detrital sinking velocity. When detritus was unable to sink, the sub-surface maximum was in the region of 5-15 meters depth when implementing function I (Figure 5-13 d and j), but much shallower (around 5 meters) with function V (Figure 5-14 d and j). When detritus were able to sink, the sub-surface chlorophyll maximum was in the region of 10-20 meters and was similar with both grazing functions [Figures (5-16 and 5-17) d and j].

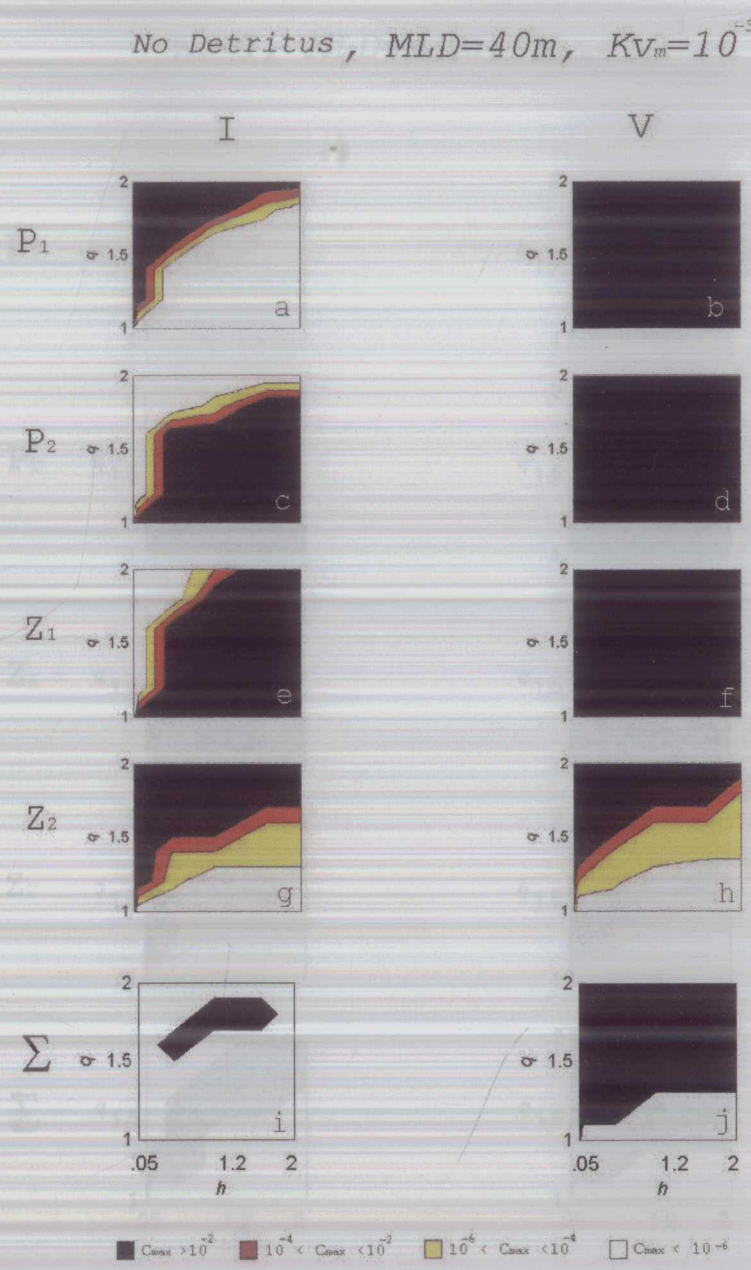

Figure 5-4 Plankton survivorship, MLD=40m, $Kv_m=10^{-3}$ m^2 s^{-1}, No detritus.
This figure similar to Figure 4-5 but re-plotted in the lower resolution *q-h* space. Concentrations are non-dimensional. First column is for grazing function I, second column is for grazing function V. For steady solutions, the maximum scaled plankton concentrations over all depths at equilibrium were used. For oscillatory solutions, the maximum plankton concentrations over all depths and over the last 200 days of a simulation were used. (i & j) black shading indicate regions where all plankton survive simultaneously (Σ).

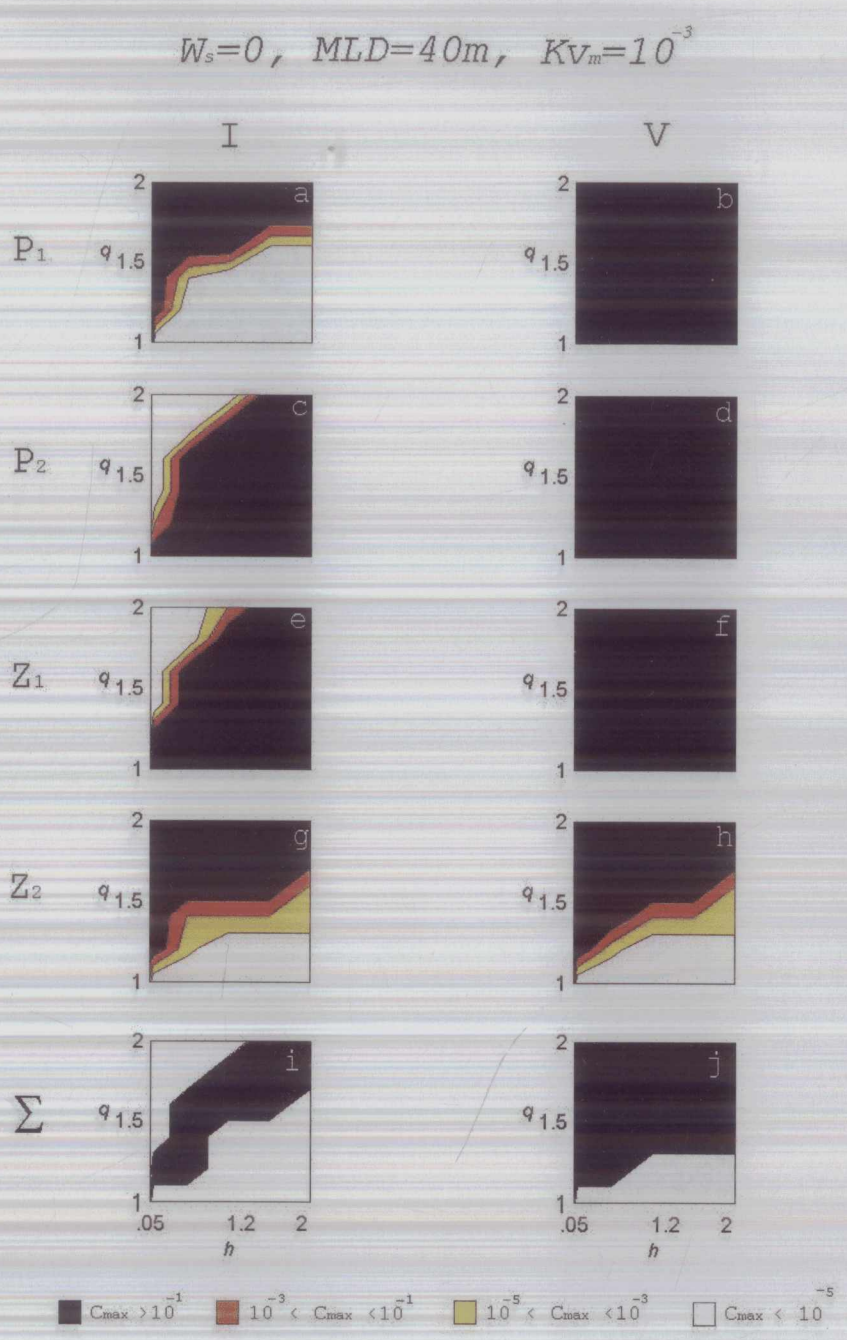

Figure 5-5 Plankton survivorship, MLD=40m, $Kv_m=10^{-3}$ m^2 s^{-1}, $W_s=0$ m day^{-1}. First column is for grazing function I, second column is for grazing function V. For steady solutions, the maximum plankton concentrations (μM N) over all depths at equilibrium were used. For oscillatory solutions, the maximum plankton concentrations over all depths and over the last 200 days of a simulation were used. (i & j) black shading indicate regions where all plankton survive simultaneously (Σ).

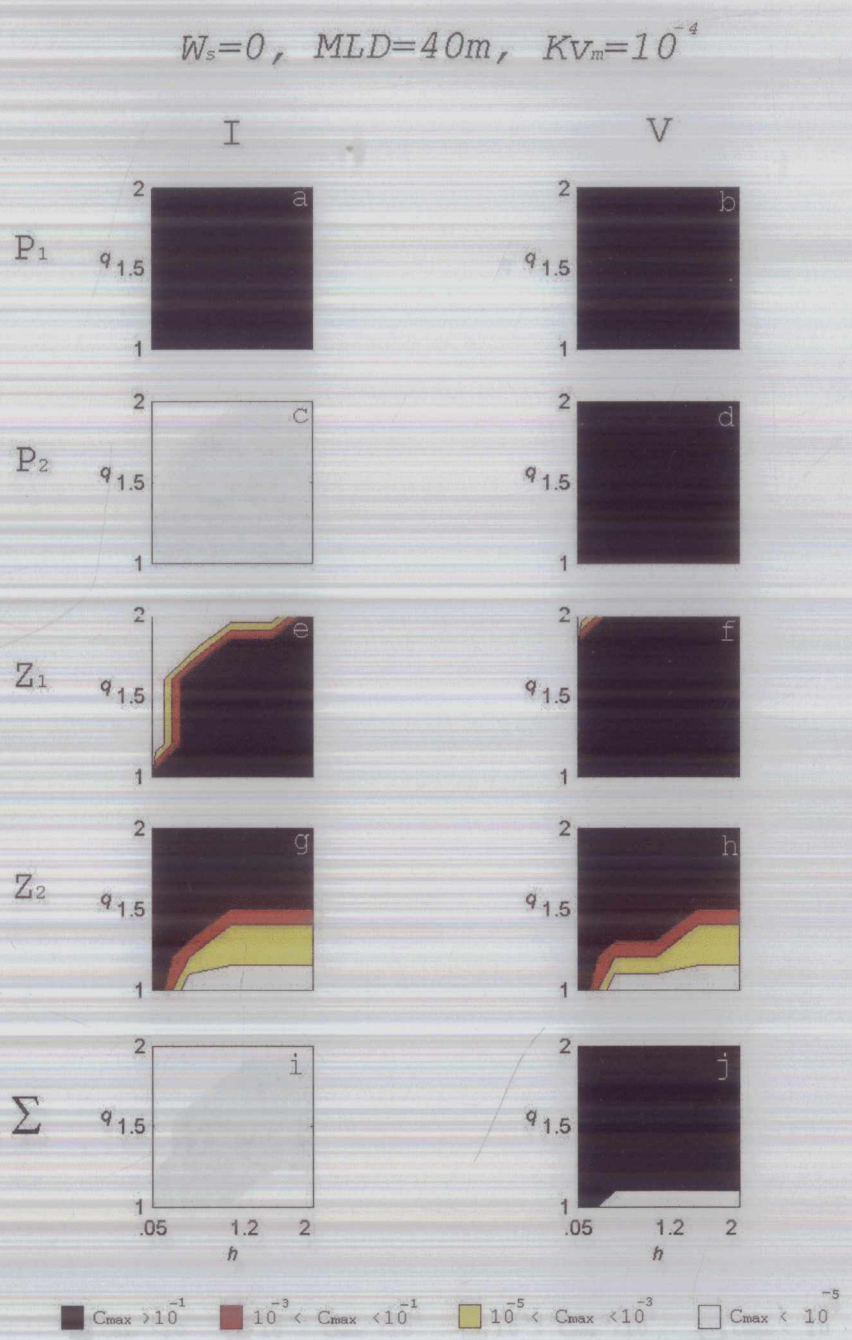

Figure 5-6 Plankton survivorship, MLD=40m, Kv_m=10^{-4} m^2 s^{-1}, W_s=0 m day^{-1}. As for Figure 5-5.

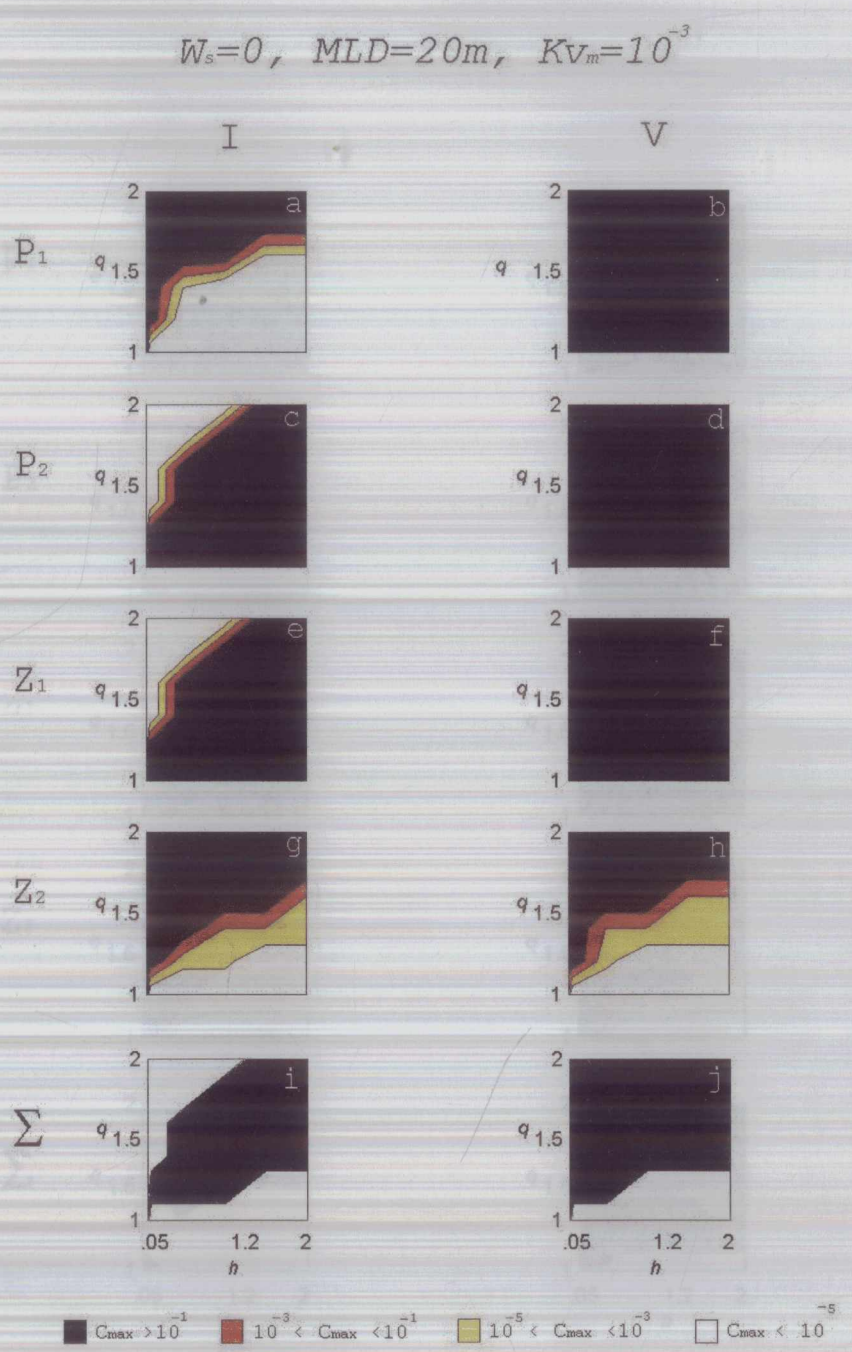

Figure 5-7 Plankton survivorship, MLD=20m, Kv_m=10^{-3} m^2 s^{-1}, W_s=0 m day^{-1}. As for Figure 5-5.

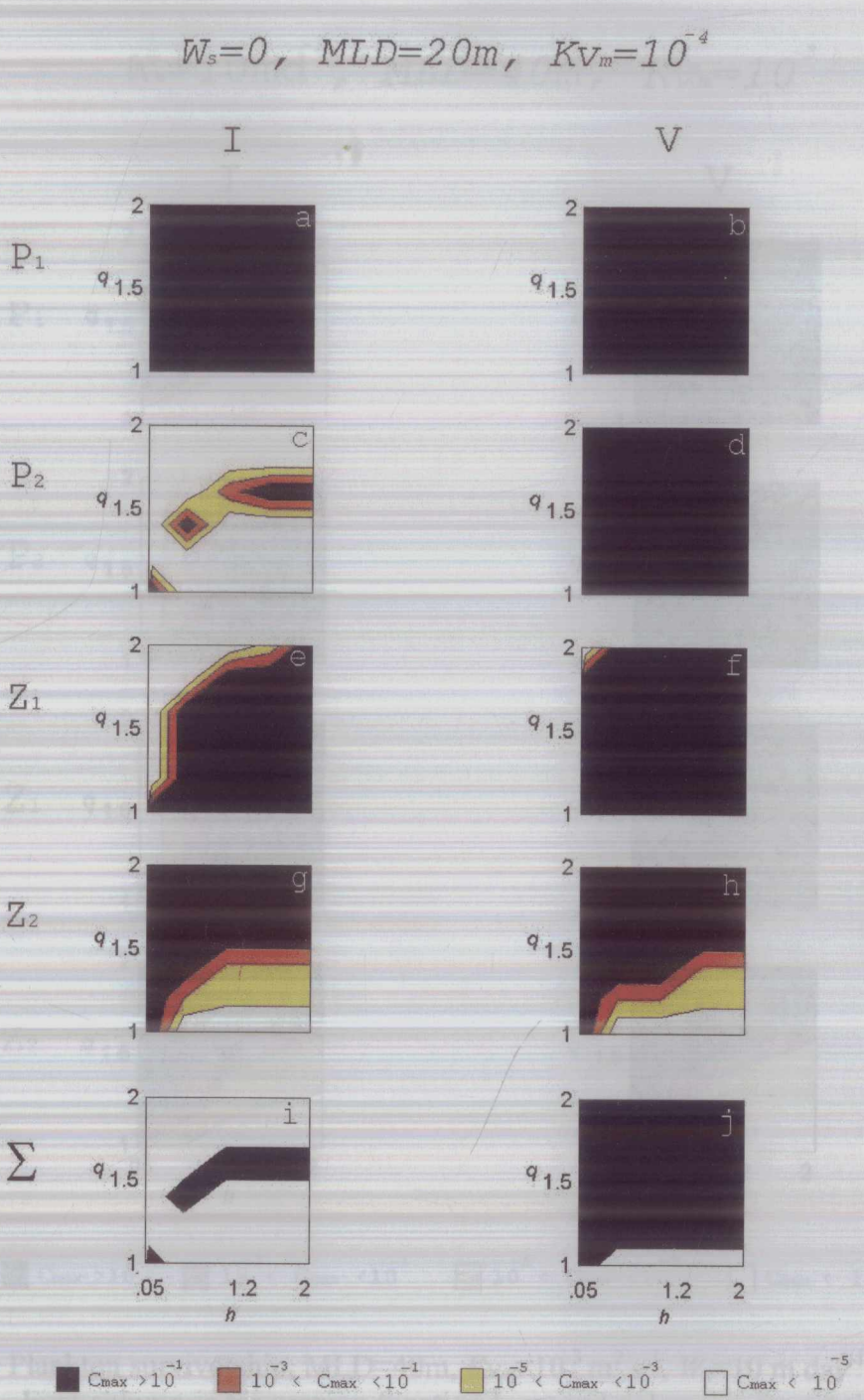

Figure 5-8 Plankton survivorship, MLD=20m, $Kv_m=10^{-4}$ m^2 s^{-1}, W_s=0 m day^{-1}. As for Figure 5-5.

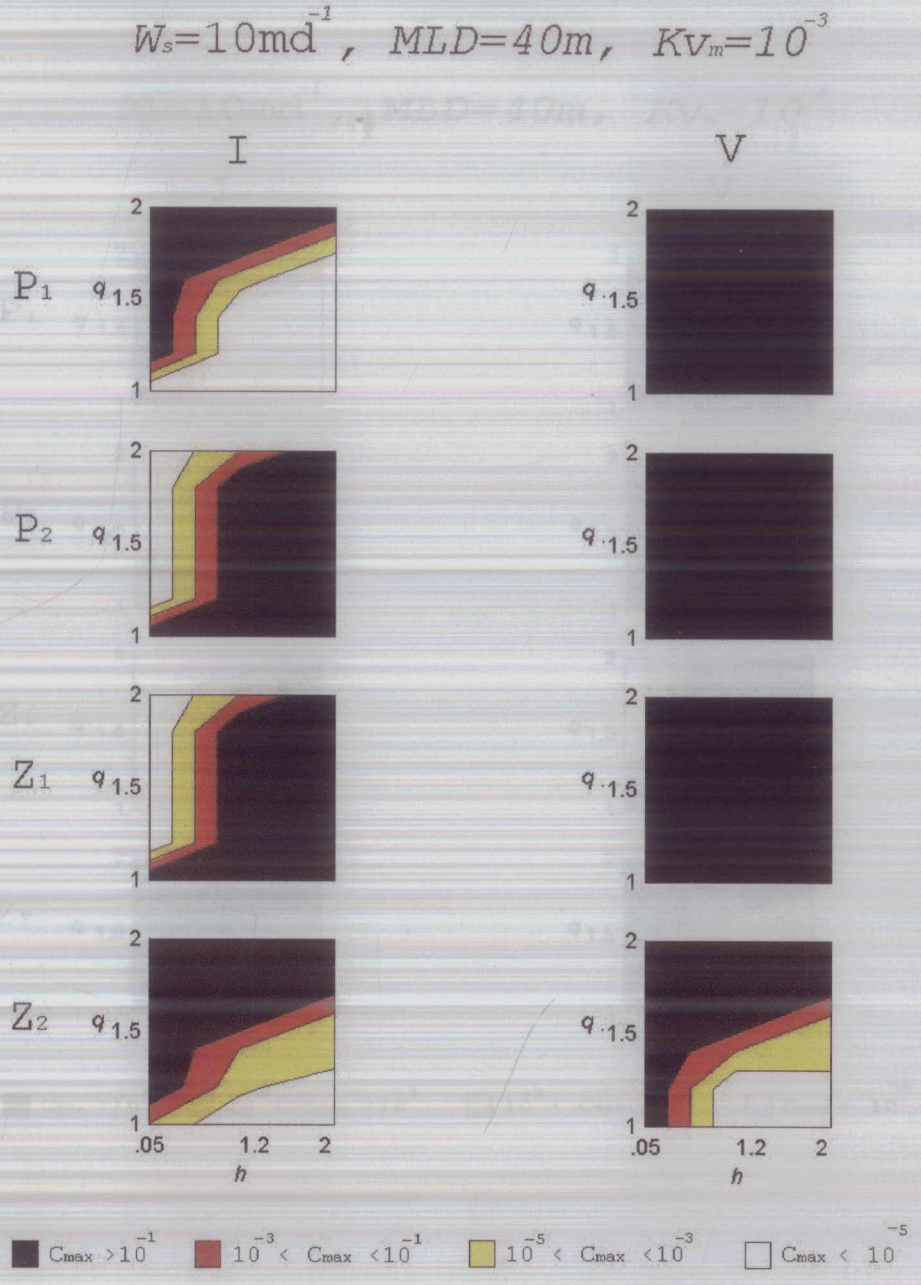

Figure 5-9 Plankton survivorship, MLD=40m, Kv_m=10^{-3} m^2 s^{-1}, W_s=10 m day^{-1}. First column is for grazing function I, second column is for grazing function V. For steady solutions, the maximum plankton concentrations (μM N) over all depths at equilibrium were used. For oscillatory solutions, the maximum plankton concentrations over all depths and over the last 200 days of a simulation were used.

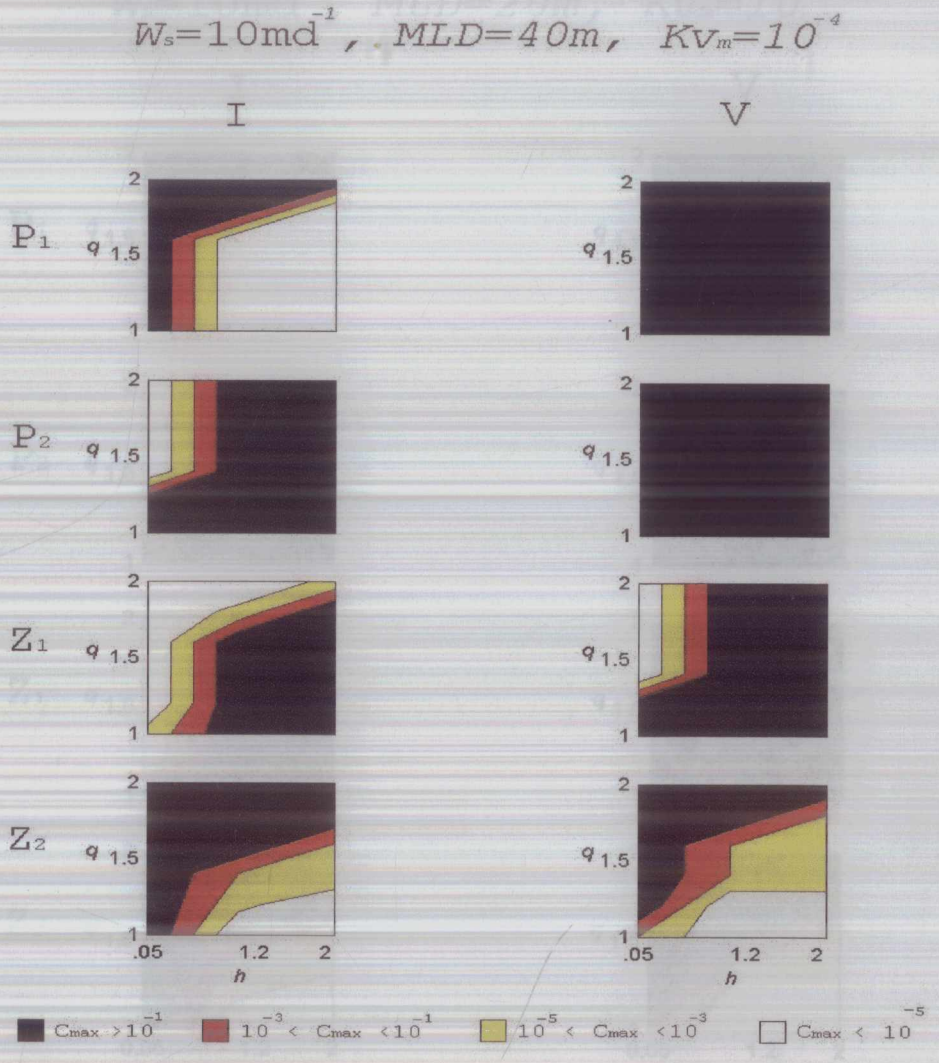

Figure 5-10 Plankton survivorship, MLD=40m, Kv_m=10^{-4} m^2 s^{-1}, W_s=10 m day^{-1}. As for Figure 5-9.

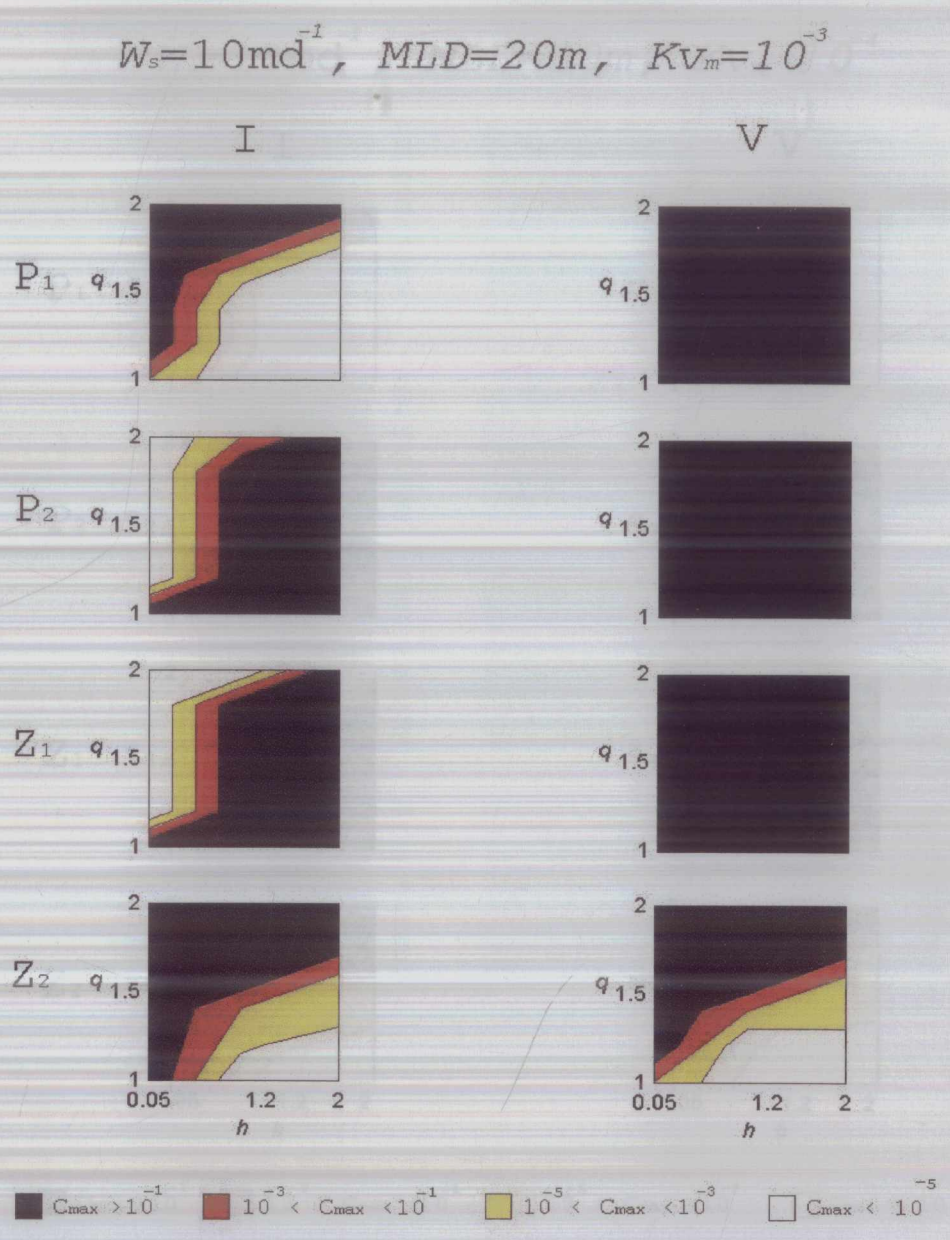

Figure 5-11 Plankton survivorship, MLD=20m, Kv_m=10^{-3} m^2 s^{-1}, W_s=10 m day^{-1}. As for Figure 5-9.

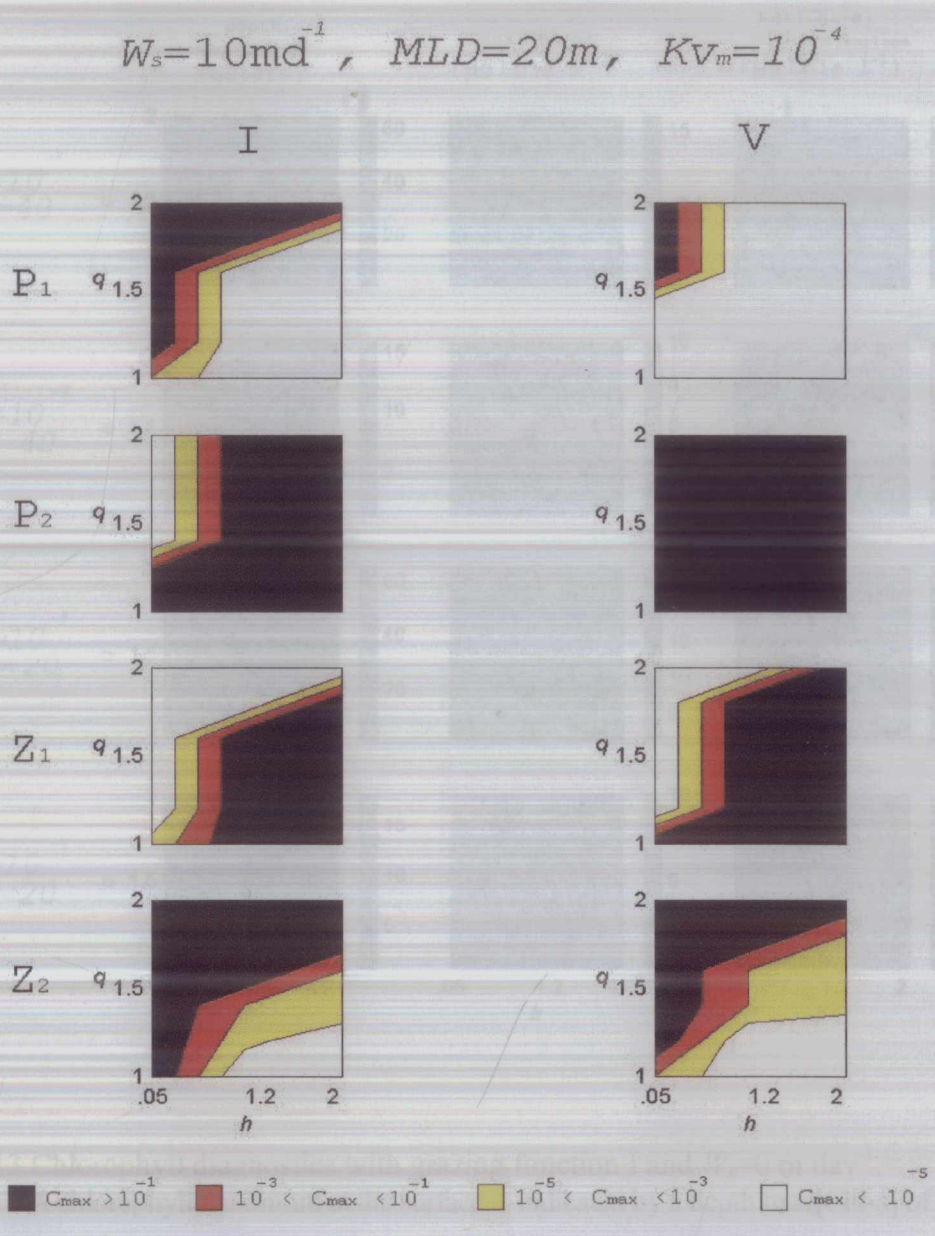

Figure 5-12 Plankton survivorship, MLD=20m, Kv_m=10^{-4} m^2 s^{-1}, W_s=10 m day^{-1}. As for Figure 5-9.

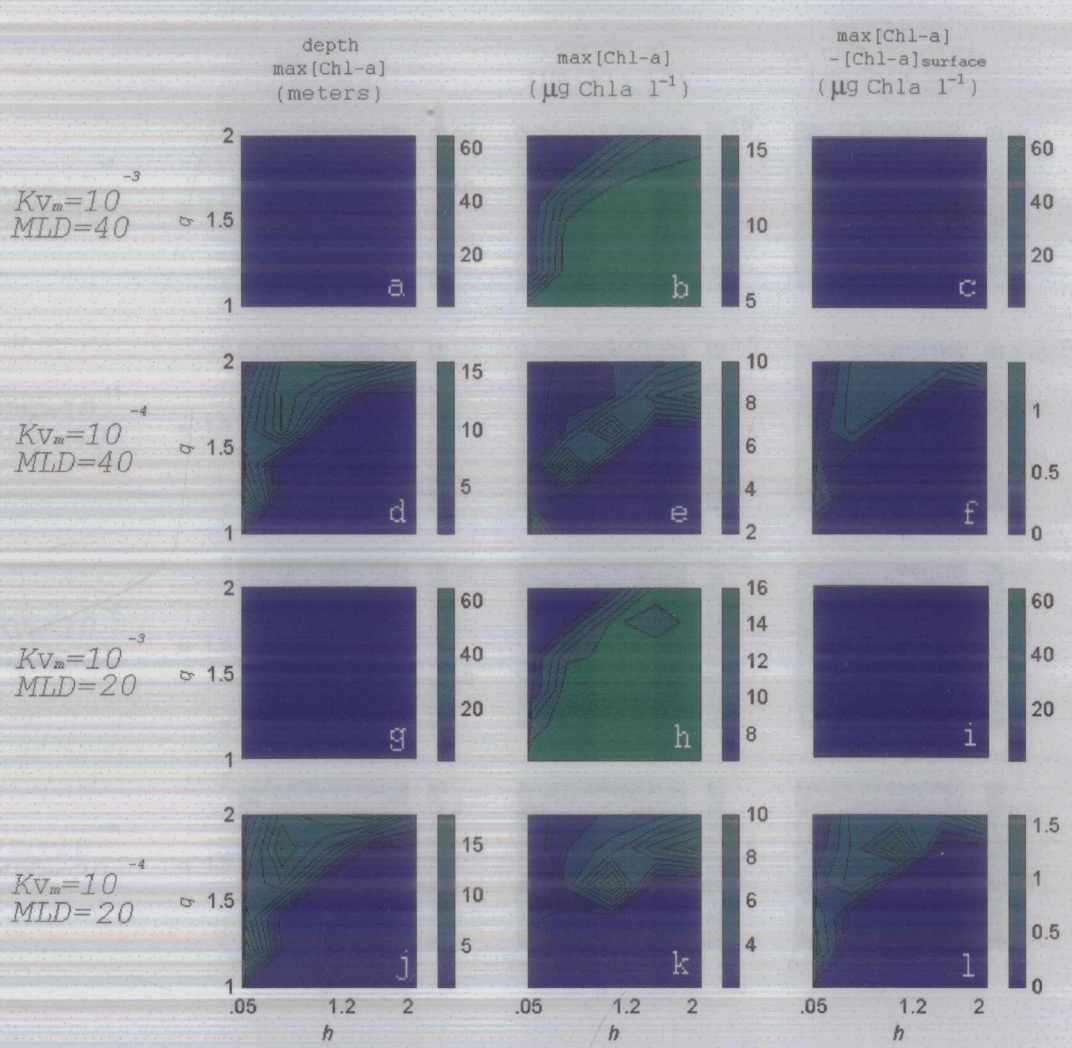

Figure 5-13 Chlorophyll diagnostics with grazing function I and W_s=0 m day^{-1}.
A chlorophyll maximum at the surface is indicated by a depth max[Chl-a] of 1.

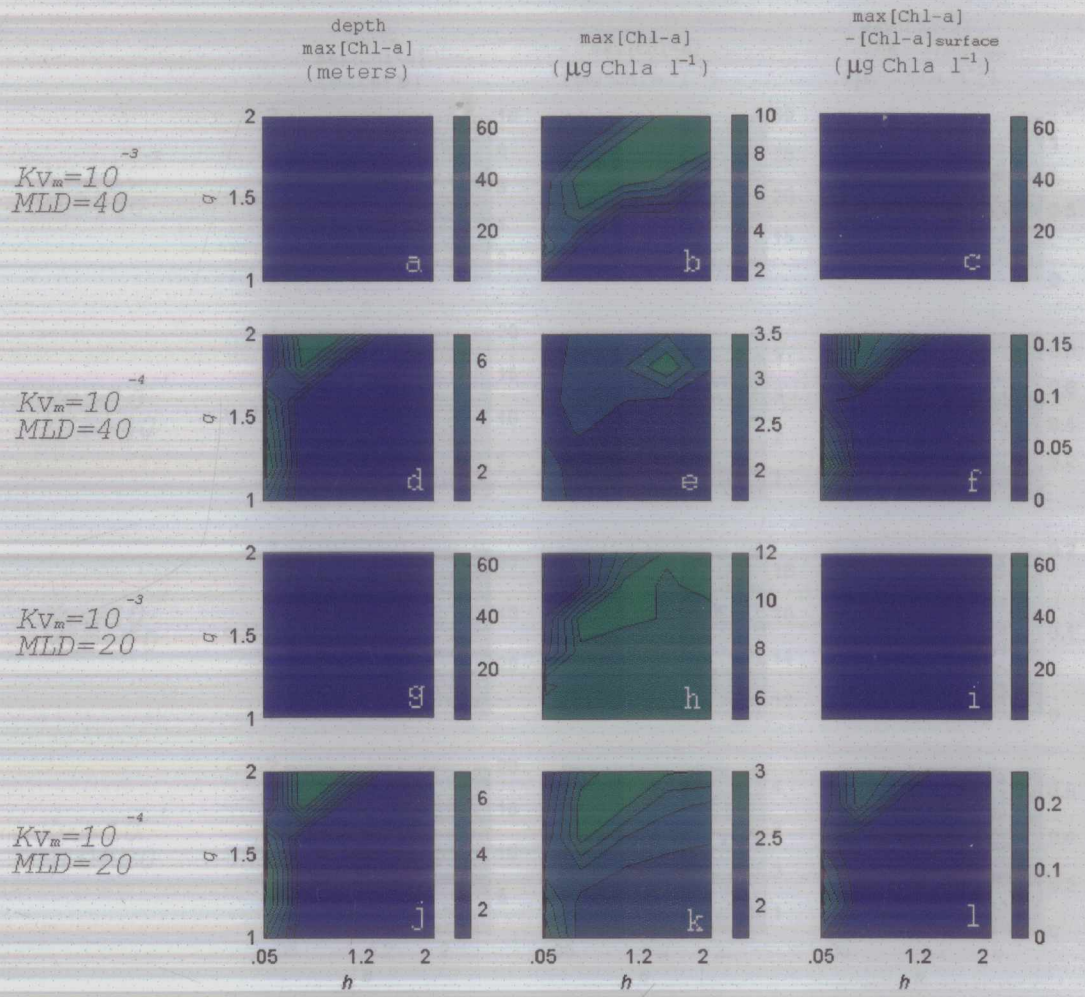

Figure 5-14 Chlorophyll diagnostics with grazing function V and W_s=0 m day^{-1}. A chlorophyll maximum at the surface is indicated by a depth max[Chl-a] of 1.

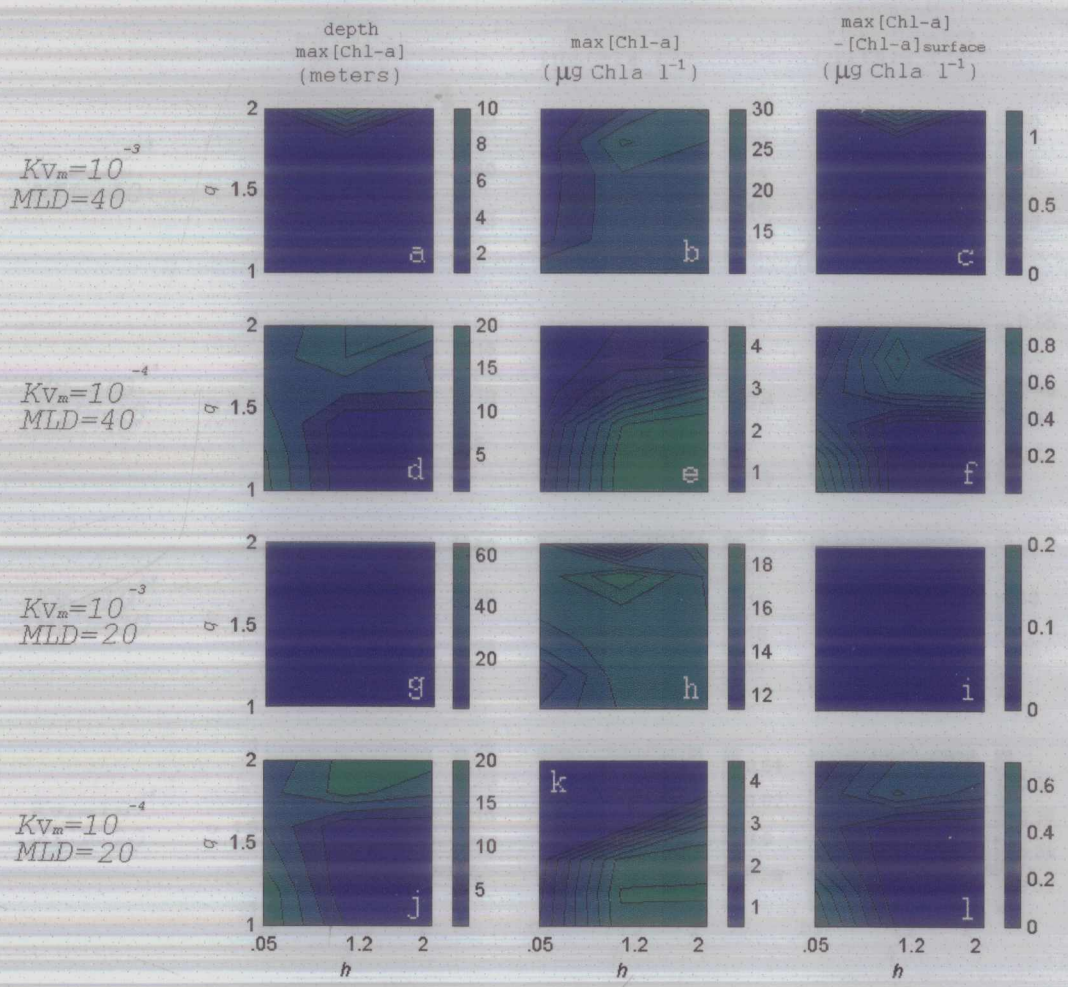

Figure 5-15 Chlorophyll diagnostics with grazing function I and W_s=10 m day^{-1}. A chlorophyll maximum at the surface is indicated by a depth max[Chl-a] of 1.

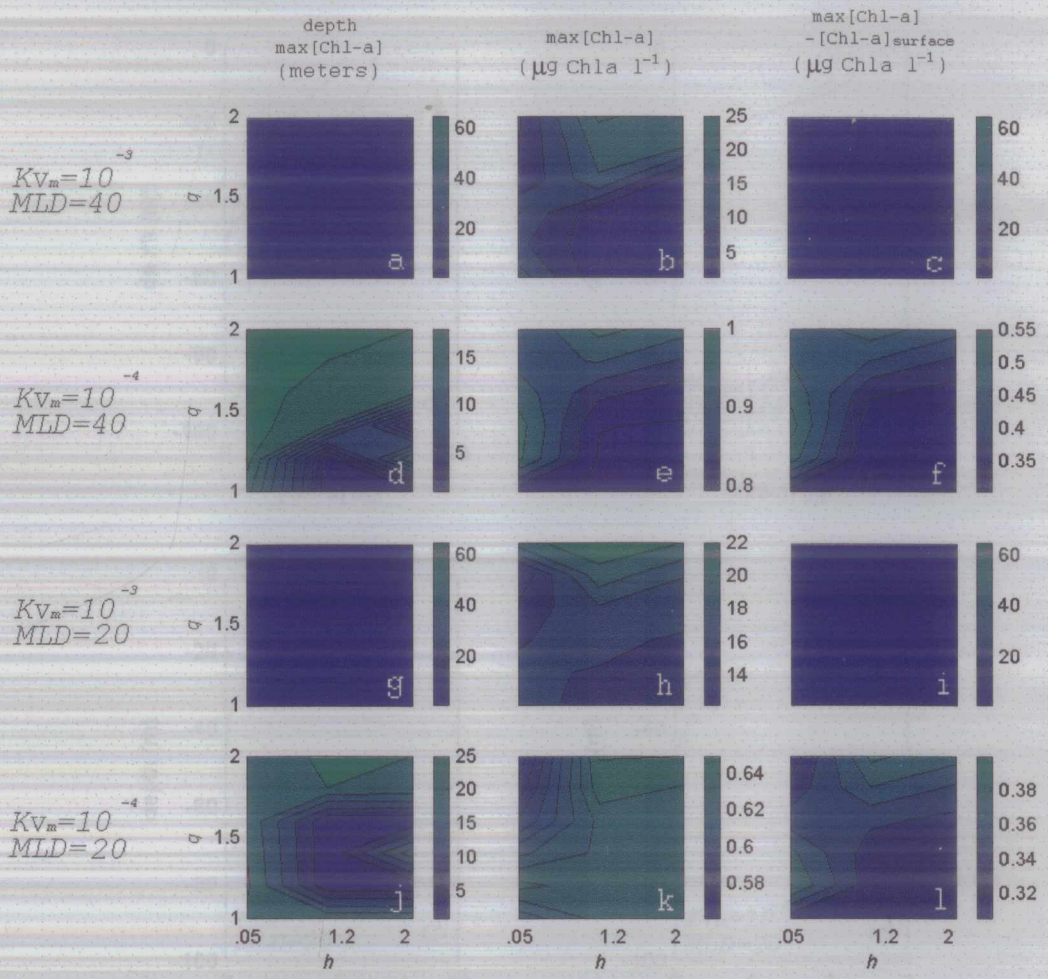

Figure 5-16 Chlorophyll diagnostics with grazing function V and W_s=10 m day^{-1}. A chlorophyll maximum at the surface is indicated by a depth max[Chl-a] of 1.

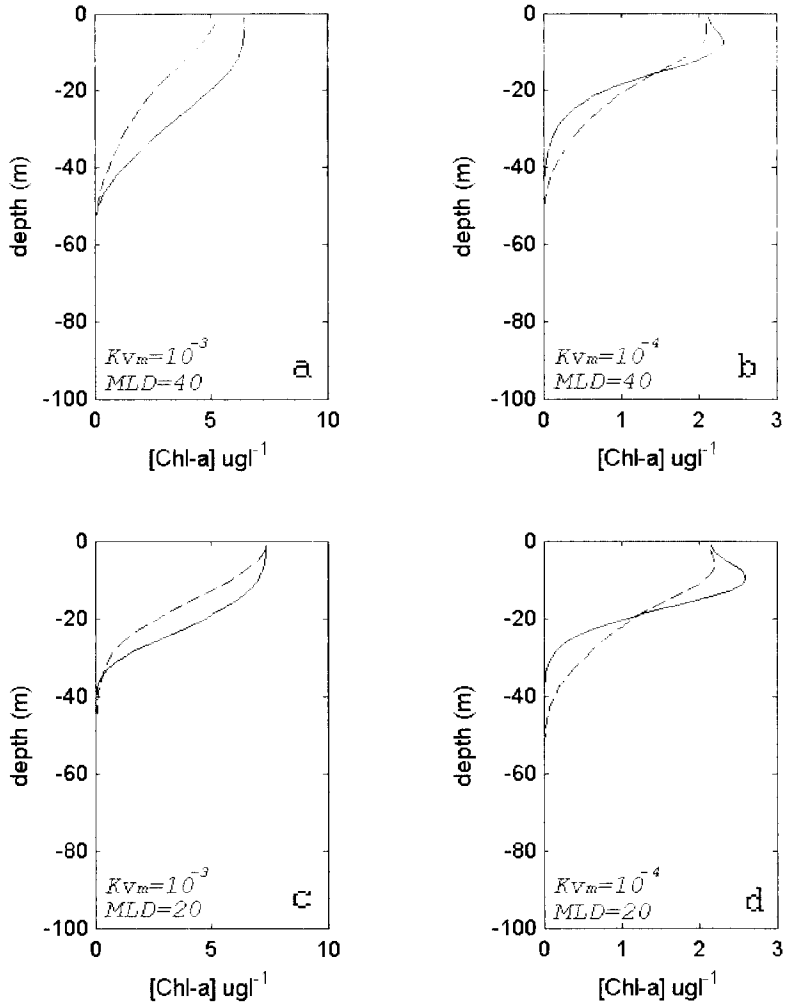

Figure 5-17 Chlorophyll concentration profiles, W_s=0 m day^{-1}.
For function I (solid line) and function V (dotted line). All profiles are shown for q=1.2, h=0.05.

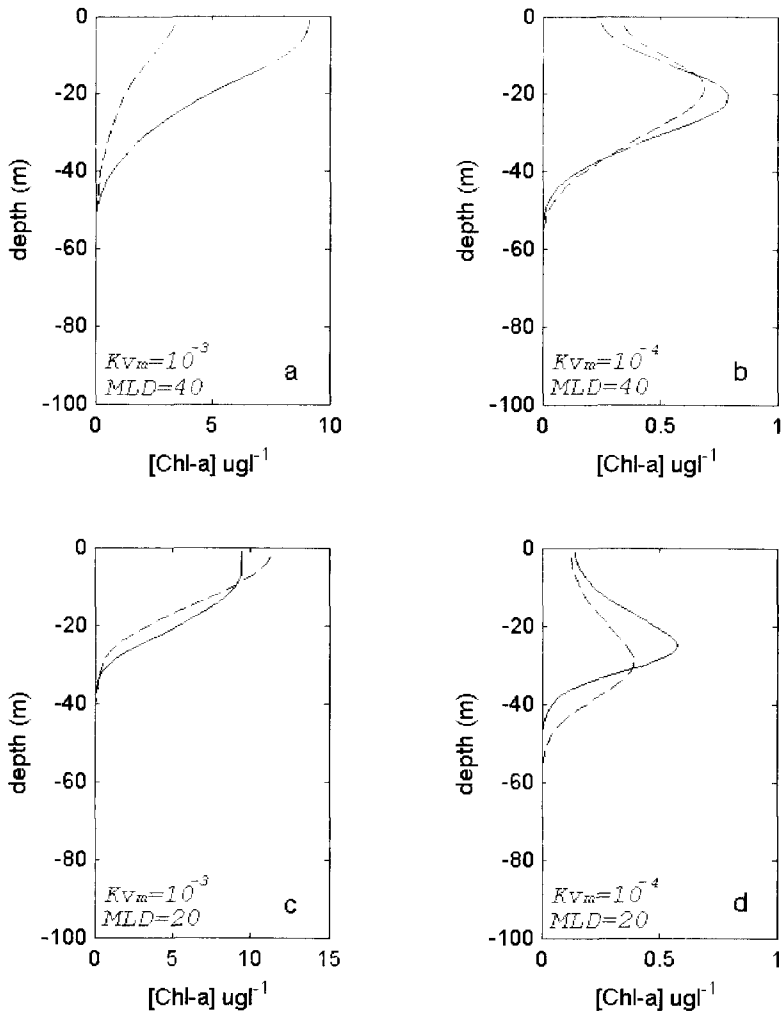

Figure 5-18 Chlorophyll concentration profiles, W_s=10 m day^{-1}.
For function I (solid line) and function V (dotted line). All profiles are shown for q=1.2, h=0.05.

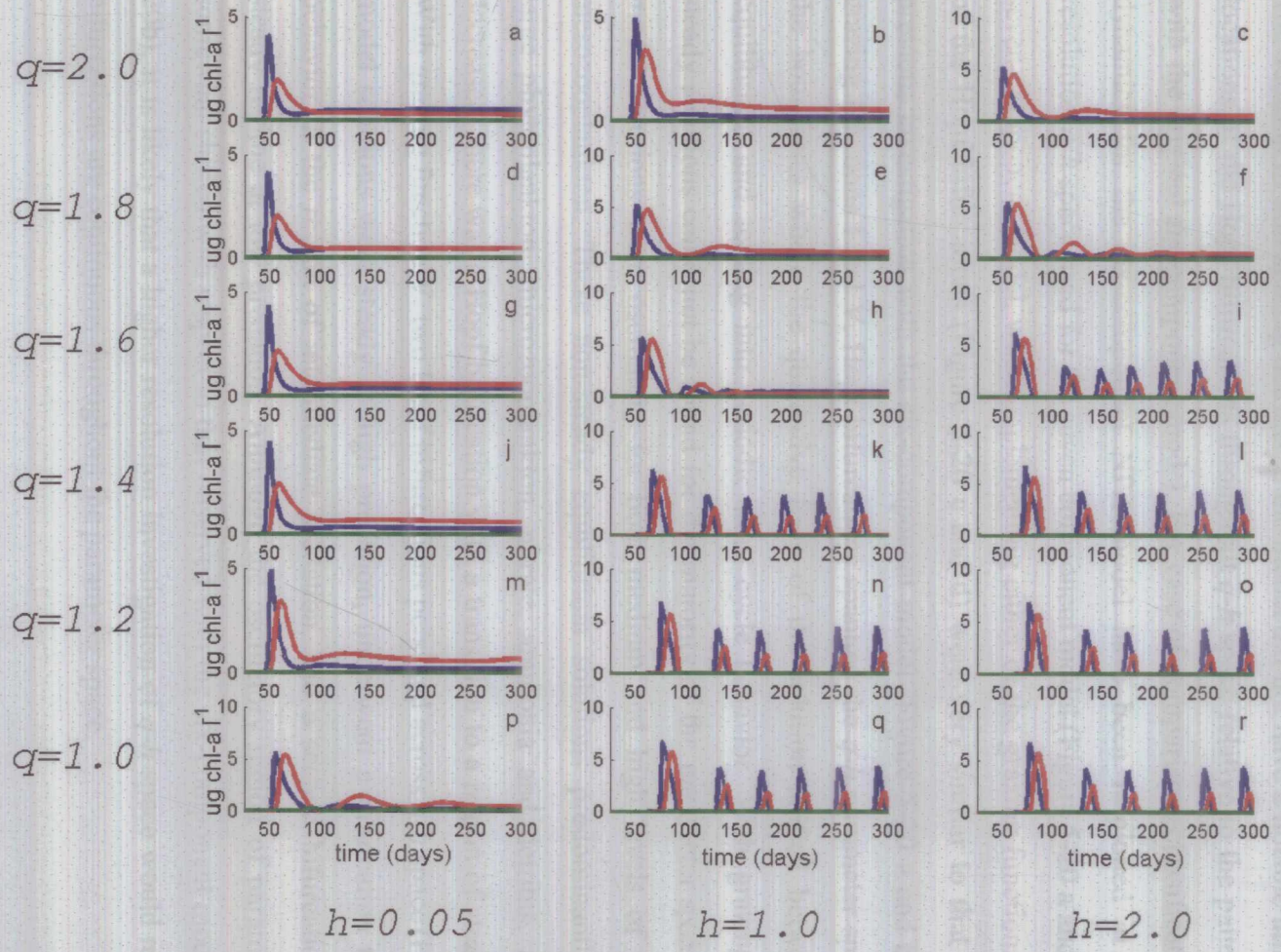

Figure 5-19 Time series of chlorophyll concentration with q and h.
For grazing function I, MLD=20m, $Kv_m=10^{-3}$ m^2 s^{-1} and W_s=10 m day^{-1}. Concentration at 1 meter (blue line), 20 meters (red line) and 40 meters (green line).

5.3.2 Dynamic model behavior

The addition of non-sinking detritus to the model did not have a notable influence on the locations of the Hopf bifurcations throughout *q-h* space relative to the patterns observed with the original six-component model. For ease of comparison, classification of model dynamics for the six-component NPZ model have been re-plotted at the reduced resolution *q-h* space used for the seven component model (Figure 5-20 a and b). With the seven-component model, when implementing either of the grazing functions the location of the Hopf bifurcations (Figure 5-20 c and d) were very similar to that found in the previous investigation with the six-component model (Figure 5-20 a and b). With both grazing functions I and V, Hopf bifurcations spanned the *q-h* parameter space, defining the boundaries where the qualitative form of the solution shifted between a steady equilibrium and settling into periodic limit cycle behavior. With grazing function I, steady solutions could not be found for the majority of the parameter space (Figure 5-20c); model solutions were oscillatory for both medium and high levels of predation on mesozooplankton. These non-steady equilibrium solutions predominantly comprised large phytoplankton, microzooplankton, nitrate, ammonia and detritus. As predation decreased, there was a Hopf bifurcation with a transition to a region of steady solutions. With grazing function V, two Hopf bifurcations persisted across *q-h* space (Figure 5-20 d); model solutions were steady at high predation, underwent a bifurcation to oscillatory behavior in the region of intermediate predation, and a second bifurcation back to a steady regime at low predation. Although the oscillatory region of parameter space is somewhat shifted with respect to that observed with the six-component model (Figure 5-20b), it is likely that a higher resolution investigation of *q-h* space would reveal that the bifurcations are continuous throughout the parameter space.

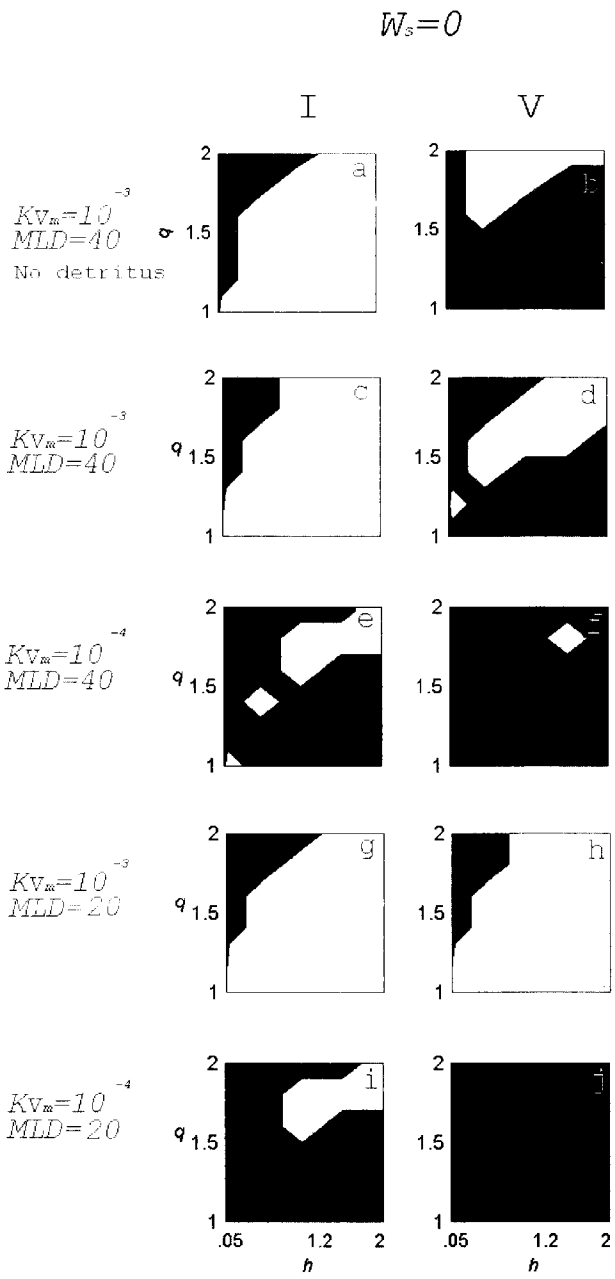

Figure 5-20 Classification of solutions over *q*-*h* parameter space, W_s=0 m day^{-1}. Regions of steady equilibrium solutions are black, regions of oscillatory solutions are white. (a & b) show results for the six-component model re-plotted in the lower resolution *q*-*h* space.

Influence of Physical Regime

The impact of reducing the mixed layer depth on the dynamical behavior of model solutions depended on which grazing function was implemented and on the magnitude of the mixed layer diffusion. With grazing function I and $Kv_m=10^{-3}$ m^2 s^{-1}, reducing the mixed layer depth from 40 to 20 meters did not notably impact the location of the Hopf bifurcation that separates the regions of oscillatory and steady equilibrium solutions (Figure 5-20 c and g). Steady solutions were confined to a small region where predation on mesozooplankton was low. With grazing function V and $Kv_m=10^{-3}$ m^2 s^{-1}, reducing the mixed layer depth from 40 to 20 meters reduced the region of *q-h* space for which model solutions were found to be steady (Figure 5-20 d and h). With the shallower mixed layer (20 meters) the bifurcation pattern was now similar to that observed with grazing function I, *i.e.,* equilibrium solutions were steady only when predation on mesozooplankton was low; solutions were oscillatory for all other regions of parameter space. This increase in model excitability was not observed with an equivalent reduction in mixed layer depth at lower diffusivities ($Kv_m=10^{-4}$ m^2 s^{-1}) in the surface mixed layer (Figure 5-20 f and j); rather solutions were now steady for the entire region of *q-h* space examined, including the previously solitary oscillatory solution. A small increase in prevalence of steady model solutions was also noted with a reduction in the mixed layer depth for grazing function I with $Kv_m=10^{-4}$ m^2 s^{-1} solution (Figure 5-20 e and i).

With both gazing functions, reducing the mixed layer diffusion by an order of magnitude resulted in a broader region of *q-h* parameter space for which solutions could be classified as steady. With this reduced mixing and grazing function I, solutions were now only oscillatory at medium levels of predation (Figure 5-20 c, e, g, i). Although clear Hopf bifurcations did not exist throughout the parameter space, this may be an artifact of the low resolution investigation. The combination of reduced diffusion and grazing function V resulted in solutions that were steady for the majority of parameter space examined (Figure 5-20 d, f, h, j]. There was, in fact, only a small region of parameter

space when the mixed layer depth was 40 meters (corresponding to q=1.8, h=1.5) that produce an oscillatory solution (Figure 5-20f). The existence of this single oscillatory solution suggests that a very narrow region of oscillatory solutions may exist in q-h space.

When detritus was able to sink, changes to the physical forcing regime had a similar impact on model dynamics as observed with non-sinking detritus. Irrespective of the mixed layer depth (20 and 40 meters) or the grazing function (I or V), decreasing the mixed layer diffusion resulted in steady equilibrium solutions for a greater region of the q-h space (Figure 5-21). The influence on dynamics of reducing the mixed layer depth was dependent on both the mixed layer depth and the grazing functions. When the mixed layer diffusion was high (10^{-3} m^2 s^{-1}) and grazing function I was implemented, the model dynamics were not notably influenced by a shift in the mixed layer depth (Figure 5-21 a and e). When function V was implemented, however, the same reduction in mixed layer depth resulted in oscillatory solutions for a greater region of q-h space, such that the pattern of dynamics looked similar to that obtained with function I (Figure 5-21 b and f). With both grazing functions and a smaller mixed layer diffusivity (10^{-4} m^2 s^{-1}), reducing the mixed layer depth did not markedly impact the location of steady/oscillatory regions (Figures 5-21 c, d, g, h].

The incorporation of a non-zero detrital sinking velocity into the NPZ model had a variable degree of impact on model dynamics depending on the grazing function and the mixed layer depth. The addition of a sinking component did, however, always result in model solutions that had similar or broader regions of oscillations throughout q-h space. For ease of comparison, the dynamics obtained for the seven-component model with non-sinking detritus have been reproduced (Figure 5-22) using data only from those points in q-h space for which model behavior with a sinking detrital component was investigated. With grazing function V incorporation of sinking detritus did not have a large impact on model dynamics; at low mixed layer diffusivity model trajectories continued to approach

equilibrium monotonically for each point in *q-h* space [Figures (5-21 and 5-22) d and h], at high mixed layer diffusivity the region of oscillatory solutions bounded by the Hopf bifurcations appeared slightly broader with sinking detritus [Figures (5-21 and 5-22) b and f]. With grazing function I and high diffusion, incorporation of sinking detritus had little or no influence on model dynamics; model trajectories remained monotonic at low predation and were oscillatory at medium to high levels of predation [Figures (5-21 and 5-22) a and e]. With lower diffusivity, the inclusion of detrital sinking resulted in oscillatory model trajectories at high predation (Figure 5-21 c and g), meaning that the *q-h* parameter space was now divided into two dynamic regimes rather than the three found previously (Figure 5-20 e and i).

5.3.3 Availability of Utilizable Nutrient

The availability of utilizable nutrients is known to have an impact on the dynamics of simple NPZ models (Popova *et al.*, 1997; Ryabchenko *et al.* 1997). Thus, the equilibrium nitrate profile is a logical place to look for an explanation of the observed changes to model behavior, resulting from the changes to the model's physical structure. Utilizable nitrogen is considered to be those pools of nitrogen that can be readily assimilated by the phytoplankton, *i.e.*, nitrate and ammonium. When detritus did not sink, while ammonium (N_2) always exhibited a subsurface maximum in the region of 30 meters, nitrate (N_1) concentration always increased monotonically with depth, from low concentrations in the mixed layer to relatively high concentrations that dominated the system below the mixed layer (*i.e.*, Figure 4.9). Nitrate concentrations were an order of magnitude greater than ammonium concentrations. Therefore, when the detrital component was unable to sink, the total utilizable nitrogen available to the phytoplankton always increased with depth.

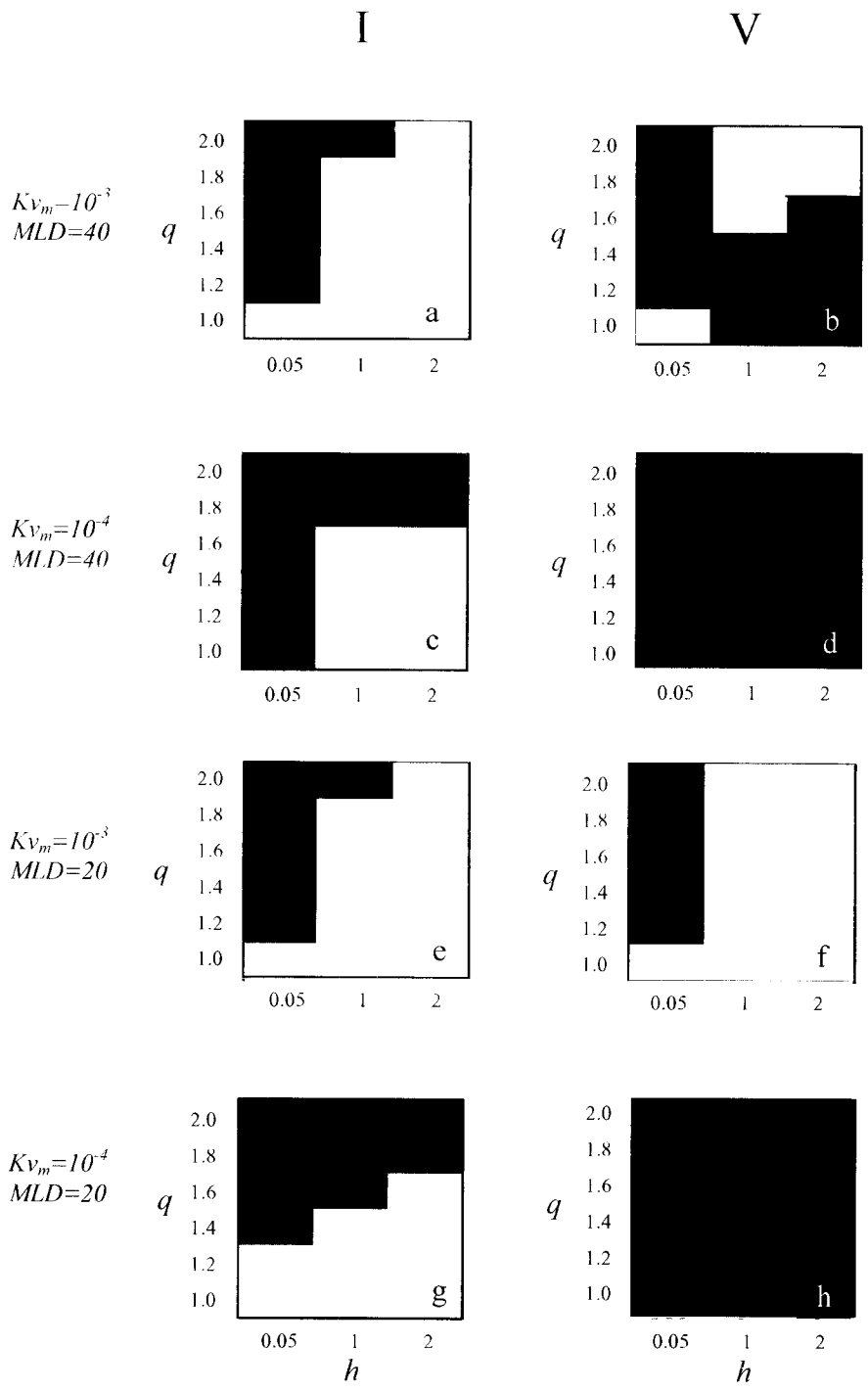

Figure 5-21 Classification of solutions over q-h parameter space, W_s=10 m day^{-1}. Regions of steady equilibrium solutions are black, regions of oscillatory solutions are white.

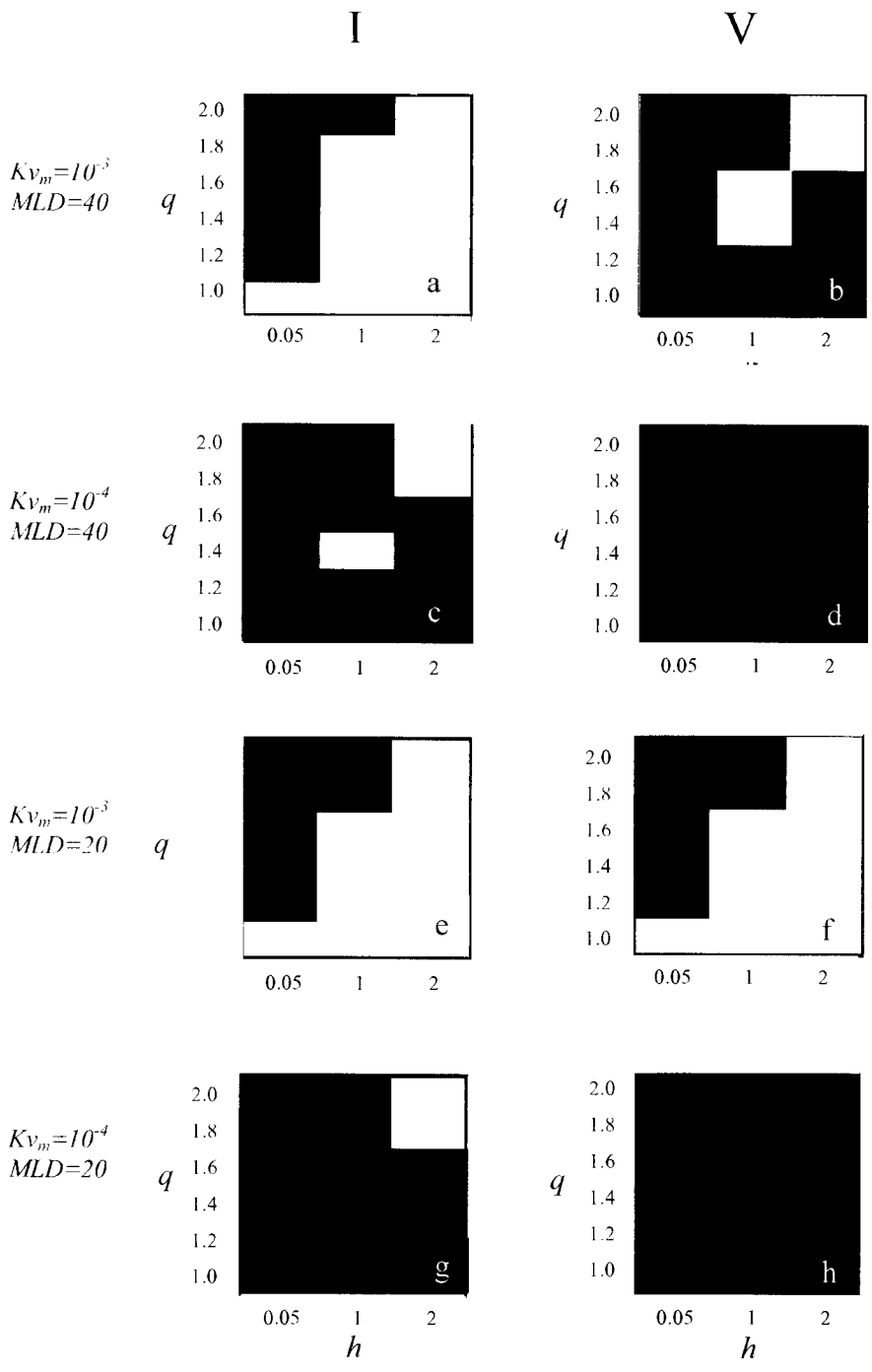

Figure 5-22 Classification of solutions over q-h parameter space, W_s=0 m day^{-1}. This is Figure 5-20 plotted at the lower q-h resolution. Regions of steady equilibrium solutions are black, regions of oscillatory solutions are white.

Profiles of utilizable nitrogen ($N=N_1+N_2$) and the flux of N are shown only for the point q=1.2 and h=0.05 [Figures (5-23 through 5-28)], this point was selected for ease of comparison between model experiments because model solutions always had a steady equilibrium here. Patterns illustrated by these plots are representative of steady solutions throughout q-h space. When detritus had a zero sinking velocity, a reduction in both the mixed layer depth and the magnitude of vertical diffusion in the surface mixed layer caused a shoaling and flattening of the nutricline in steady equilibrium solutions. Irrespective of which of the two grazing functions was implemented, decreasing the mixed layer depth from 40 meters to 20 meters raised the depth of the nutricline [Figures(5-23 and 5-24) e and k]; a larger shift in nutricline position was observed with the larger mixed layer diffusion coefficient (Kv_m=1x10^{-3} m^2 s^{-1}). Decreasing the mixed layer diffusion by an order of magnitude had a greater impact on nutricline position when the mixed layer depth was deeper [Figures (5-23 and 5-24) b]; when the mixed layer depth was at 20 meters only a slight shift in the position of the nutricline was observed with a reduction in diffusion [Figures (5-23 and 5-23) h]. Similar shifts in position of the nutricline were observed irrespective of which grazing function was implemented. Therefore, changes in model dynamics therefore cannot be explained purely by a shift in the steady state nitrate profile.

Although the equilibrium nitrate profiles cannot explain the observed changes in model dynamics with changes to the model's physical structure, changes in the vertical flux of utilizable nitrogen at equilibrium are very revealing. The flux of utilizable nitrogen is given by:

$$FLUX = Kv\frac{\partial(N_1+N_2)}{\partial z} \quad \frac{\mu M\, N}{m^2 \cdot s} \qquad \text{Eq. 5.10}$$

This meant that the flux of utilizable nitrogen ($N=N_1+N_2$) was always positive upwards in the case of non-sinking detritus. When detritus had a non-zero sinking velocity, due to the boundary condition (N_{2b}=10μM N) enforced, the flux of nitrogen could be positive downwards. Throughout *q-h* space, a decrease in the mixed layer diffusion (Kv_m) reduced the peak upwards flux of N by an order of magnitude. This was true irrespective of the depth of the mixed layer (20 or 40 meters) or which grazing function (I or V) was implemented [Figures (5-23 and 5-24) c and i]. When $Kv_m=10^{-3}$ m^2 s^{-1}, decreasing the mixed layer depth from 40 to 20 meters reduced the peak flux by approximately 6μM N m^{-2} s^{-1} when grazing function I was implemented (Figure 5-23 f), however, when function V was implemented an increase in peak flux of approximately 6μM N m^{-2} s^{-1} resulted from the same change in mixed layer depth (Figure 5-24 f). With both grazing functions and $Kv_m=10^{-4}$ m^2 s^{-1}, decreasing the mixed layer depth did not cause a notable change to the magnitude of the peak flux of N at equilibrium [Figures (5-23 and 5-24) l]. It thus appears that the observed changes in model dynamics with alternative diffusivity profiles can be explained by the resultant change in the flux of utilizable nitrogen at equilibrium. An increase in flux of utilizable nitrate enhanced the excitability of the model, giving rise to oscillatory model solutions for a broader region of *q-h* parameter space. Conversely, a decrease in the upwards flux on utilizable nitrate has the opposite effect, enhancing model stability and creating steady equilibrium solutions for a broader region of the parameter space investigated. An increase in N flux of only 6 μM N m^{-2} s^{-1} was sufficient to shift model dynamics from steady equilibrium to oscillatory limit cycles.

With sinking detritus, as with non-sinking detritus, the changes to model dynamics, brought about by the changes in the physical forcing regime, appeared to be related to the strength of peak flux of utilizable nitrate, which generally coincides with the nutricline. The region of *q-h* space for which model solutions approached oscillatory equilibrium dynamics was broader when the change to the physical forcing regime caused an increase in the flux of utilizable nitrate. Decreasing the mixed layer diffusion caused a reduction

in peak flux by an order of magnitude [Figures (5-25 and 5-26) c and i] and steady equilibrium solutions were observed for a broader region of q-h space [Figure 5-21(a, c, b, d)]. Decreasing the mixed layer depth when the mixed layer diffusion was large (10^{-3} m^2 s^{-1}) resulted in a smaller peak flux when grazing function I was implemented (Figure 5-25 f), but a larger flux when function V was implemented (Figure 5-26 f); thus potentially explaining the different response observed in the dynamics. With a lower mixed layer diffusion (10^{-4} m^2 s^{-1}) an equivalent reduction in mixed layer depth resulted in much smaller fluxes of utilizable nutrient with both grazing functions [Figures (5-25 and 5-26)l]; however, little change was observed in the pattern of dynamics (Figure 5-21 c, g, d , h).

Comparing the dynamics of the model with sinking and non-sinking detritus [Figures(5-21 and 5-22)] reveal that changes in the peak flux of utilizable nitrogen cannot solely explain the observed changes in model behavior resulting from changes to model structure. When mixed layer diffusion was large (10^{-3} m^2 s^{-1}) and mixed layer shallow (20 meters), the addition of sinking resulted in an increase in the flux of nitrate [Figures (5-27 and 5-28) i], and more oscillatory solutions [Figures (5-21 and 5-22) e and f]. However with a deeper mixed layer the addition of sinking also resulted in a larger flux [Figures (5-27 and 5-28) c], but did not have much impact on model dynamics [Figures (5-21 and 5-22) a and b]. Additionally, when the mixed layer diffusion was smaller (10^{-4} m^2 s^{-1}), irrespective of the mixed layer depth, adding sinking detritus resulted in a smaller flux of utilizable nitrogen [Figures (5-27 and 5-28) f and l] yet model solutions were more oscillatory with function I [compare Figures (5-21 and 5-22) c and g] and unchanged with function V [compare Figures (5-21 and 5-22) d and h]. For the case of lower mixed layer diffusion the depth of the nutricline was quite depressed relative to the no sinking case [Figures (5-27 and 5-28) e and k]. This leads to the speculation that in addition to the flux of nitrogen into the mixed layer, model excitability is in part related to the equilibrium nitrogen concentration within the mixed layer.

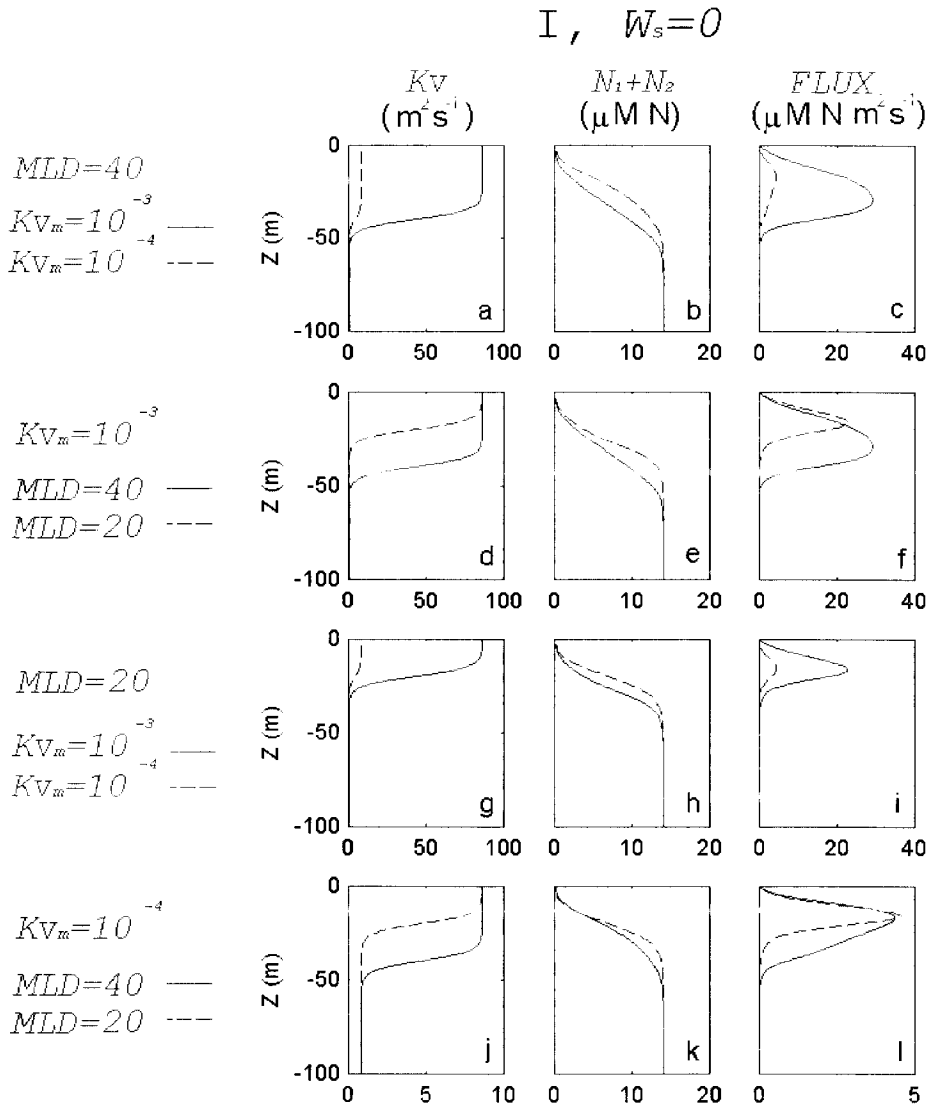

Figure 5-23 Profiles of Kv, [N], and flux. Grazing function I, W_s=0 m day^{-1}. All profiles are for q=1.2 and h=0.05.

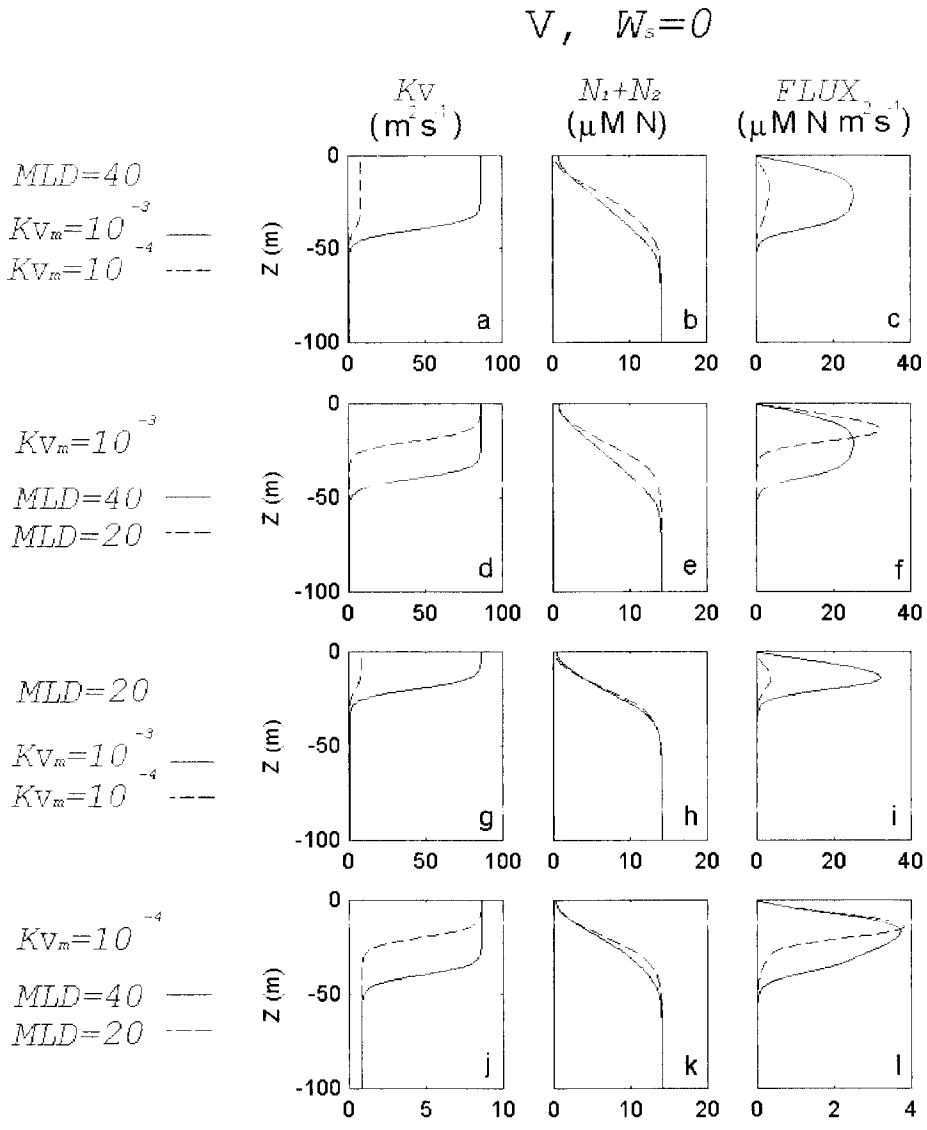

Figure 5-24 Profiles of Kv, [N], and flux. Grazing function V, W_s=0 m day^{-1}. All profiles are for q=1.2 and h=0.05.

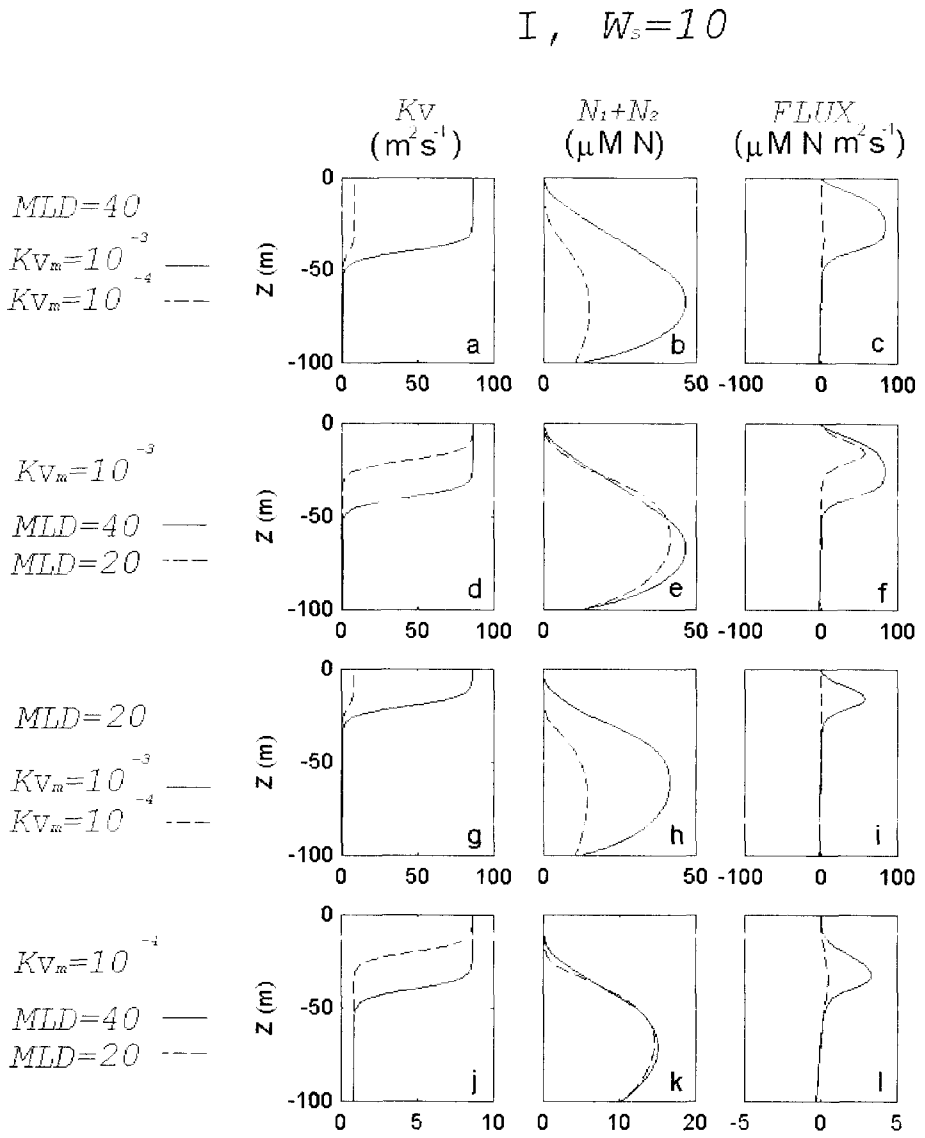

Figure 5-25 Profiles of Kv, [N], and flux. Grazing function I, W_s=10 m day^{-1}. All profiles are for q=1.2 and h=0.05.

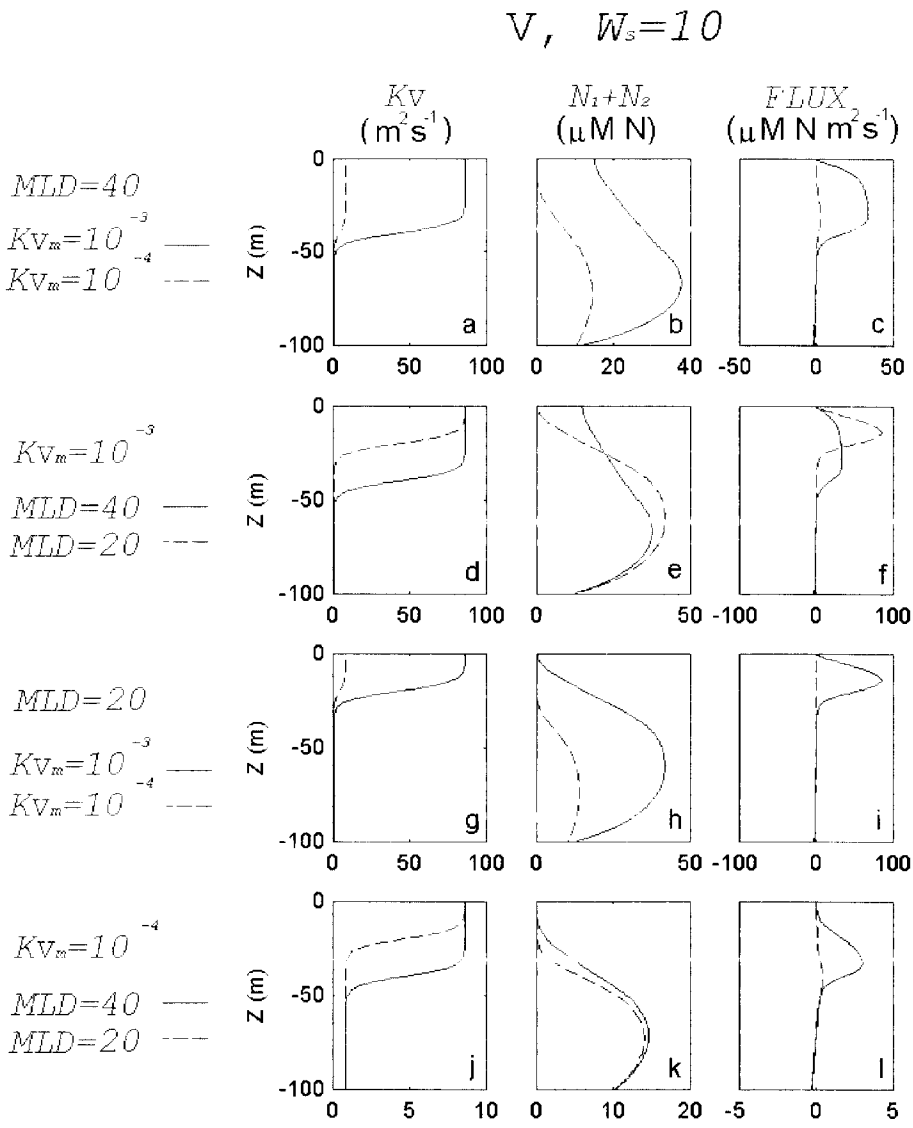

Figure 5-26 Profiles of Kv, [N], and flux. Grazing function V, W_s=10 m day^{-1}. All profiles are for q=1.2 and h=0.05.

I

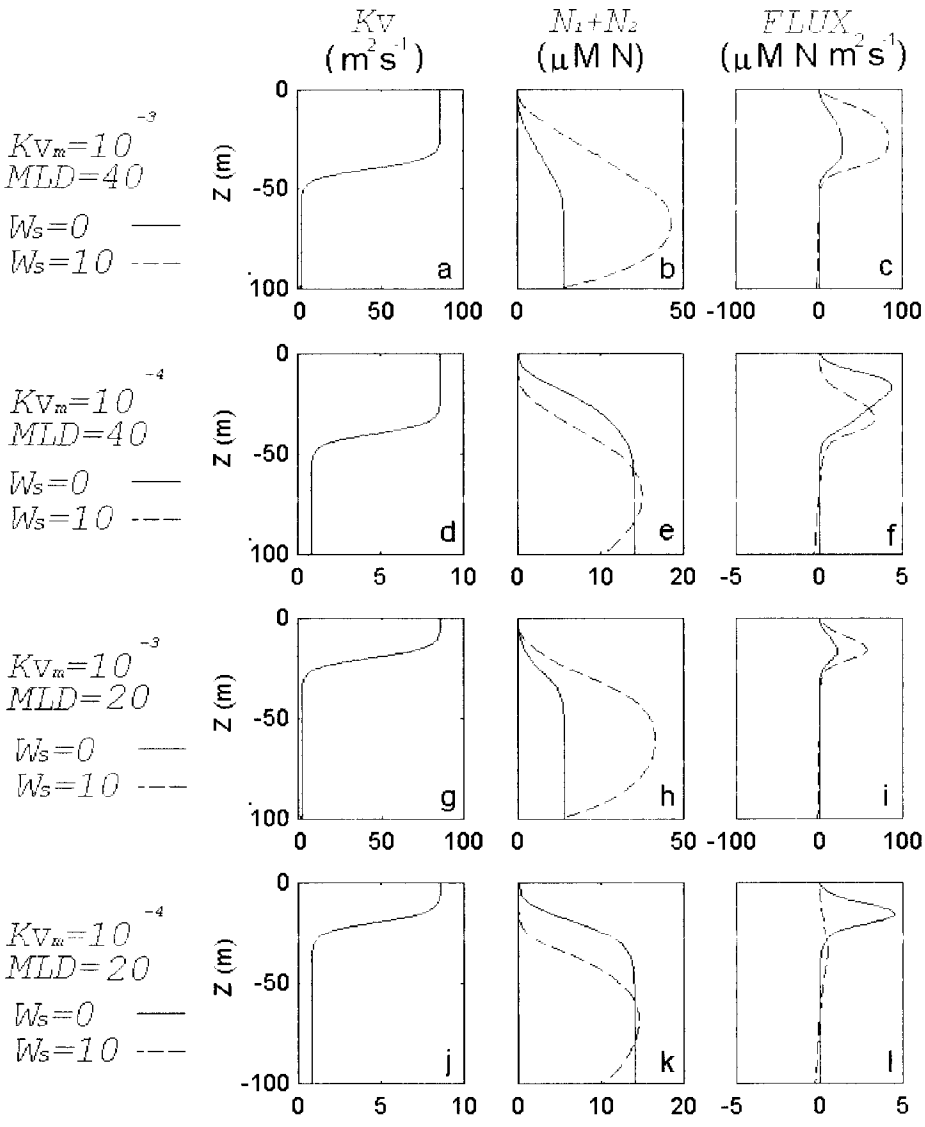

Figure 5-27 Profiles of Kv, [N], and flux. Grazing function I, W_s=0 and 10 m day^{-1}. All profiles are for q=1.2 and h=0.05.

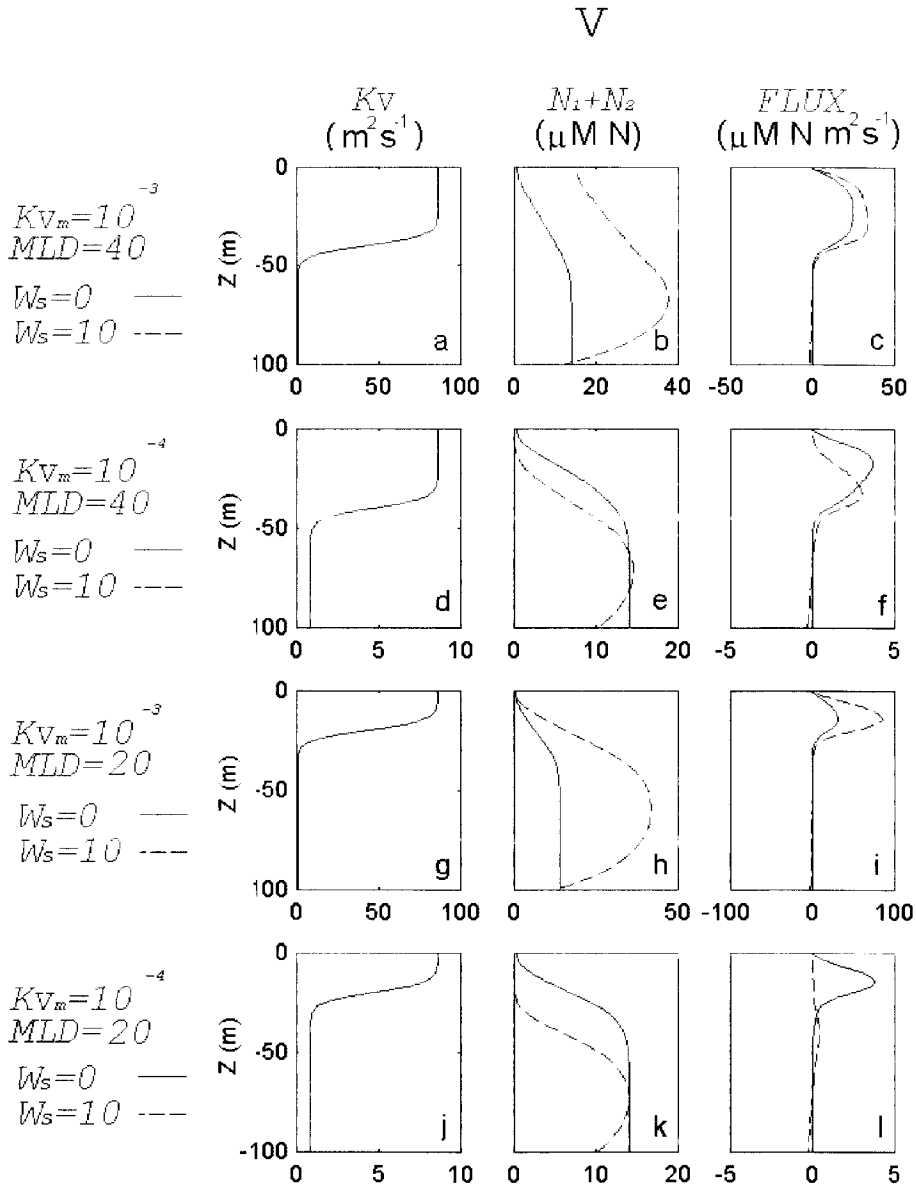

Figure 5-28 Profiles of Kv, [N], and flux. Grazing function V, W_s=0 and 10 m day^{-1}. All profiles are for q=1.2 and h=0.05.

5.4 Discussion

It is becoming more common for a detritus component to be included in NPZ marine ecosystem models. Such an inclusion allows more explicit representation of the nutrient regeneration loop and allows for the export of nitrogen from the euphotic zone. The detritus component is effectively a nitrogen store that delays the return of organic matter to inorganic nutrients, and reduces the total system nutrient availability through the loss of sinking material. Explicit representation of the regeneration loop in NPZ models, through the inclusion of detritus, is commonly thought, although not shown, to act as a 'brake' on the model, reducing excitability.

This investigation explored the non-linear dynamics of a depth-explicit, one-dimensional, seven-component NPZ model in which zooplankton could graze on multiple nutritional resources. The dynamic behavior of the NPZ model was investigated for alternative detrital sinking rates and alternative diffusivity profiles. The survivorship of equilibrium solutions and the existence of a sub-surface chlorophyll maximum were also explored. Alternative stationary parameterizations for the mixed layer diffusivity (Kv_m= 10^{-3} m^2 s^{-1} or 10^{-4} m^2 s^{-1}) and the mixed layer depth (20 or 40 meters) were implemented. The model was parameterized for the coastal Gulf of Alaska ecosystem but the specific predation rate (h=0.05-2 $[gCm^{-3}]^{1-q}$ day^{-1}), and the form of the predation function ($1 \leq q \leq 2$) were systematically varied. Model behavior was initially explored with zero sinking velocity for detritus (W_s=0 m day^{-1}), this was subsequently increased to 10 m day^{-1}. Two alternative forms for the grazing function (grazing function I and V) were implemented. These two functional forms were considered to be the most dissimilar structurally and were found previously to give rise to the 'end member' behavior (Chapter 4).

At present no general method for analysis of non-stationary systems of non-linear differential equations exists. It is not possible to find analytical solutions to the intermediately complex, spatially explicit NPZ model under investigation here, therefore

the classic approach to stability analysis, is of limited use for classifying model behavior. To gain insight into the behavior of this system model solutions were examined in time and space, in order to numerically seek and classify solutions. Such an approach provides a useful insight into the behavior of depth-explicit models comprising multiple grazers and prey types.

Many of the past studies on model dynamics consider ecosystem models that comprise only a single phytoplankton or zooplankton component and so do not address survivorship of multiple plankton types. However, the findings presented in Chapter 4 revealed that with some forms of the grazing function, all model component thrived simultaneously only in very small regions of parameter space. This is an important issue, especially with the majority of modern ecosystem modeling studies using models that comprise multiple grazers and multiple prey types, and observational data most often shows coexistence. The results presented here re-enforce the conclusions from Chapter 4, *i.e.,* that when implementing a Michaelis-Menten grazing function extended to multiple nutritional resources (function I) the model was oscillatory for a broad region of *q-h* parameter space; commonly steady solutions comprised only small phytoplankton, mesozooplankton, nitrate, ammonium and detritus, and were only found when predation on zooplankton (H) was low. Conversely, with a sigmoidal grazing function extended to multiple nutritional resources (function V), the model approached steady solutions for a much broader region of *q-h* parameter space, and solutions comprising all model components were common. As discussed in Chapter 4, the difference in model structure and dynamics when implementing grazing function I and V is related to the inherent assumptions underlying the formulations. With function I, prey are provided no refuge from grazing pressure no matter how rare, whereas with function V, rare prey experience a reprise from grazing irrespective of the concentrations of the other available prey types.

The addition of a detritus component to a previously six-component (P_1,P_2,Z_1,Z_2,N_1,N_2) model was shown not to have a notable impact on the structure of model solutions or on

the dynamic behavior of the model if the detritus was unable to sink. However, if detritus has a non-zero sinking velocity, the survivorship in the model solutions was little altered, but the vertical profiles of model components were impacted significantly. For example, although in some instances it is possible to get a sub-surface chlorophyll maximum without sinking detritus, only with the incorporation of sinking detritus was a sub-surface chlorophyll maximum of a reasonably realistic depth and magnitude observed consistently throughout the parameter space investigated. The depth of the sub-surface chlorophyll maximum with grazing function I was still a little shallow relative to observations (Figure 5-1). Additionally, with the inclusion of sinking detritus, model dynamics tended to be more excitable; exhibiting oscillatory behavior for a broader region of parameter space investigated. It has previously been shown that the addition of a sinking detritus compartment to a simple three-component NPZ model hardly changes the nature of the qualitative dynamics so long as the zooplankton was unable to graze upon it (Edwards, 2001). It is likely that this discrepancy arises because the model investigated by Edwards (2001) was not depth-explicit, rather it was a simple mixed layer model and sinking detritus was modeled as a constant loss rate from the system. Edwards (2001) suggested that if the size of the detritus pool is not required, then a simpler model without detritus could be used to investigate model dynamics. The results presented here illustrate that with depth-explicit ecosystem models, such as those commonly used in ecosystem studies today, the incorporation of sinking detritus has a large impact on the position of the nutricline, and thus the flux of utilizable nitrogen into the mixed layer and the resulting model dynamics. Therefore, an understanding of model dynamics and the correct simulation of depth-explicit concentrations will require explicit inclusion of a detritus component within the NPZ model. It is important to note that in the model investigated here only the detritus component was able to sink; both large and small phytoplankton components were considered to be non-sinking. In reality, while small phytoplankton may not sink, large phytoplankton could have a significant sinking velocity. Additionally, the various constituents of detritus, *i.e.*, dead plankton and fecal pellets could sink at very different rates. The model results presented here provide a good

first approximation of the behavior of a depth-explicit NPZ model that incorporates sinking detritus. However, it is important to consider that non-zero sinking rates for the phytoplankton or alternative sinking rates for the detritus component could have a large impact on model behavior. It is likely that this could have a significant impact on the vertical concentration profiles influencing the existence of structural features such as the sub-surface chlorophyll maximum.

The addition of diffusion to the simple three-component NPZ model has been shown to stabilize the water column for certain model parameterization, and does so more strongly at higher levels of mixing (Edwards *et al.,* 2000). The transition from unstable to stable model solutions was found to occur at $Kv = 4x10^{-7}$ m^2 s^{-1} which is significantly below diffusivities associated with even background levels of mixing. At stronger levels of mixing ($1x10^{-2}$ m^2s^{-1}) associated with wind mixing all oscillations were eliminated. Although the model under investigation here was originally based on this simple model the findings presented for the more complex model are in stark contrast. It is likely that this discrepancy has roots in the structure of the vertical diffusion profile. Although Edwards *et al.* (2000) used a model that had a depth-explicit vertical structure they assumed diffusion was vertically homogenous for the 100 meters considered; his is not a realistic assumption for most regions of the world's ocean.

The existence of short term oscillations has been previously addressed for an NPZ model in which a zooplankton grazer can feed on multiple prey types (Ryabchenko *et al.*, 1997). In this previous investigation a mixed layer model was forced with seasonally varying mixed layer thickness. Model oscillations were found to be initiated by abrupt changes of the mixed layer depth in the spring or fall, but the existence of these oscillations required a combination of a shallow mixed layer, significant mean annual entrainment velocities and high nutrient concentration in the seasonal pycnocline (Ryabchenko *et al.*, 1997). In agreement with these findings, it was shown here that both the magnitude of the mixed layer diffusivity and the mixed layer depth could potentially have an impact on dynamics

of a depth-explicit NPZ model. It appears that degree of impact of these physical properties depends on the resultant change in flux of utilizable nitrate to the mixed layer. In general, a change in physical forcing that gave rise to an increase in flux (an increase in mixed layer diffusivity or a reduction in mixed layer depth) resulted in a more excitable model that exhibited oscillations for a broader region of parameter space. However, a comparison of model dynamics with and without sinking detritus indicates that an increase in the flux of utilizable nitrogen to the mixed layer does not universally increase the prevalence of model oscillations. The net export of nitrogen from the mixed layer, resulting from the sinking detritus, depressed the nutricline and consistently resulted in a smaller upward flux of nitrogen back to the mixed layer. However, rather than stabilizing the model as we might expect, this reduced availability of nitrogen either had no influence on, or enhanced, model excitability. It is possible that while sometimes an increase in availability of nitrogen can cause oscillations, so too can the lack of available nitrogen.

Long term periodic (>1 year), quasi-periodic, and chaotic solutions have also been proposed to result from strong upwelling and high availability of utilizable nitrogen in the seasonal pycnocline (Popova *et al.,* 1997). The model used in this previous investigation assumed a homogeneous mixed layer and, nitrogen was fluxed into/out of the mixed layer using an 'entrainment' function that was dependent on the changing mixed layer depth. This is a similar model structure to that used by Ryabchenko *et al.* (1997). Here, using stationary forcing, but a more sophisticated approach to representing vertical diffusion, oscillations were found to be intrinsic to the NPZ model, their existence independent of seasonal forcing. Quasi-periodic or chaotic variability was not found in this investigation, however, the time dependent solutions considered were significantly shorter than those used by Popova *et al.,* (1997) and forcing was stationary in time. It is possible that with seasonal forcing some of these more complex behaviors may be observed.

5.5 References

Childers, A.R., Whitledge, T.E. and Stockwell, D.A. (in press) Seasonal and interannual variability in the distribution of nutrient and chlorophyll a across the Gulf of Alaska shelf: 1998-2000. *Deep-Sea Res.*

Denman, K. L. and Peña, M. A. (1999) A coupled 1-D biological/ physical model of the northeast subarctic Pacific Ocean with iron limitation. *Deep-Sea Res. II,* **46,** 2877-2908.

Edwards, A. M. (2001) Adding Detritus to a Nutrient Phytoplankton Zooplankton Model: A Dynamical-Systems Approach. *J. Plankton Res.*, **23**, 389-413.

Edwards, C. A., Powell, T. A. and Batchelder, H. P. (2000) The stability of an NPZ model subject to realistic levels of vertical mixing. *J. Mar. Res.*, **58**, 37-60.

Fasham, M. J. R., Ducklow, H. W. and McKelvie, S. M. (1990) A nitrogen-based model of plankton dynamics in the oceanic mixed layer. *J. Mar. Res.*, **48**, 591-639.

Frost, B.W. (1993) A modelling study of processes regulating plankton standing stock and production in the open subarctic Pacific Ocean. *Prog. Oceanog.*, **32**, 17-56.

Kish M.J., Motono, H., Kashiwai, M. and Tsuda A. (2001) An Ecological-Physical Coupled Model with Ontogenetic Vertical Migration in the Nortwestern Pacific. *J. Oceanogr.*, **57**, 499-507.

Lancelot, C., Hannon E., Becquevort, S., Veth, C. and De Baar, H. J. W. (2000) Modeling phytoplanktonblooms and carbon export production in the Southern Ocean: dominant controls by light and iron in the Atlantic sector in Austral spring 1992. *Deep-Sea Res. I,* **47**, 1621-1662.

Legendre, L. and Rassoulzadegan, F. (1995) Plankton and nutrient dynamics in marine waters. *Ophelia*, **41**, 153-172.

Leonard, C. L. McClain C. R., Murtugudde, R., Hofmann, E. E. and Harding Jr. L. W. (1999) An iron-based ecosystem model of the central equatorial Pacific. *J. Geophys. Res.*, **104**, 1325-1341.

Loukos, H., Frost, B. W., Harrison, D. E. and Murray, J. W. (1997) An ecosystem model with iron limitation of primary production in the equatorial Pacific at 140°W. *Deep-Sea Res. II,* **44,** 2221-2249.

Popova, E. E., Fasham, M. J. R., Osipov, A. V. and Ryabchenko, V. A. (1997) Chaotic behaviour of an ocean ecosystem model under seasonal external forcing. *J. Plankton Res.,* **19,** 1495-1515.

Ryabchenko, V. A., Fasham, M. J. R., Kagan, B. A. and Popova, E. E. (1997) What causes short-term oscillations in ecosystem models of the ocean mixed layer? *J. Mar. Res.,* **13,** 33-50.

Sarmiento, J. L., Slater, R. D., Fasham, M. J. R., Ducklow, H. W., Toggweiler, J. R. and Evans, G. T. (1993) A seasonal three-dimensional ecosystem model of nitrogen cycling in the North Atlantic euphotic zone. *Global Biogeochem. Cycles*, **7**, 417–450.

Stabeno, P. J., Bond, N. A., Herman, A. J., Kachel, N. B., Mordy, C. W. and Overland, J.E. (2004) Meterology and oceanography of the Northern Gulf of Alaska. *Continental Shelf Research*, **24**, 859-897.

Strom, S. L., Brainard, M. A., Holmes, J. L. and Olson, M. B. (2001) Phytoplankton blooms are strongly impacted by microzooplankton grazing in coastal North Pacific waters. *Mar. Biol.,* **138,** 355-368.

Weingartner, T., Coyle, K., Finney, B., Hopcroft, R., Whitledge, T., Brodeur, R., Dagg, M., Farley, E., Haidvogel, D., Haldorson, L., Hermann, A., Hinckley, S., Napp, J., Stabeno, P., Kline, T., Lee, C., Lessard, E., Royer, T. and Strom, S. (2002) The Northeast Pacific GLOBEC Program: Coastal Gulf of Alaska. *Oceanography,* **15**, 48-63.

Chapter 6 . Discussion and conclusions

6.1 Summary

A full understanding of marine ecosystem dynamics requires knowledge of the influence of physical forcing on the spatiotemporal distribution and abundance of plankton, and of the interaction between the different trophic levels. Economical and logistical barriers prevent the ideal large geographic scale, high temporal resolution collection of observational data that would help us address many key questions that exist on marine ecosystem functionality. In light of this, Nutrient-Phytoplankton-Zooplankton (NPZ) computer simulation models are becoming increasingly prevalent in marine ecosystem studies. These models are used to gain insights into how a system works or to make predictions of the future state of the ecosystem. These models can provide synchronous 'coverage' of an ecosystem of interest, and are a relatively inexpensive research tool. While such computer simulation models are not a substitute for the traditional observational approach, they do provide a valuable way of exploring the details of the links between physical forcing (wind-mixing, heating, freshening, *etc.*), the nutrient and light fields, and plankton dynamics. As such, they are very useful in application of the 'bottom up' approach to ecosystem studies.

The observation of oscillations in concentrations of NPZ model components (*i.e.*, the plankton and the nutrients) is common (May, 1973; Oaten and Murdoch, 1975; Steel and Hendersen, 1992; Edwards and Brindley, 1996; Edwards *et al.*, 2000). Such oscillations have also been observed, albeit to a lesser extent, in nature. The most notable example being the oscillations observed in chlorophyll concentration at OWS 'India' (Ryabchenko *et al.*, 1997; Yool, 1998). It is possible that more systems exhibit oscillations but that our resolution of data collection is not of an appropriate scale to capture them. Investigations in to the non-linear dynamics of simple, zero dimensional, models (May 1973; Oaten and Murdoch, 1975; Franks, 1986) have shown that oscillations are an intrinsic property of

NPZ models, and are thought to result primarily from the predator-prey interactions. The investigation into NPZ model dynamics has also been extended to temporally forced models (Ryabchenko *et al.*, 1997; Popova *et al.*, 1997). These investigations suggest that oscillations observed in nature are related to the availability of inorganic nitrogen to the phytoplankton, and their existence requires high nutrient concentrations in the pycnocline and a shoaling mixed layer (Ryabchenko *et al.*, 1997). While either of the above explanations could be the cause of the oscillations observed at OWS 'India', it is also possible that these observations are related to unmeasured factors such as the advection of successive blooms past the mooring (Yool, 1998). Whether or not such oscillations truly exist in nature, it is important to understand the dynamics intrinsic to NPZ models. Relatively complex ecosystem models, comprising multiple phytoplankton and zooplankton component, are now commonly used in ecosystem studies. However, to date, little has been done in the way of exploring the behavior of these models when subjected to steady, depth-explicit forcing. In the absence of this knowledge the time dependent behavior of coupled biological-physical ecosystem models could mistakenly be attributed to variable physical forcing rather than as an inherent property of the biology model. An improved understanding of model behavior will also help in the search for an explanation for oscillations observed in nature.

The objective of this dissertation was to explore the dynamical behavior of intermediately complex NPZ models in which multiple grazers could feed on multiple prey types. The role of the functional forms for grazing and predation on the behavior of a multiple prey NPZ subject to depth-explicit but stationary forcing was explored. Initially the model investigated comprised six-components. Subsequently, a seventh detritus component was added. The model was subjected to stationary physical forcing. Model dynamics and the structure of the model solutions were determined when implementing alternative forms of the zooplankton grazing function and systematically vary the specific predation rate (h=0.05-2.4 [g C m^{-3}]$^{1-q}$ day^{-1}), and the predation exponent ($1 \leq q \leq 2$), which determines the form of the model closure term. Additionally, the survivorship of the various model

components was investigated. Previous studies on NPZ model stability have not addressed survivorship. It is likely that this is because those studies considered a model with only a single phytoplankton and zooplankton component and survivorship was not an issue. However, it has been shown here, with some forms of the grazing function all model components thrived simultaneously only in very small regions of parameter space. This is an important issue, because the majority of modern ecosystem modeling studies use a model that comprises multiple grazers and multiple prey types.

The models investigated here were parameterized to represent the coastal Gulf of Alaska, a very productive, commercially important marine ecosystem. Many questions exist regarding the mechanisms behind the high productivity of this system, and the observed variability in productivity on a decadal time scale. Computer simulation models of the Gulf of Alaska ecosystem are being developed in order to supplement the traditional observational approach to ecosystem understanding. The ability to accurately model the details of the influence of physical forcing on primary (phytoplankton) and secondary (zooplankton) production will provide valuable insight into marine ecosystem functionality and contribute towards our understanding of observed spatial and temporal variations in ecosystem productivity. It is hoped that the work presented in this dissertation will provide a valuable addition to our understanding of complex ecosystem models parameterized for this region, and also to modelers of other ecosystems in which multiple phytoplankton and zooplankton groups are known to play an important role in ecosystem dynamics.

The models investigated here were depth-explicit in the vertical, and each layer was coupled by the action of diffusion. The inclusion of a realistic diffusion profile represents a major advance in studies of NPZ non-linear dynamics. At present, no general method for analysis of diffusive, depth-explicit NPZ models exists. Here I have demonstrated that because it is not possible to solve such complex systems analytically, the traditional approach to studying dynamics, *i.e.*, determination of the eigenvalues of the Jacobian (community) matrix, was of limited use for classifying model behavior. Model dynamics

were instead explored by examining model trajectories in time and space, numerically seeking and classifying the form of solutions. Such an analysis provides a useful insight into behavior of the more complex NPZ models commonly used in ecosystem studies.

6.2 Discussion

It was demonstrated that with each of the grazing functions tested, Hopf bifurcations, where the form of the solution transitioned between steady equilibrium and periodic limit cycles, span the q and h parameter space explored. While these transitions in dynamic behavior have been previously noted for simple, one-predator one-prey, NPZ models (Edwards and Bees, 2001) it has been shown here that with more complex ecosystems, where a zooplankton can graze on a mixed prey field, the location of the bifurcations in parameter space is highly dependent on the form of the grazing function. The period of the oscillatory, limit cycle solutions was also found to depend predominantly on the form of the grazing function. The period of limit cycles associated with a three-component NPZ model is commonly reported to be about constant and of the order of 34–35 days (Steele and Henderson, 1992; Edwards and Brindley, 1996), however, in such investigations only one form (sigmoidal) was used to simulate zooplankton grazing on a single prey. This investigation demonstrates that when zooplankton can graze on a mixed prey field, alternative forms of the grazing function can result in very different oscillation periods, and regions in q-h space of near constant period may not exist.

Permanent coexistence of model components at equilibrium was also found to be strongly influenced by the choice of grazing function. With some forms of the grazing function it was rare for all predators and prey to exist simultaneously, while with others, all components coexisted simultaneously for large regions of the parameter space explored. It was proposed that the difference depends on the assumptions inherent in the form of the grazing function, *i.e.,* if and when rare prey types are provided with a refuge from grazing. If no prey refuges exists, or if the refuge applies only when the concentration of the total prey is low, regardless how rare any one prey type may be, then the system

typically purges itself until only one predator and one prey remain. The non-linear dynamics of the remaining components are then determined by the efficiency of the remaining grazer to capture the remaining prey.

The addition of detritus to an NPZ model was thought of little consequence for model dynamics (Edwards, 2001). In this study, the dynamic behavior and structure of solutions for a six-component model was not notably impacted by adding a detritus component, if the detritus were unable to sink. If detritus has a non-zero sinking velocity, such that utilizable nitrogen was exported from the upper mixed layer, the structure of model solutions, with regards to survivorship of model component, was little altered, but a downwards shift in the position of the nutricline and a concomitant reduced upwards flux of utilizable nitrogen was observed. This export of nitrogen from the mixed layer enhanced the probability of simulating the sub-surface chlorophyll maximum and also increased the excitability of the model. Detritus therefore plays an important role in NPZ model dynamics and must be included in the model to correctly simulate the depth-explicit concentrations of model components or to have a understanding of the potential excitability of the system.

The existence of short term oscillations for an NPZ model in which a zooplankton grazer can feed on multiple prey types has been previously addressed (Ryabchenko *et al.*, 1997). The susceptibility to oscillations was attributed to abrupt changes of the mixed layer depth in the spring or fall, and was dependent on a small mixed layer thickness, significant mean annual entrainment velocity and high nutrient concentration in the seasonal pycnocline. This past investigation used an upper mixed layer model which was forced with seasonally varying upper mixed layer thickness. Both the magnitude of the mixed layer diffusivity and the mixed layer depth (through their impact on flux of utilizable nitrogen to the mixed layer) were shown to impact the dynamics of a depth-explicit NPZ model. Here, changes to physical forcing that increased the upward nutrient flux (*i.e.*, an increase in mixed layer diffusivity or a reduction in mixed layer depth)

resulted in a more excitable model that exhibited oscillations for a broader region of parameter space. However, oscillations were found to be intrinsic even in the physically stationary models investigated here; their existence is not dependent on variable seasonal forcing. Additionally, by comparing model dynamics with and without sinking detritus, it was shown that a reduction in the availability of utilizable nitrogen to the mixed layer does not universally decrease the prevalence of model oscillations. The net export of nitrogen from the mixed layer, resulting from the sinking detritus, depressed the nutricline and consistently resulted in a smaller flux of nitrogen back to the mixed layer. Rather than stabilizing the model as one might expect, this reduced availability of nitrogen either had no influence on, or enhanced, model excitability. This illustrates that while sometimes an increase in availability of nitrogen can cause oscillations, so too can the lack of available nitrogen.

Through this dissertation the dynamical behavior of intermediately complex NPZ models in which multiple grazers could feed on multiple prey types has been shown to be greatly impacted by the choices of functional forms, both for predation and grazing. Balancing the 'best' form for simulation of a biological process from a modeler's point of view and from an observationalist's point of view can present a challenge. For example, an observationalist may seek a form for the grazing function that appears to best describe the grazer under investigation. However, usually only one, or a few, species are considered at a time. Conversely, due to the necessary aggregation that modelers perform when seeking to describe an ecosystem, such a functional form may not be appropriate. Often, trophic levels rather than individual species are considered, and so certain functional forms may not make sense from a biological point of view. I do not wish to advocate that any one functional form for grazing or predation is better than the others available, however, the elimination of model components or the production of oscillatory model solutions are generally considered undesirable traits, and a functional form that promotes such behavior may be less favored. It is important that prior to attempting interpretation of results from simulations using coupled biological and physical models, users and

developers of ecosystem models should be aware of the potential impact their choice of function may have on the intrinsic oscillatory nature of the model.

6.3 Future Work

There is much left for study in this area of research. Although the models investigated here represent major advance in terms of biological complexity and depth-explicit forcing, the forcing was temporally stationary. The next logical step in the progression of investigations into NPZ non-linear dynamics would be to explore the impact of seasonal forcing on a depth-explicit model in which zooplankton can graze on multiple prey items and detritus are able to sink. Expansion of model dimensions in space would also prove insightful. It is possible that the incorporation of two or three dimensional physics into the model would act to dampen or enhance the model excitability. Further expansion of the biological complexity could also be an interesting path to follow. Stability studies, including this one, generally focus on the impact of the predation function and/or the grazing function. This is because several alternative forms have been presented in the literature to simulate these biological processes, and it is not known which is most 'correct'. There is less uncertainty associated with the other process functions in the model, *i.e.,* the functional form for nutrient uptake, and as a result the impact of the form of these other terms on model dynamics is generally overlooked. Many of the more complex NPZ models used today in ecosystem studies incorporate additional complexity whose impact on dynamics has been little considered. For example, the self shading of phytoplankton, the temperature dependent growth of phytoplankton and zooplankton, and the capture efficiency of a zooplankton for the available prey. As we come to rely more on these models as a tool to interpret marine ecosystem functionality it will be important to continue to expand our understanding of the non-linear behavior inherent in these models.

6.4 Closing Remarks

Despite the simplicity of the models investigated here, with regard to the time dependency and biological complexity, the results do represents a significant advance of our understanding into NPZ model dynamics. These findings contribute towards the more general understanding of non-linear dynamics and structural stability of complex NPZ models in which multiple grazers can select from multiple prey types. I have provided an insight into the impact that the choice of commonly used multiple resource grazing functions and mortality functions can have on model dynamics. These findings have important implications for modeling efforts in environments where multiple prey and predator classes persist simultaneously. It is hoped that this analysis will be of value during construction of models for such ecosystems, and for interpreting results from biophysical model simulations in which the physical forcing is varied over a seasonal cycle.

6.5 References

Edwards, C. A., Powell, T. A. and Batchelder, H. P. (2000) The stability of an NPZ model subject to realistic levels of vertical mixing. *J. Mar. Res.*, **58**, 37-60.

Edwards, A. M. and Bees, M. A. (2001) Generic dynamics of a simple plankton population model with a non-integer exponent of closure. *Chaos, Solutions & Fractals,* **12**, 289-300.

Edwards, A. M. and Brindley, J. (1996) Oscillatory behaviour in a three-component plankton population model. *Dyn. Stabil. Syst.*, **11**, 347-370.

Edwards, A. M. (2001) Adding detritus to a Nutrient Phytoplankton Zooplankton model: A dynamical-systems approach. *J. Plankton Res.*, **23**, 389-413.

Franks, P. J. S. and Chen, C. (2001) A 3-D prognostic numerical model study of the Georges bank ecosystem. Part II: biological-physical model. *Deep-Sea Res.*, **48**, 457-482.

May, R. M. (1972) Limit cycles in predator-prey communities. *Science,* **177**, 900-902.

May, R. M. (1973). Stability and complexity in model ecosystems, Princeton University Press. Princeton, N.J.

Oaten, A. and Murdoch, W. W. (1975) Switching, functional response, and stability in predator-prey systems. *American Naturalist,* **109**, 299-318.

Popova, E. E., Fasham, M. J. R., Osipov, A. V. and Ryabchenko, V. A. (1997) Chaotic behaviour of an ocean ecosystem model under seasonal external forcing. *J. Plank. Res.,* **19**, 1495-1515.

Ryabchenko, V. A., Fasham, M. J. R., Kagan, B. A. and Popova, E. E. (1997) What causes short-term oscillations in ecosystem models of the ocean mixed layer? *J. Mar. Res.,* **13**, 33-50.

Steele, J. H. and Henderson, E. W. (1992) The role of predation in plankton models. *J. Plankton Res.,* **14**, 157-172.

Yool, A. (1998). The dynamics of open-ocean plankton ecosystem models, Ph.D. diss, University of Warwick.